L-Proline and Glutamatergic Neurotransmission:

Clarifying the Modulatory Role of Neuronal

L-Proline Transporter

Dissertation

zur

Erlangung des Doktorgrades (Dr. rer. nat.)

der

Mathematisch-Naturwissenschaftlichen Fakultät

der

Rheinischen Friedrich-Wilhelms-Universität Bonn

vorgelegt von

Daniel Schulz

aus

Troisdorf

Bonn 06.12.2011

Angefertigt mit Genehmigung der Mathematisch-Naturwissenschaftlichen Fakultät der

Rheinischen Friedrich-Wilhelms-Universität Bonn

1. Gutachter: Prof. Dr. Eva Kostenis

2. Gutachter: Prof. Dr. Klaus Mohr

Tag der Promotion: 26.03.12

Erscheinungsjahr: 2012

Abstract

The neuronal high affinity L-proline transporter (PROT) is a putative neurotransmitter transporter whose contribution to neurotransmission is still unknown. PROT is expressed exclusively in brain by subpopulations of glutamatergic neurons and is assumed to conduct the reuptake of L-proline, which is released upon depolarization. Since to date no specific high-affinity receptor for L-proline has been discovered, the amino acid has been suggested to play a role regulating glutamatergic neurotransmission. To uncover the *in vivo* modulatory function of PROT, a mouse strain lacking functional PROT was generated and confirmed. The analysis of these PROT-knockout mice provided new insights into the modulatory functional roles of this transporter. Biochemical alterations within the central nervous system of PROT lacking mice were identified. Thus, PROT-deficient mice exhibit increased expression levels of N-methyl-D-aspartic acid (NMDA), α-amino-3-hydroxy-5 methylisoxazolepropionic acid (AMPA) and kainate (KA) receptor subunits. Furthermore, levels of the dopamine receptor D_2 (DRD2) as well as levels of the dopamine synthesizing enzyme tyrosine hydroxylase (TH) are elevated. Behavioral analyses of PROT-knockout mice unveiled decreased locomotor activity, increased anxiety like behavior, and better learning abilities compared to wild-type littermates. The changes in behavioral profiles of analyzed PROT-deficient animals are in line with the observed biochemical adaptive alterations. Collectively, the presented studies indicate that the functional role of PROT within neurotransmission is primarily the modulatory fine tuning of glutamatergic signaling, by controlling the levels of L-proline in synaptic clefts.

Zusammenfassung

Bei dem neuronalen hochaffinen L-Prolin-Transporter (PROT) handelt es sich vermutlich um einen Neurotransmitter Transporter, dessen Einfluß auf die Neurotransmission bislang kaum erforscht ist. Dieser Transporter wird ausschließlich im Gehirn von einer Teilpopulation glutamaterger Neurone exprimiert und es wird angenommen, dass er der Wiederaufnahme von depolarisations-abhängig ausgeschüttetem L-Prolin dient. Da bisher noch kein spezifischer L-Prolin-Rezeptor im ZNS nachgewiesen werden konnte, wird vermutet, dass diese Aminosäure eine Funktion bei der Regulation der glutamatergen Neurotransmission ausübt. Um die modulatorische Funktion von PROT *in vivo* aufzuklären, wurde eine Mauslinie generiert, der das funktionsfähige PROT-Protein fehlt. Durch die Analyse dieser PROT-Knockout Mäuse konnten neue Erkenntnisse über die modulatorische Funktion dieses Transporters gewonnen werden. Zahlreiche biochemische Veränderungen konnten im ZNS von PROT-defizienten Tieren identifiziert werden. PROT-Knockout Mäuse weisen eine erhöhte Expression von N-methyl-D-aspart (NMDA), α-amino-3-hydroxy-5 methylisoxazolepropionsäure (AMPA) und Kainat (KA) Rezeptor Untereinheiten auf. Weiterhin sind die Expressions-Level des Dopamin Rezeptors D_2 (DRD2), sowie des Dopamin synthetisierenden Enzyms Tyrosin Hydroxylase (TH) erhöht. Darüber hinaus zeigen PROT-defiziente Tiere veränderte Verhaltensprofile. PROT-Knockout Mäuse zeichnen sich im Vergleich zu Wild-Typ Tieren durch eine verminderte lokomotorische Aktivität, ein erhöhtes Angst-Verhalten und eine bessere Lernfähigkeit aus. Diese veränderten Verhaltensphänotypen der PROT-defizienten Tiere passen zu den beobachteten adaptiven Veränderungen der Glutamat Rezeptor Expression. Insgesamt deuten die dargestellten Studien darauf hin, dass die Funktion, die PROT in der Neurotransmission ausübt, in erster Linie der modulatorischen Feinabstimmung der glutamatergen Signalgebung dient, indem dieses Protein die L-Prolin-Level im synaptischen Spalt kontrolliert.

Table of Contents

List of Figures

1   Introduction

1.1   Synaptic Transmission in the Central Nervous System

The activities of the nervous system operate through ongoing electrical and chemical signals. These alternations are based on the process of synaptic transmission, also called neurotransmission. Synaptic transmission is a process reporting the intercellular communication of neuronal cells through signal transduction at specialized junctions (synapses). At these synapses, signaling molecules (neurotransmitters) are released from the presynaptic neurons into the synaptic cleft to activate corresponding receptors of postsynaptic cells upon binding. The activation of these neurotransmitter receptors leads to conformational changes, which either result in induction of intracellular signal transduction cascades or in the diffusion of ions through molecular pores (ion channels), which can be part of receptors and play a central role in membrane excitation. Synaptic transmission arises when signaling through neurotransmitters causes the development of an electric current (action potential) in the postsynaptic neuronal cell. It can be either excitatory or inhibitory, depending on the ion-selectivity of the activated receptor. This is because neuronal cells have a negative membrane potential, or in other words, the cytoplasm is electrically more negative than the external fluid, leading to a potential drop across the plasma membrane. Incoming ions that make the cytoplasm more positive depolarize the membrane, and vice versa, those making it more negative are said to hyperpolarize the membrane. If a receptor is selectively permeable for positive charged ions, activation induces an excitatory postsynaptic potential (EPSP). On the other hand, selectivity for negatively charged ions leads upon activation of the respective receptors to an inhibitory postsynaptic potential (IPSP). Thereby, the development or abortion of an action potential is triggered. The main neurotransmitter activating excitatory receptors is glutamate, and main inhibitory neurotransmitters are gamma-aminobutyric acid (GABA) and glycine. To terminate the synaptic transmission induced upon neurotransmitter release from the presynaptic neuron, neurotransmitters have to be inactivated. This is achieved either by enzymatic degradation or by active transport back into neuronal cells (or into glial cells) through membrane located neurotransmitter transporters. These transporters are highly selective and bind their substrates with high affinity. Neurotransmitter transporters use the electrochemical gradient across the cell membrane as a driving force to carry their substrate. This means that the energy is obtained by cotransport of ions like sodium and chloride, or antiport of potassium.

1.2   An Overview about the Amino Acid L-Proline

L-proline (shown in **Figure 1**) is an exceptional amino acid; it differs from others in its imino group instead of a primary amino group. Its side chain is bound to both nitrogen and α-carbon atoms resulting in a special molecule that exhibits conformational rigidity. Therefore, L-proline has an important role for the structure of proteins and is as well excluded from the regular amino acid metabolism, namely the pyridoxal 5-phosphate coenzyme catalyzed decarboxylation and transamination reactions. Besides the abundant presence of L-proline in regular food, pathways exist for its synthesis from glutamate or ornithine as precursors (Hu et al. 2008). As shown in **Figure 2**, the initial reactions of these pathways occur in the mitochondria. The common intermediate is glutamic-γ-semialdehyde that spontaneously cycles to Δ^1-pyrroline-5-carboxylate (P5C) (Adams 1970; Phang et al. 1979). The enzymes required for synthesis are ornithine-aminotransferase (OAT) and P5C-synthase, respectively. P5C is then released to the cytoplasm and converted to L-proline by P5C-reductase (Pycr). L-proline is reshuttled into the mitochondria and there degraded by the enzyme L-proline dehydrogenase (PRODH) that converts L-proline back to P5C. Subsequently, P5C is non-enzymatically converted back to glutamic-gamma-semialdehyde, which can be transformed into glutamate (by Δ^1-pyrroline-5-carboxylate dehydrogenase) or ornithine (by ornithine-aminotransferase).
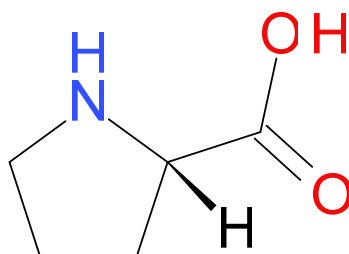
Figure 1 Chemical structure of L-proline
Image was designed with the help of Symyx® Draw 3.3 (Symyx Solutions, Inc.)
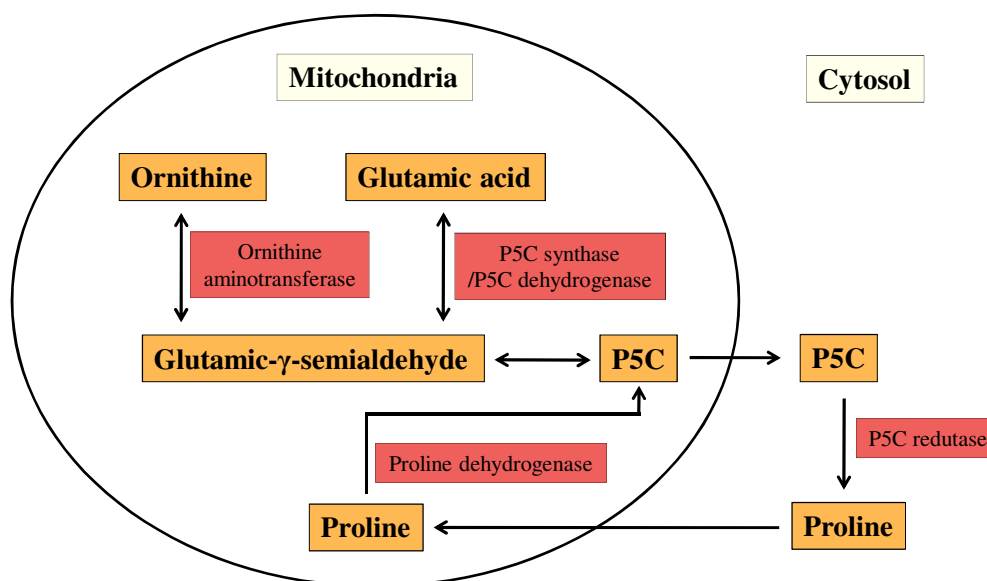
Figure 2 Schematic depiction of the L-proline cycle (modified from Wyse and Netto 2011)
Abbreviation: P5C = Δ^1-pyrroline-5-carboxylate

Dysfunctions of the described primary metabolism of L-proline are known to be associated with various diseases (Mitsubuchi et al. 2008). The disorder hyperprolinemia is an autosomal recessive inherited disease caused by insufficient L-proline catabolism and present in two forms. Hyperprolinemia type I (HPI) results from the hepatic deficiency of the enzyme proline dehydrogenase (PRODH) with subsequent tissue accumulation of L-proline. Plasma L-proline levels of patients suffering from HPI are elevated from five- to ten times (700 to 2400 μM) above normal values (51 to 271 μM) (Wyse and Netto 2011). Hyperprolinemia type II (HPII) is characterized by insufficiency of P5C-dehydrogenase activity again resulting in accumulation of L-proline (Flynn et al. 1989). This form of hyperprolinemia leads to higher increase in L-proline plasma concentrations (1500 to 3700 μM) compared to HPI. In state of hyperprolinemia, concentrations of L-proline are increased in all tissues, thus as well in the cerebrospinal fluid. As a result, the disease is associated with cognitive symptoms like hyperactivity, amnesia, epilepsy and deafness (Mitsubuchi et al. 2008). In addition, there is evidence for association of hyperprolinemia with schizophrenia (Clelland et al. 2011). In mouse models of hyperprolinemia the animals are found to exhibit learning deficits in short-term memory examining tasks like T-maze as well as in aversive learning tasks (Baxter et al. 1985; Davis et al. 1987). Furthermore, chronic hyperprolinemia provokes a long-term memory deficit, shown by Morris water maze test analysis (Bavaresco et al. 2005).

1.3   The Role of L-Proline in the Brain

There is a long history of evidence suggesting that certain amino acids or their metabolites are able to modulate synaptic transmission in the central nervous system (Snyder et al. 1973; Yoneda and Roberts 1982; Fremeau et al. 1992; Gogos et al. 1999). While L-glycine and L-glutamate are well established as neurotransmitters, little is known about the role of the non-essential amino acid L-proline in the CNS. However, in addition to its essential roles in primary metabolism and protein synthesis L-proline fulfills several criteria of well characterized amino acid neurotransmitters.

First, the neurotransmitter candidate L-proline shows a heterogeneous regional distribution in brain. By using an L-proline conjugated antibody, L-proline was observed in areas corresponding to the amygdala, piriform cortex and hippocampus as well as in a group of fibers and neuronal cell bodies in the brainstem and hypothalamus (Takemoto and Semba 2006). Furthermore, a differential distribution of radioactivity can be found after injection of ^{3}H-leucine and ^{3}H-proline into cortex (Felix and Kunzle 1974).

A synaptosomal biosynthetic pathway from ornithine has been found in the rodent brain, where L-proline is synthesized by the enzymes ornithine-δ-aminotransferase and pyrroline 5-carboxylate reductase (Yoneda and Roberts 1982). However, this synthetic pathway is not required to offer substrate for protein synthesis because L-proline is sufficiently present in conventional food. Furthermore, L-proline is one of the most abundant amino acids in any tissue, being readily available from decomposition of the extracellular matrix, which is built-on predominately of collagen, which in turn contains 25% L-proline and its derivative hydroxyproline.

Another piece of evidence of the transmitter role of L-proline arises from experiments in which intrahippocampal injections of L-proline at high doses produce lesions at the injection site similar to those appearing after injections of L-glutamate (Nadler et al. 1988). The neurodegenerative activity of L-proline could result directly from a putative ability to depolarize affected cells.

An additional hint to the possible role of L-proline as a neurotransmitter comes from the observation that in rat cerebral cortex and spinal cord slices, radiolabeled L-proline is released from neurons by potassium-induced depolarization in a Ca^{2+}-dependent manner (Snyder et al. 1973). Furthermore, a Ca^{2+}-dependent release of exogenously loaded radiolabeled L-proline was also described in synaptosomes prepared from rodent brain cortex (Nickolson 1982). Such a Ca^{2+}-dependent release is a typical hint for neurotransmitters.

Although specific sodium-independent binding of radiolabeled L-proline to rodent brain synaptic membranes has been described (Greene et al. 1986; Cordero et al. 1991), so far no specific high-affinity receptor has been found for L-proline in the CNS, suggesting that it is a neuromodulator rather than a neurotransmitter (Shafqat et al. 1995). Indeed, the amino acid L-proline reportedly plays a role in regulating synaptic transmission, which is the most striking remark for its neuromodulatory function. Already in 1976 it was published that intracerebral administration of L-proline selectively disrupts memory formation and recall in chicks (Cherkin et al. 1976). Another study about the contribution of L-proline to synaptic transmission displayed that high concentrations of this amino acid could be shown to activate N-methyl-D-aspartic acid (NMDA) receptors, α-amino-3-hydroxy-5 methylisoxazolepropionic acid (AMPA) receptors and kainate (KA) receptors in mouse brain slices (Ault et al. 1987; Henzi et al. 1992; Martin et al. 1992). As well it was reported that more physiological concentrations of L-proline potentiate the transmission mediated by NMDA-receptors (Cohen and Nadler 1997b). Different studies showed that L-proline applied to neurons can exhibit excitatory actions (Ault et al. 1987; Henzi et al. 1992; Martin et al. 1992; Felix and Kunzle 1974). Furthermore, it was observed that in chicks under acute stressful conditions the amount of L-proline in brain was reduced whereas intracerebroventricular injection of L-proline induced sedative and hypnotic effects (Hamasu et al. 2009; Hamasu et al. 2010).

Another important piece of evidence that L-proline is a neurotransmitter or neuromodulator candidate is displayed through the interesting finding that a high affinity sodium-dependent transporter for L-proline (PROT) was detected in the CNS (Cohen and Nadler 1997c; Fremeau et al. 1992; Renick et al. 1999). In general, neurotransmitter systems have mechanisms to terminate signaling through removing the ligands via rapid reuptake by sodium-dependent transporters. Typically, for high affinity uptake of amino acids into obvious neurotransmitter pools, sodium-dependency is more characteristic than for low affinity uptake of the same amino acids, particularly in metabolic processes through different types of transporters (Mulder and Snyder 1974).

1.4   The Neuronal High Affinity L-Proline Transporter PROT

Although already in 1976 a high affinity sodium-dependent L-proline uptake was described in rodent brains (Balcar et al. 1976), it was not before 1992 that this could finally be related to the neuronal high affinity sodium-dependent L-proline transporter (PROT) (Fremeau et al. 1992). First, PROT was cloned and characterized using rat brain cDNA (Fremeau et al. 1992) and later on as well using human sources (Shafqat et al. 1995). Sequence analysis revealed that PROT belongs to the family of sodium-dependent neurotransmitter transporters, which enclosed among others the transporters for dopamine, serotonin, glycine, norepinephrine or GABA (Fremeau et al. 1992). These transporters use transmembrane electrochemical ion gradients to drive active transport of substrates across the plasma membrane (Amara and Kuhar 1993; Kanner 1989). The structural properties of this transporter family are the existence of 12 hydrophobic transmembrane domains, intracellular amino- and carboxy-termini, and N-glycosylation sites between transmembrane domains 3 and 4. PROT shares with its family of sodium-dependent neurotransmitter transporters an overall sequence identity of 45% (Fremeau et al. 1992; Shafqat et al. 1995).
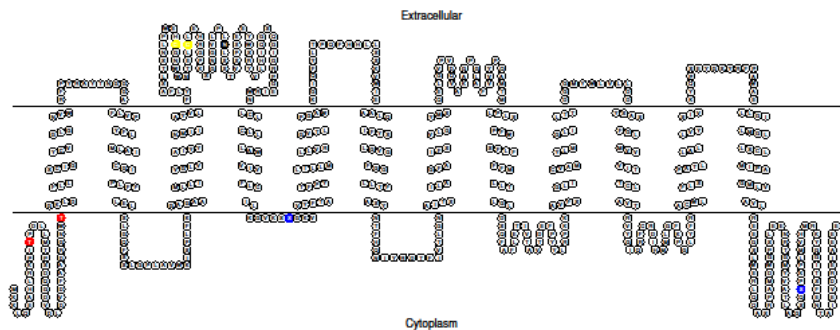
Figure 3 Snake plot of murine high affinity L-proline transporter PROT

The schematic representation of PROT as a serpentine model demonstrates conserved structural features with other members of the sodium-dependent neurotransmitter transporter family by exhibiting an intracellular N-terminus, 12 transmembrane domains linked by 5 intracellular and 6 extracellular loops as well as an intracellular C-terminus. Cysteine residues are highlighted as yellow circles and potentially phosphorylation sites are highlighted as red circles (threonine-residues) and blue circles (serine-residues).
Plot was designed with the help of an online available TM prediction server and a snake plot construction program from http://www.enzim.hu/hmmtop/html/submit.html (HMMTOP prediction of TM helices) and http://www.sacs.ucsf.edu/TOPO (TOPO2 Transmembrane Protein Display Page).

Northern blot analysis detected for both human and rat origins a ~4 kb mRNA transcript [murine PROT: NCBI accession no. NM 201353.1, mRNA =3362 bp, cDNA = 1914 bp] coding for the transporter. Immunoblots of rat and human brain tissues identified a 68 kDa glycosylated protein. As deduced from treatment with peptide-N-glycosidase F, the molecular mass of the primary translation product is 53 kDa (Velaz-Faircloth et al. 1995). It was shown that human PROT (hPROT) exhibits 636 amino acids, lacking one of the glutamate residues present at positions 630-634 in the carboxy-terminus, compared to 637 amino acids of rat PROT (rPROT) and murine PROT (mPROT) (Shafqat et al. 1995). Expression of the corresponding cDNAs in HeLa cells revealed the characteristics of high affinity transport for L-proline with apparent Michaelis constants (K_m) of 9.7 µM for the rPROT and 6.2 µM for hPROT (Shafqat et al. 1995). Moreover, PROT shows a stoichiometry of one L-proline molecule to two sodium ions and one chloride ion per net transport (Galli et al. 1999).

PROT is expressed in the hippocampal formation, the cerebral cortex (Velaz-Faircloth et al. 1995), corpus striatum, hypothalamus, amygdala, thalamus and subthalamic nucleus (Shafqat et al. 1995) of the brain. In these regions PROT is localized in a subset of neuronal cells, mainly in glutamate pathway fibers (Nadler 1987; Nadler et al. 1992) and within synaptic terminals (Fremeau et al. 1992; Velaz-Faircloth et al. 1995). Labeling of PROT revealed that this transporter is localized both in membranes of small synaptic vesicles (SSVs) and in the plasma membrane of axon terminals (Renick et al. 1999). Furthermore, the topology of PROT in synaptic vesicles was found to be inverted with respect to the plasma membrane. This orientation suggests that PROT-containing vesicles are generated by a process involving endocytosis from the plasma membrane (Renick et al. 1999).

PROT-function has been found to be regulated by calcium (Ca^{2+}) and Ca^{2+}-dependent protein kinases (Jayanthi et al. 2000). These authors reported that Ca^{2+} acts as an acute activator of PROT, suggesting that this ion is involved not only in the release of transmitters but also in its fast removal from the synaptic cleft. On the other hand, it was observed that calcium acts indirectly and more slowly by down-stream events inhibiting PROT-function through Ca^{2+}-dependent protein kinases, maybe due to long-term modulation of synaptic transmission (Jayanthi et al. 2000). In addition, PROT was found to be potently inhibited by exogenously applied enkephalins in both rat brain synaptosomes and HeLa cells recombinantly expressing PROT (Fremeau et al. 1996; Galli et al. 1999), which suggests a potential role for PROT in analgesia.

In summary, all data strongly support an important role of L-proline as neuromodulator of synaptic neurotransmission in brain. In addition, PROT codes for the brain-specific high-affinity L-proline transporter previously described in rat brain synaptosomes and slices. Moreover, its pattern of expression in glutamatergic neuronal cells suggests that PROT does not represent a ubiquitous transporter that might have a general function, but rather supports a specific role for L-proline and its transporter in neurotransmission, particularly at glutamatergic synapses.

1.5   An Overview about Glutamatergic Neurotransmission

As mentioned above, it was published that L-proline can modulate glutamatergic synaptic transmission either by potentiating it at physiological concentrations or by directly activating N-methyl-D-aspartic acid (NMDA) receptors, α-amino-3-hydroxy-5 methylisoxazolepropionic acid (AMPA) receptors and kainate (KA) receptors at high concentrations (Ault et al. 1987; Henzi et al. 1992; Martin et al. 1992).

Glutamate-receptors are classified into two groups: ionotropic glutamate-receptors, which are ligand-gated ion channels, and metabotropic glutamate-receptors that work through a signaling cascade, which involves G proteins (Nakanishi 1992). Ionotropic glutamate-receptors can be further divided into three major subtype families as a result of their ability to bind specific chemicals more selectively than glutamate, their native ligand (Watkins and Evans 1981). Therefore, glutamate-receptors are rationed into NMDA-, AMPA- and KA-receptors.

Functional NMDA-receptors are heteromeric complexes that consist of two obligatory NR1 subunits and two identical or different NR2 (NR2A, NR2B, NR2C and NR2D) subunits and possibly the NR3A subunit (Dingledine et al. 1999). AMPA-receptors are tetramers made up of four subunits, GluR1-GluR4 (encoded by *Gria1-4*). Kainate-receptors as well form tetrameric complexes built of one dimer out of GluR5-GluR7 (*Grik1-Grik3*) subunits and one dimer of KA1 (*Grik4*) or KA2 (*Grik5*), which is the main KA-receptor subunit expressed all over the brain (Ozawa et al. 1998).

The class of the ionotropic glutamate-receptors conveys most excitatory neurotransmission in the mammalian CNS (Dingledine et al. 1999). Most ionotropic AMPA- and KA-receptors allow, upon activation through glutamate, Na^+-entry but little Ca^{2+}-influx into the neuronal cells. In contrast, NMDA-receptors allow the slipping of Na^+ and Ca^{2+} (Dingledine et al. 1999). Furthermore, NMDA-receptors require an additional stimulus to become activated together with glutamate-binding, like depolarization by a previously

activated AMPA-receptor (Angulo et al. 1999). Therefore, NMDA-receptors act as "coincidence detectors" (Tsien et al. 1996) that contribute to Ca^{2+} mediated synaptic plasticity, which is suggested to be important for learning and memory formation (Clayton and Browning 2001).

Rapid excitatory neurotransmission is only mediated by ionotropic glutamate-receptors (Collingridge and Lester 1989). AMPA-receptors contribute to the fast component of the rapid excitatory postsynaptic currents (time to peak 200 μs or less, decay time 1-3 ms) whereas the slower component of the rapid excitatory postsynaptic currents (time to peak 10 ms or less, decay time 100 ms or more) is mediated by NMDA-receptor channels (Sprengel and Single 1999). Moreover, presynaptically localized KA-receptors can act as conditional amplifiers of preexisting glutamatergic neurotransmission by facilitating subsequent transmitter release (Lerma 2006). These presynaptic KA-receptors regulate transmitter release at both inhibitory and excitatory synapses (Rodriguez-Moreno et al. 1997; Kamiya and Ozawa 2000), thus modulating neuronal network activity throughout the CNS.

1.6   An Overview about Knockout Mice

Evans, Kaufman and Martin (Evans and Kaufman 1981; Martin 1981) were the first to report the isolation and culture of murine pluripotent embryonic stem cells, thus becoming pioneers for the generation of genetically engineered animals. Arise of this technology to manipulate genomes of mammalian model organisms by mutating a selected gene (Shastry 1994) is an effective and powerful method to investigate functions of the encoded protein(s) *in vivo*. By this technology, manipulated artificial DNA acquires the opportunity to recombine with the genome of ES cells and thereby knocks out a user-defined DNA locus. This technique facilitates to relate a particular gene directly with a particular behavior. Moreover, the phenotypically screening of knockout mice can help to delineate valuable new targets for pharmaceutical development. An advantage of knockout animals is that they can be used as "filters" for the physiological significance of potentially new drug targets when their deletion in the mouse modulates mammalian physiology in a therapeutically relevant manner (Zambrowicz and Sands 2003).

1.7   Intention of this Work

Taken together all the given information, little is known about the particular role that L-proline and the high affinity transport of L-proline by PROT play in neurotransmission. In order to uncover the *in vivo* role of PROT, it is the goal of this doctoral thesis to generate mice that lack the expression of a functional PROT-protein. Initially, the recombinant mouse strain should be analyzed in order to evaluate whether deletion of PROT has effects on brain morphology and to examine the contribution of PROT on L-proline uptake. Moreover, as described above, it is known that PROT is localized primarily at glutamatergic synapses (Nadler et al. 1992). Thus, it should be investigated if PROT-deficient animals display changes in the expression of specific components of glutamatergic neurotransmission. Existing association studies observe a relationship of L-proline levels in CNS with some diseases, including prevalent ones like schizophrenia (Clelland et al. 2011; Jacquet et al. 2002; Willis et al. 2008). Hence, PROT$^{-/-}$ mice should be consequently investigated to identify potential behavioral alterations within nociception, as it has previously been proposed that L-proline might play a role in analgesia (Fremeau et al. 1996; Galli et al. 1999). Since it has been reported that animals possessing reduced proline oxidase activity and high plasma L-proline levels exhibit sluggish behavior (Kanwar et al. 1975; Hayward et al. 1993) as well as altered locomotor activity (Paterlini et al. 2005), PROT$^{-/-}$ mice should be also analyzed in order to look for possible changes in their locomotor abilities. Furthermore, it would be of interest to investigate potentially modified prepulse inhibition in PROT-mutants, since abnormalities in sensorimotor gating have also been reported for proline dehydrogenase knockout mice (Gogos et al. 1999). In summary, via these investigations, it would be analyzed whether PROT-deficient animals exhibit CNS symptoms similar to those found in human metabolic diseases related to altered levels of L-proline.

2 Materials

Contact information of the listed manufacturers is given in the annex (9.3).

2.1 Enzymes and Molecular Weight Markers

Enzyme	Product Number	Manufacturer
Antarctic Phosphatase	M0289S	NEB
BamHI	R0136S	NEB
EcoRI	R0101S	NEB
GoTaq Flexi DNA Polymerase	M8305	Promega
HindIII	R0104S	NEB
KpnI	R0142S	NEB
NheI	R0131S	NEB
NotI	R0189S	NEB
1 kb DNA Ladder	N3232	NEB
100 bp DNA Ladder	N3231	NEB
Pfu DNA Polymerase	M7741	Promega
Proteinase K	82560	Fluka
Revertaid Reverse Transkriptase	EP0442	Fermentas
Ribolock RNase Inhibitor	EO0382	Fermentas
SpeI	R0133S	NEB
SYBR® Green JumpStart™ Taq ReadyMix™	S4438	Sigma
T4 DNA Ligase	M0202S	NEB
XbaI	R0145S	NEB
XhoI	R0146S	NEB

2.2 Antibodies

Antigen	Type	Species	Product Number	Manufacturer
Goat IgG	polyclonal	rabbit	NB710-H	Novus Biologicals
Gria2 / GluR2	polyclonal	rabbit	PAB9628	Biozol
Grik3 / GluR7	polyclonal	mouse	ABIN302159	antibodies-online
KA2 / Grik5	polyclonal	rabbit	06-315	Millipore™
Mouse IgG	polyclonal	goat	A 4416	Sigma
NR1	monoclonal	mouse	556308	BD Pharmingen™
NR2A	polyclonal	rabbit	4205	Cell Signaling
NR2B	polyclonal	rabbit	4207	Cell Signaling
PROT	polyclonal	rabbit	-	AG Milenz
PSD95	monoclonal	rabbit	04-1066	Millipore™
Rabbit IgG	polyclonal	goat	A 6154	Sigma
Tubulin	polyclonal	goat	3708-100	BioVision

2.3 Molecular and Cellular Biological Kits

Kit	Product Number	Manufacturer
QIAquick® Gel Extraction Kit	28706	QIAGEN GmbH
QIAprep® Spin Miniprep Kit	27106	QIAGEN GmbH
NucleoBond® Xtra Maxi	740414.50	Macherey-Nagel
G-50 Micro Column Kit	27-5335-01	Amersham
RNeasy® Micro Kit	74004	QIAGEN GmbH
InnuPREP DNA Mini Kit	845-KS-1040050	Analytik Jena
Random Primed DNA Labeling Kit	11004760001	Roche

2.4 Oligonucleotides

All oligonucleotide primers applied in this thesis were synthesized either by Promega or Invitrogen and reconstituted in UltraPure™ distilled water to obtain 100 μM stock solutions.

Name	Acc.-No	Primer Sequence [5´-3´]	bp
ProT Exon7S	NM_201353.1	TCT CTA GGA GTG GGC TTT GG	20
ProT Exon8AS	NM_201353.1	CTG AGA CAT GTA GCC CAG CA	20
b-Actin Forward	NM_007393.3	TGT TAC CAA CTG GGA CGA CA	20
b-Actin Reverse	NM_007393.3	GGG GTG TTG AAG GTC TCA AA	20
GAPDH Forward	NM_008084.2	ACC CAG AAG ACT GTG GAT GG	20
GAPDH Reverse	NM_008084.2	CAC ATT GGG GGT AGG AAC AC	20
neoS	XM_001387562.1	CAG CTC ATT CCT CCC ACT CAT GAT	24
WTAS	NM_201353.1	GCT ATC CCC CAT CTT GCC TG	20
WTSIII	NM_201353.1	AGA ACA TCT ACA GGT CAG TG	20
*PRODH-*Forward	NM_011172.2	AGC AGG ACC CGG CTC TCC AG	20
*PRODH-*Reverse	NM_011172.2	GGT CAG GCG GCT GAT GGC TG	20
Pycr1 Forward	NM_144795.3	AGC TAC GGT CTC GGC CCT CC	20
Pycr1 Reverse	NM_144795.3	GAT GGT GAC CCC TGC CGC AC	20
Gria1 Forward	NM_001113325.1	GGG AAT GTG AAG CA AGG ACT CCG	24
Gria1 Reverse	NM_001113325.1	CCG CTT CGA CTC GCT ACG GG	20
Gria3 Forward	NM_016886.3	ACA GCG CTG GGT GAG ACT GG	20
Gria3 Reverse	NM_016886.3	CTC CAG CAC TGC CTC TGC GG	20
Grin2A Forward	NM_008170.2	CAA CCA CCT CAG CAT TGT C	19
Grin2A Reverse	NM_008170.2	ACT TCT TCA CAT TCA TCC CTT C	22
PSD95 Forward	Q62108	ACA ACC AAG AAA TAC CGC TAC	21
PSD95 Reverse	Q62108	TCC TCA TAC TCC ATC TCC CC	20

Name	Acc.-No	Primer Sequence [5´-3´]	bp
SR Forward	NM_001163311	GCT GCT GAG CCC TCG AAT GCA	21
SR Reverse	NM_001163311	CTC CCC CAC ACC AGC TGG GT	20
DRD1 Forward	NM_010076	GGC CTG CCA GTG GAG AGG GA	20
DRD1 Reverse	NM_010076	ACC TTG GAC CGC AGG TGT CG	20
DRD2 Forward	NM_010077	GCT CAC CCT CCT CAT CTT TAT C	22
DRD2 Reverse	NM_010077	ATT TCC ACT CAC CCA CCA C	19
COMT Forward	NM_001111062	AAG ACC GCT ACC TTC CAG AC	20
COMT Reverse	NM_001111062	TAG ACT GCC TTC TCC AAG CC	20
TH Forward	NM_009377.1	TGA AGC CAA AAT CCA CCA C	19
TH Reverse	NM_009377.1	GAC ACT TAT CCA CT CTG ACA C	22
GlyT1 Forward	NM_008135	GTG GAT GAG GTA GGG AAT GAG	21
GlyT1 Reverse	NM_008135	GAG ATG ACA ACC AAG GAG AAG	21
ProT Forward	NM_201353.1	TCT TAA CCT CAG CAG CAC C	19
ProT Reverse	NM_201353.1	GAA ATA CAC CAC CTT GCC C	19
ProT Reverse	NM_201353.1	GAA ATA CAC CAC CTT GCC C	19
3´-PHext F.	NM_201353.1	GGG GAC TAA GTG GTG AAT GT	20
3´-PHext R.	NM_201353.1	TGT CCC TTC CTG CTT CCC AG	20
5´-probe Forward	NM_201353.1	TTT GGT ACC TGG CTT CTT CCC TC	24
5´-probe Reverse	NM_201353.1	TTA GAA TTC CAG ACA TTT CCC AAG CCC AC	29
Ex2 Forward	NM_201353.1	TTT GCG GCC GCT TTC CCT ACC GAG CCT AC	29
Ex6 Reverse	NM_201353.1	TTA CTC GAG GAT GAG GTA GGG AAA GGT	27
Ex8 Forward	NM_201353.1	CGC GGA TCC AGA CAC CTT CAT TGT CAC TC	29
Ex10 Reverse	NM_201353.1	TTA GAA TTC TCA TCA GTC ACT GCA GTC AC	29

2.5 Chemicals

Substance / Reagent	Product Number	Manufacturer
Agar	05040	Fluka
Agarose UltraPure	15510027	Invitrogen™
Albumin, bovine	A6003	Sigma
Ampicillin	K029.1	Roth
Ammonium Persulphate	A3678	Sigma
Bromophenol blue	18030	Fluka
Calcium chloride, dihydrate	21097	Fluka
DMSO	A1584	AppliChem
D-glucose	G7021	Merck
Ethylendiamine tetra acetic acid (EDTA)	CN06.3	Roth
Ethanol absolute	08-205	KMF
Ethidiumbromide	2218.1	Roth
Enhanced Chemoluminescence Reagent	RPN2132	GE Healthcare
Gelatine	G2500	Sigma
Glycine	11016	Grüssing
Glucose	G7021	Merck
Glycerol	11052	Grüssing
HEPES (4-(2-hydroxyethyl)-1-piperazineethanesulfonic acid)	54457	Fluka
Hydrochloric acid	08-721	KMF
Kaleidoscope Marker	161-0324	Bio-Rad
MagicMark XP Protein Standard	LC5602	Invitrogen
Magnesium chloride	63072	Fluka
Magnesium Sulfate	0261.1	Roth
Methanol	20847.307	VWR International

Substance / Reagent	Product Number	Manufacturer
NuPage Antioxidant	NP0005	Invitrogen
NuPage Sample Buffer	NP0007	Invitrogen
NuPage Sample Reducing Agent	NP0004	Invitrogen
NuPage Transfer Buffer	NP0006-1	Invitrogen
Potassium acetate	1.04820.1000	Merck
Potassium chloride	12008	Grüssing
Potassium dihydrogen phosphate	1.04873.5000	Merck
Propan-2-ol	P-7507-15	Fisher Scientific
Roti-Block	A151.2	Roth
Rotiphorese Gel 40 (19:1)	A515.1	Roth
Rubidium chloride	R-2252	Sigma
Sodium acetate anhydrous	4555	Applichem
Sodium chloride	12123	Grüssing
Sodium dodecyl sulfate	CN30.0	Roth
Di-sodium hydrogen phosphate	71640	Fluka
Sodium hydroxide	12156	Grüssing
Sucrose	84105	Fluka
Sulfuric acid	00731.2511	Merck
Tetramethylethylenediamine	T9281	Sigma
Tris	A2264	AppliChem
Tris-HCl	90.90.3	Roth
Triton X-100	93420	Fluka
Tryptone	A1553	AppliChem
Tween 20	P1379	Sigma
Yeast extract	2363.3	Roth
β-Mercaptoethanol	31350	Invitrogen

2.6   Solutions and Buffers for Molecular Biology

If not indicated differentially, all buffers and solutions were prepared with purified demineralized (dH_2O) water.

Lysis buffer (for DNA isolation from murine stem cells)

Constituent	Amount	Final Concentration
1 M Tris-HCl	10 ml	0.1 M
0.25 M EDTA	2 ml	0.025 M
10% SDS	2 ml	1%
1 M NaCl	20 ml	0.1 M

Chemicals were dissolved in 100 ml dH_2O, pH adjusted to 7.2 with NaOH, and afterwards the solution was sterilized via sterile filtration and stored as 10 ml aliquots at -20°C.

Phosphate buffered saline (1X PBS)

Constituent	Amount	Final Concentration
KCl	0.2 g	2.7 mM
KH_2PO_4	0.2 g	1.76 mM
NaCl	8.0 g	137 mM
Na_2HPO_4	2.88 g	10.0 mM

Chemicals were dissolved in 1000 ml dH_2O, pH adjusted to 7.4 with HCl, and the solution was sterilized by autoclaving.

3 M Sodium acetate (for precipitation of linearized plasmid DNA)

Constituent	Amount	Final Concentration
Sodium acetate anhydrous	2.46 g	3 M

Sodium acetate was dissolved to a final volume of 10 ml with dH_2O, the pH was adjusted up to 5.1 with glacial acetic acid and the solution was sterilized via sterile filtration.

DNA Loading Buffer

Constituent	Amount	Final Concentration
Bromophenol blue	25 mg	0.25%
Xylene cyanol	25 mg	0.25%
Sucrose	4 g	4%

Tris-Acetate-EDTA (50X TAE-buffer)

Constituent	Amount	Final Concentration
Tris	242 g	2 M
Glacial acetic acid	57.1 ml	5.71%
0.5 M EDTA (pH 8.0)	100 ml	0.05 M

Chemicals were dissolved in 1000ml dH$_2$O.

TE-Buffer

Constituent	Amount	Final Concentration
1M Tris	1 ml	10 mM
0.5 M EDTA (pH 7.4)	0.2 ml	1 nM

2.7   Solutions and Buffer for Southern-Blotting

Depurination-Solution

Constituent	Amount	Final Concentration
HCl	-	250 mM

Denaturation-Solution

Constituent	Amount	Final Concentration
NaOH	19.99 g	500 mM
NaCl	87.66 g	1.5 M

Neutralisation-Solution

Constituent	Amount	Final Concentration
Tris/HCl	60.57 g	500 mM
NaCl	87.66 g	1.5 M

20x SSC

Constituent	Amount	Final Concentration
Na-citrat dihydrate	88.23 g	300 mM
NaCl	175.32 g	3 M

Maleic Acid-Buffer

Constituent	Amount	Final Concentration
Maleic acid	11.6 g	100 mM
NaCl	8.76 g	150 mM

10x Blocking Solution

Constituent	Amount	Final Concentration
Blocking reagent	10 g	10%
Maleic acid buffer	90 ml	-

Solution was autoclaved at 121°C for 20 min.

Hybridization Buffer

Constituent	Amount	Final Concentration
20x SSC	25 ml	25%
10x Blocking solution	10 ml	10%
SDS	0.2 g	0.2%
N-lauroylsarcosine	1 g	1%

Washing Buffer

Constituent	Amount	Final Concentration
Maleic acid buffer	997 ml	-
Tween 20	3 ml	0.3%

2.8   Chemicals, Solutions and Media for Cell Culture

Media & Additives	Product Number	Manufacturer
Dulbecco's Modified Eagle Medium (DMEM)	41965	Gibco/Invitrogen™
ES Cell Qualified Fetal Bovine Serum (Mexiko)	10439024	Gibco/Invitrogen™
ESGRO® (10^7 Units) = leukemia inhibitory factor (LIF)	ESG1107	Chemicon®
FIAU (1-(2-Deoxy-2-fluoro-ß-D-arabinofuranosyl)-5-iodouracil)	M251	Moravek Biochemicals
G418, liquid (Geneticin)	Ant-gn-5	InvivoGen
Hank's balanced salt solution (HBSS)	14025050	Gibco/Invitrogen™
L-Glutamine, 200 mM, liquid	25030	Gibco/Invitrogen™
2-Mercaptoethanol, 50 mM	31350010	Gibco/Invitrogen™
Minimum Essential Medium (MEM)	31095029	Gibco/Invitrogen™
MEM Non Essential Amino Acids Solution	11140035	Gibco/Invitrogen™
Penicillin-Streptomycin solution	15140130	Gibco/Invitrogen™
Sodium Pyruvate, 100 mM, liquid	11360	Gibco/Invitrogen™
Trypsin / EDTA (0.05%/0.02%)	P10-02318P	PAN™ Biotech GmbH
Trypsin, 0.25% (1x) with EDTA 4Na, liquid	25200	Gibco/Invitrogen™
UltraPure™ Distilled water	10977	Gibco/Invitrogen™

ES Cell Medium

Constituent	Volume [ml]	Final Concentration
Dulbecco's Modified Eagle Medium (DMEM)	500	-
Fetal Bovine Serum (ES Cell approved)	56	10%
L-Glutamine, (200 mM)	5.6	2 mM
Penicillin-Streptomycin	5.6	0.6%
Sodium pyruvate (100 mM)	5.6	2 mM
Non-Essential Amino Acids	5.6	0.1 mM
2-Mercaptoethanol, (50 mM)	1.1	0.1 mM
ESGRO® (10^7units/ml)	0.05	1000 units/ml

ES Cell Selection Medium

Constituent	Volume [ml]	Final Concentration
Dulbecco's Modified Eagle Medium (DMEM)	500	-
Fetal Bovine Serum (ES Cell approved)	56	10%
FIAU	0.5	0.2 μM
G418	4	600 μg/ml
L-Glutamine, (200 mM)	5.6	2 mM
Penicillin-Streptomycin	5.6	0.6%
Sodium pyruvate (100 mM)	5.6	2 mM
Non-Essential Amino Acids	5.6	0.1 mM
2-Mercaptoethanol, (50 mM)	1.1	0.1 mM
ESGRO® (10^7units/ml)	0.05	1000 units/ml

ES Cell Freezing Medium (2x)

Constituent	Volume [ml]	Final Concentration
Dulbecco's Modified Eagle Medium (DMEM)	50	-
Fetal Bovine Serum (ES Cell approved)	40	40%
DMSO	10	10%

Fibroblast Medium

Constituent	Volume [ml]	Final Concentration
Dulbecco's Modified Eagle Medium (DMEM)	500	-
Fetal Bovine Serum	56	10%
L-Glutamine, (200 mM)	5.6	2 mM
Sodium pyruvate (100 mM)	5.6	2 mM
Penicillin-Streptomycin	5.6	0.6%

Gelatin Solution (for ES Cell Cultivation)

Constituent	Amount	Final Concentration
Gelatin	2.0 g	1%
UltraPure™ Distilled Water	Ad 200 ml	-

Gelatin was dissolved in cell culture grade water (UltraPure™ Distilled water), autoclaved twice (second time on the following day) and stored at 4-8°C. For usage a working dilution (0.1% in UltraPure™ Distilled Water) was prepared.

FIAU (1-(2-Deoxy-2-fluoro-ß-D-arabinofuranosyl)-5-iodouracil, 0.2 mM)

Constituent	Amount	Final Concentration
FIAU	1.0 mg	0.2 mM
UltraPure™ Distilled water	Ad 13.4 ml	-

FIAU solution was always sterilized by filtration, divided in aliquots (500 µl) and stored at -20°C.

10X HBS (ES cell electroporation)

Constituent	Amount	Final Concentration
D-Glucose	2.0 g	1%
HEPES	10.0 g	20 mM
KCl	0.74 g	50 mM
NaCl	16 g	280 mM
Na_2HPO_4	0.252 g	1.5 mM
UltraPure™ Distilled water	Ad 200 ml	-

Chemicals were dissolved in water; the pH was adjusted to 7.2 and solution was sterilized via sterile filtration.

2.9   Media and Solutions for Bacteria Culture

Rubidium Chloride Solution 1

Constituent	Amount	Final Concentration
KAc	0.088 g	30 mM
$MnCl_2$ (x 4 H_2O)	0.297 g	50 mM
RbCl	0.363 g	100 mM
$CaCl_2$ (x 2 H_2O)	0.044 g	10 mM
Glycerol	4.5 ml	15%

Chemicals were dissolved in 4.5 ml water; the pH was adjusted to 5.8 with HCl and solution sterilized via sterile filtration.

Rubidium Chloride Solution 2

Constituent	Amount	Final Concentration
RbCl	0.012 g	10 mM
$CaCl_2$ (x 2 H_2O)	0.110 g	75 mM
MOPS	0.021 g	10 mM
Glycerol	1.5 ml	15.0%
dH_2O	ad 10 ml	-

Chemicals were dissolved in 10 ml water, the pH was adjusted to 6.8 with HCl and the solution was sterilized via sterile filtration.

Super Optimal Broth (SOB Medium)

Constituent	Amount	Final Concentration
Tryptone	6.0 g	2.0%
Yeast extract	1.5 g	0.5%
NaCl	0.175 g	10 mM
KCl	0.055 g	2.5 mM
1 M $MgCl_2$	3.0 ml	10 mM
1 M $MgSO_4$	3.0 ml	10 mM

All constituents were dissolved in Milli-Q water up to a final volume of 300 ml and sterilized by autoclaving. $MgCl_2$ and Mg_2SO_4 solutions were added directly before usage.

LB Agar

Constituent	Amount	Final Concentration
Agar	15 g	1.5%
NaCl	10 g	1%
Tryptone	10 g	1%
Yeast extract	5 g	0.5%

Constituents were dissolved in Milli-Q water up to a final volume of 1000 ml, and the pH was adjusted to 7.5 with NaOH. The solution was heated to dissolve the agar and sterilized by autoclaving.

LB Medium

Constituent	Amount	Final Concentration
NaCl	10 g	1%
Tryptone	10 g	1%
Yeast extract	5 g	0.5%

Constituents were dissolved in Milli-Q water up to a final volume of 1000 ml, the pH was adjusted to 7.4 with NaOH, and the solution was sterilized by autoclaving.

2.10   Water Purification

All solutions were prepared with purified demineralized (dH_2O) water obtained from a Milli-Q® Water System (Millipore, Eschborn) or with sterile UltraPure™ Distilled Water (Gibco/Invitrogen™).

2.11   Sterilization Method

For molecular and cellular biological experiments all heat stable materials, equipments, solutions and media were autoclaved in a Varioklav® (H+P Labortechnik AG, Oberschleißheim) at 121°C and 1.2 bar for 21 min. Sterilization of heat sensitive solutions and buffers was accomplished by the use of sterile filters (pore wide 0.2 μm).

2.12   Plasmids, Bacterial Strains and Cell-Lines

XpPNT: Targeting vector for the mutation of the murine *ProT* gene locus. The XpPNT-vector is described in detail (9.1) and pictured in the annex (**Figure 41**). It was kindly provided by Prof. Dr. Jesús Gomeza.

pBS: pBluscript II KS (+/-) vector was used for the amplification of parts of the *ProT* gene. This vector (2961 bp) consists of an origin of replication in *E.coli,* a multiple cloning site (MCS), and an ampicillin resistance gene (amp).

XL1-Blue: This *E.coli* strain obtained from Agilent Technologies (200249) was used for the amplification of recombinant plasmids.

HM1: This embryonic stem cell line was derived from mice strain Ola/SV129. These cells were kindly provided by Prof. Dr. Volkmar Gieselmann (Institute of Physiological Chemistry, University of Bonn) (Magin et al. 1992).

2.13   Consumables

Consumables	Product Number	Manufacturer
Cell culture flasks	430168 / 430729 / 431079	Corning
Centrifuge tubes	430791 / 430829	Corning
Combitips plus	0030 069. 447/455/463/390	Eppendorf
Costar® 6 / 12 / 24 well plates	3506 / 3512 / 3527 / 3548	Corning
Cryogenic vials	5000-1020	Nalgene®
Culture dishes	430166 / 430167	Corning
Disposable filter unit 0.2 µl	FB30/0.2 CA-s	Whatman®
ELISA microplate (96 well)	9017	Corning
Filter tips SSNC	B95012 / B95020 / B 90222 / B95210	Bioplastics BV
Gene Pulser® cuvette	165-2088	Bio-Rad
Incubation tubes	294718727	Labomedic
1.5 ml	115105	Labomedic
2.0 ml	115106	Labomedic
Nitrocellulose membranes	RPN203E	GE Healthcare
Parafilm™	1447011	Labomedic
Pasteur pipettes, glass	447016	Labomedic
Pasteur pipettes, PP, sterile	297804239	Labomedic
PCR tubes	0030 124.332	Eppendorf
Oxygen crystal tips 10 µl	110727	Labomedic
Whatman paper	GB005	Biometra

Consumables	Product Number	Manufacturer
Yellow 200 µl tips	70.760.002	Sarstedt
Blue 1000 µl tips	686290	Greiner bio-one
Stripette® serological pipettes	4486 – 4490	Corning

2.14 Laboratory Instruments and Equipment

Type	Format	Manufacturer
Autoclave	Varioklav®	H&P Labortechnik
Balance	TE64	Sartorius
Balance	TE6101	Sartorius
Balance	BL310	Sartorius
Camera	CoolSNAPHQ^2	Roper Scientific
Centrifuge	MiniSpin	Eppendorf
Centrifuge	Galaxy Mini	VWR
Centrifuge	Centrifuge 5810	Eppendorf
CO_2 incubator	Heraeus®HERAcell® 240	Thermo Fisher Scientific
Counting chamber	Fuchs-Rosenthal	Labomedic
Dry block heater	Thermomixer® comfort	Eppendorf
Dry block heater	QBT2	Grant Instruments
Electronic pipet filler	Easypet®	Eppendorf
Electrophoresis chamber	Mini-Sub® cell GT	Bio-Rad
Electrophoresis chamber	Wide Mini-Sub® cell GT	Bio-Rad
Freezer (-80°C)	Heraeus®Herafreeze®	Thermo Fisher Scientific
Freezer (liquid nitrogen)	MVE 815P-190	Chart BioMedical Ltd.
Microplate reader	Sunrise-Basic Tecan	Tecan Austria GmbH
Microscope	CKX31SF	Olympus
Microscope	Leica DM IL LED Fluo	Leica
Microwave	Intello Wave	LG
PCR cycler	GeneAmp® PCR System 9700	Applied Biosystems
PCR cycler	2720 Thermal Cycler	Applied Biosystems
qPCR cycler	Realplex2 S	Eppendorf
pH-meter	SevenEasy™	Mettler Toledo

Type	Format	Manufacturer
Photo documentation system	De Vision DBOX	Decon Sience Tec
Pipettes	0.5-10 µl; 10-100 µl; 100-1000 µl	Eppendorf
Power supplie	PowerPac HC™	Bio-Rad
Safety cabinet	HeraSafe HS12	Thermo Electron
Shaking water bath	Herlev	Buch& Holm
Sponge Pad	Sponge	Invitrogen™
UV/VIS spectrophotometer	SmartSpec™ Plus	Bio-Rad
Vacuum pump system	AP 15	HLC BioTech
Vortex	Milli-Q® Water System	Millipore
Water purification system	Reax Top	Heidolph
Infrared-tracking system	Actimot	TSE Systems
Liquid scintillation counter	Wallac 1409	Wallac
Detection system	DeVision DBOX	Decon Science Tec
Blotting module	XCell II Blot Module	Invitrogen™
Blotting chamber	XCell SureLock™ Mini-Cell	Invitrogen™

2.15 Software

Name	Company
Actimot	TSE Systems
Citavi v3.0	Swiss Academic
DeVision G v1.0	Decon Science Tec GmbH
Gel Pro Analyzer	Media Cybernetics
Gel Scan Software	BioSciTec
Office Excel 2007	Microsoft® Corporation
Office PowerPoint®	Microsoft® Corporation
Office Word 2007	Microsoft® Corporation
Prism® 4.02	GraphPad Software
Symyx® Draw 3.3	Symyx Solutions, Inc.
Vector NTI 8	Invitrogen™
Quantity One	Bio-Rad
XFluor4	Microsoft® Corporation/Tecan sunrise

3   Methods

3.1   Cell Culture Methods

3.1.1   Cultivation of Cells

All cells were cultivated at 37°C in an incubator with 5% CO_2 and humid atmosphere (96% humidity). Every operation was carried out under aseptic conditions in safety cabinets with laminar air flow. HM1-embryonic stem (ES) cells, which derive from Ola/SV129 mice strain (Magin et al. 1992), were kindly provided by Prof. Dr. Volkmar Gieselmann (Institute of Physiological Chemistry, University of Bonn). These cells where cultured on monolayers of mitotically inactivated mouse embryonic fibroblasts (MEF) as feeder cells. ES cells were passaged three times a week, splitted at a ratio of 1:3 to 1:10, depending on their growth rate, to reach approximately 70% confluence. For trypsinization growth medium was removed from the flask and cells were washed with pre-warmed PBS (2.8). Afterwards, cells were incubated with ES cell trypsin at 37°C for up to 3 min until cells were detached. Trypsinization was stopped by adding ES cell medium (2.8). After trypsinization, cells were dispensed on fresh feeder plates, which had been prepared in advance. Medium exchange was performed daily.

3.1.2   Generation of Embryonic Mouse Fibroblasts (Feeder Cells)

Mouse Embryonic Fibroblast (MEF) were derived from mouse embryos carrying a neomycin resistance gene and required to support the growth of undifferentiated ES cells by releasing cytokines such as LIF to the culture media. These cells were kindly provided by Dr. Jesús Gomeza (Institut für Pharmazeutische Biologie, AK Kostenis, University of Bonn).

3.1.2.1 Gamma Ray Treatment of Embryonic Mouse Fibroblasts

Feeder layer fibroblasts need to be mitotically inactive in order to seed a monolayer with a defined cell number. Therefore, cells were treated by irradiation to stop mitosis, while maintaining the ability to secrete growth factors. The irradiation was performed by Dr. Stefan Garbe (Radiology, University Medical Center of Bonn) by treating the fibroblasts with gamma rays (96 Gray for 5 min). The same day feeder cells became cryopreserved (3.1.3). Usually, one day before ES cell plating was conducted, cell culture dishes were gelatinized with 10 ml of a gelatin working solution (0.1%) and incubated for 10 min. After aspiration of gelatin solution, a calculated amount of feeder cells was seeded on these plates, which were used for up to four days.

3.1.3   Cryopreservation and Re-Cultivation of Cell Lines

In order to prepare permanent cell line stocks, cells were frozen at − 80°C, and after 1–2 days they were transferred into liquid nitrogen (-180°C) for long-term storage. For this purpose, cells were trypsinized, dispersed in freezing medium (+20% FCS and 10% DMSO), and stored in cryotubes. For thawing cells after long-term storage, they were unfrozen rapidly in a 37°C water bath, diluted in medium, and after resuspension spun down at 800 g (4 min). Afterwards, the supernatant was discarded in order to remove DMSO, and cells were resuspended in fresh medium before being transferred to cell culture flasks or dishes.

3.1.4   Electroporation of Murine Embryonic Stem Cells

For electroporation, a culture of densely grown early-passage ES cells ($55cm^2$ cell culture dishes) was used. The medium was changed 1–2 hours before harvesting the cells. ES cells were trypsinized, and centrifuged twice (4 min, 800 rpm) in order to reduce the amount of feeder cells. After final resuspension in 10 ml of fresh ES medium, the cell number was determined in a hemacytometer in order to utilize ~$10\text{-}20x10^6$ ES cells per electroporation. The appropriate amount was again spun down and resuspended in 980 µl of electroporation buffer (1x HBS). This suspension and 20 µl of the linearized targeting DNA construct (2 µg/µl) were transferred to an electroporation cuvette (0.4 cm) and incubated for 5 min (RT). Electroporation was carried out with one pulse of 230 V and 500 µF with a time constant of 118 ms. The short high voltage pulse of the electroporator disturbs the membrane potential with subsequent formation of pores across the membranes to allow incorporation of the DNA (Sukharev et al. 1992). After a further 10 min, cells were resuspended in an appropriate volume of ES medium ($1\text{-}2x10^6$ cells per 10 ml per 55 cm^2) and transfered to feeder cell covered plates.

Selection of cells harboring the desired construct was initiated 24 hours later by first switching to selection medium containing G418 (600 µg/ml), and from the following day on G418 (600 µg/ml) as well as FIAU (0.2 µM) were used. Whereas the neomycin analog G418 serves for the maintenance of cells with stably integrated *neo* resistance gene of the targeting construct, FIAU selects for cells that do not exhibit an integration of the *HSV-TK* gene. Medium was changed daily over a selection time of 9 days. Thereafter, single colonies appearing on the plates were isolated. For this purpose, selection medium was replaced by prewarmed PBS, and cell clones were picked by use of a 200 µl pipette already containing 100 µl ES cell trypsin/EDTA. The suspensions were transferred into 24-well plates. After trypsinization, cells were singularized by pipetting, dispersed in 1 ml of

ES cell medium, and transferred into new 24-well cell culture dishes, already coated with monolayers of feeder cells. After 24 hours, medium was renewed, and cells were grown until they reached a confluence of approximately 80-90%. For storage, two-thirds of these cells were cryopreserved. The remaining cells were kept in culture until they reached full confluence to obtain highest rates of DNA yields.

3.2 Methods in Molecular Biology

3.2.1 Transformation of Chemical Competent Bacteria

Transformation of bacteria with plasmid DNA was performed in order to increase plasmid amount in relation to the genomic DNA. This was achieved by chemical pretreatment with rubidium chloride and a subsequent heat shock.

3.2.1.1 Preparation of Rubidium Chloride Competent E.coli Cells

An initial culture was prepared by inoculating 5 ml of SOB medium with 5 µl of XL-1 blue bacteria. The suspensions were grown over-night at 37°C and 220 rpm. The next day, 100 ml of SOB medium were inoculated with 1 ml of the over-night culture and grown at 37 C° and 220 rpm until the OD_{550} reached 0.5. Afterwards, cells were put on ice for 10 min and subsequently pelleted at 2800 g for 10 min in pre-cooled tubes at 4 C°. Thereafter, the supernatants were removed, and the bacteria pellets were resuspended in 25 ml of ice-cold rubidium chloride solution 1 (2.9). The suspension was incubated on ice for 10 min followed by centrifugation at 2800 g (4°C). Finally, bacteria became resuspended again in 8 ml of rubidium chloride solution 2 (2.9), were aliquoted, immediately frozen in liquid nitrogen, and stored at -80°C until usage.

3.2.1.2 Transformation by Heat Shock

For the transformation procedure, aliquots (100 µl) of rubidium chloride competent bacteria were thawed on ice, and after unfreezing an appropriate amount of plasmid DNA (~0.05-100 µg) was added and mixed by pipetting up and down. This solution of XL1-blue bacteria was incubated 30 min on ice, followed by a 30 seconds heat-shock at 42°C in a block heater. After the heat-shock, the suspension was placed on ice again and incubated for a further 2 min. Thereafter, 300 µl of SOC medium were added, and suspension was incubated at 37°C and 220 rpm for 60 min (allowing formation of antibiotic resistance encoded on the plasmid DNA). After that, the bacteria suspensions were distributed (50-200 µl) on prewarmed LB agar plates containing the appropriate selective antibiotic (usually ampicillin), and incubated over-night at 37°C.

3.2.2   Isolation of Plasmid DNA

Plasmid DNA was isolated according to the required amount of DNA using special commercial available kits QIAprep® Spin Miniprep Kit or NucleoBond® Xtra Maxi as recommended by the manufacturer.

3.2.3   Isolation of Genomic DNA

To isolate genomic DNA from mouse tail biopsies, a commercially available kit was used (InnuPREP DNA Mini Kit).

For isolation of genomic DNA from ES cells cultured in 24-well cell culture dishes the following protocol was applied. After the medium was aspirated, cells were incubated in 300 μl of lysis buffer (10 mM Tris-HCl pH 8.0, 5 mM EDTA, 0.2 % SDS, 200 mM NaCl) at 55°C with agitation (600 rpm), for two hours up to over-night. Afterwards, a centrifugation step was carried out to pellet the non-soluble material. The DNA of the supernatant was purified via ethanol and NaCl ion precipitation. Therefore, 150 μl of saturated NaCl-solution and 900 μl of absolute ethanol were added, and the resulting DNA-filaments were transferred into reaction tubes, prefilled with 500 μl of 70% ethanol. Subsequent, DNA was spun down (12000 rpm for 5 min), the pellet was air-dried, and dissolved in 100 μl of UltraPure™ distilled water or TE-buffer.

3.2.4   Cryoconservation of Bacterial Strains

In order to prepare permanent stocks of bacterial strains containing favored plasmids and thereby saving retransformation, the respective bacteria were cryopreserved. This was done by addition of 200 μl glycerol to 800 μl of the respective bacterial suspension and subsequent storage at -80°C.

3.2.5   Ethanol Precipitation

Ethanol precipitation was performed in order to concentrate nucleic acids, or to transfer them into a new set of buffer and salts. The (cleaved) DNA was well mixed with 1/10 volume of sterile 3 M sodium acetate (pH 5.1) and with 2 volumes of absolute ethanol. Afterwards, the DNA was pelleted for 5 min at 13000 rpm. After decantation of the supernatant, the pellet was washed with 500 μl of 70% ethanol and spun down once more for 5 min at 13000 rpm. The supernatant was discarded and after the DNA pellet was air-dried, it was dissolved in the desired amount of buffer (e.g. TE buffer) or UltraPure™ distilled water.

3.2.6 Determination of Nucleic Acid Concentration

The concentration of nucleic acids was determined photometrically by measurement of the absorption at a wavelength of 260 nm. To calculate nucleic acid concentrations (µg/ml), the following formula was used:

$$C \; [\mu g/\, mL] = A_{260} \; x \; D \; x \; F$$

c	concentration
A_{260}	Absorption at 260 nm
D	Dilution factor
F	Multiplication factor (for DNA 50)

1 absorbance corresponds to 50µg DNA per ml water

The quotient of A_{260}/A_{280} is a determinant of the purity and should range between 1.6 and 2.0 (in water) so as to protein impurities can be disregarded.

3.2.7 Agarose Gel Electrophoresis

For agarose gel electrophoresis varying concentrations of agarose (0.5-1.5% agarose) were diluted in 100 ml of electrophoresis buffer (1xTAE, pH 8; 2.6) and boiled to form a matrix. After cooling down, ethidium bromide (0.5 µg/ml) was added to the solution to enable visualization of the separated DNA fragments by fluorescence in UV light (302 nm). Electrophoresis was carried out at 20-120 V. For determination of the size of the applied fragments, a DNA size marker was always loaded in parallel. Prior to loading, the samples were always supplemented with loading buffer (2.6).

3.2.8 Purification of DNA-Fragments

DNA-fragments were purified using a commercial Gel Extraction-Kit (Qiagen) following the manufacturer's instructions. For that purpose, a gel slice containing the DNA fragment of interest was cut off and solubilized by mixing it with the appropriate buffer and thermal heating. Afterwards, the solution was applied to a spin column where the DNA binds to the silica gel membrane and impurities were washed away. Finally, the pure DNA was eluted in 30 µl of UltraPure™ distilled water or TE-buffer.

3.2.9 Restriction Endonuclease Cleavage of DNA

Sequence-dependent cleavage of DNA was carried out using commercially available restriction endonucleases and the appropriate buffers (and if needed BSA) at the required temperature. Restriction of DNA was performed for analytical purpose (e.g. identification of plasmid or a targeting event in genomic DNA) or for preparative purpose (e.g. isolation of a fragment for cloning). For analytical purposes up to 1 µg of plasmid DNA was cleaved

with one or more restriction enzymes (1-10 units each) in a volume of 10-20 μl for at least one hour. For preparative purposes vector DNA and/or PCR products were cut with similar restriction enzymes to obtain compatible, sticky ends.

3.2.10   Dephosphorylation of Cleaved Vector DNA

Antarctic Phosphatase was used to catalyze the removal of 5′phosphate groups from restriction enzyme cleaved products of vector DNA prior to ligation reactions. The cleaved vector DNA was incubated in a mixture of 1 x Antarctic Phosphatase reaction buffer and 5 U of Antarctic Phosphatase at 37°C for 15 min. Afterwards, the enzyme was heat-inactivated at 65°C for 5 minutes.

3.2.11   Ligation of DNA Fragments

DNA ligase of the phage T4 was used to catalyze the formation of phosphodiester bonds between 5'-phosphate and 3'-hydroxyl termini for ligation reactions. For this purpose, fragments with sticky ends of digested and dephosphorylated vector DNA (50-500 ng) and the respective insert DNA were mixed in a molecular ratio of 1:5 (vector to insert). This reaction mixture was supplemented with ligation buffer; UltraPure™ distilled water and 2 U of T4 DNA Ligase to a total volume of 10 μl and incubated over-night at 16°C.

3.2.12   Sequencing of Cloned DNA Constructs

Sequencing reactions were conducted by GATC Biotech AG (Konstanz). Thus, the correct sequence and especially the absence of point mutations (in PCR products) were ensured.

3.2.13   RNA-Isolation

After tissue sample preparation (3.3.2), RNA was isolated either by the RNeasy® Micro Kit (Qiagen) or through the following protocol: Tissue (~50 mg) was homogenized (20 strokes) in 800 μl of denaturating solution (4 M guanidinium-thiocyanate, 25 mM sodium citrate, 0.5% sarcosyl, and 0.1 M 2-mercaptoethanol in RNase-free water, autoclaved, pH 7.0) on ice. Subsequently, 80 μl of sodium acetate (2 M, pH 4.1), 800 μl of Phenol (water saturated) as well as 160 μl of a chloroform-isoamylalcohol mixture (49:1) were added to the homogenates, mixed well, and samples were incubated 15 min on ice before centrifugation (20 min, 13000 rpm, 4°C). The upper aqueous phase was mixed with one volume of isopropanol in a new cap, spun down shortly and incubated at -20°C for 1 h to over-night to precipitate the RNA.

Then, samples were centrifuged (20 min, 13000 rpm, 4°C), and the supernatants were discarded. Pellets were dissolved again in denaturating solution (300 μl) and mixed with one volume of isopropanol and incubated at -20°C for 1h to overnight. After a subsequent centrifugation step (20 min, 13000 rpm, 4°), the pellets became dissolved in 70% ethanol

spun down once more (20 min, 13000 rpm, 4°), and finally dissolved in 30 µl RNase free water.

3.2.14 Reverse Transcription

For the cDNA synthesis, Revert Aid reverse transcriptase (Fermentas) was incubated for 1 h at 37°C together with 200 ng of RNA, the RiboLock™ RNase Inhibitor (Fermentas) and 250 pmol of random hexamer primer (Invitrogen) in a final volume of 20 µl. "No-reverse transcriptase" controls were performed by omitting reverse transcription, and "no-template" controls were carried out by addition of ultra-pure water instead of the DNA template. For qPCR experiments the cDNAs were diluted 1:4 with ultra-pure water.

3.2.15 Polymerase Chain Reaction (PCR)

The temperature profiles and reaction outlines of the different PCRs, performed in the scope of this thesis, were specifically adjusted according to the thermodynamic properties of the oligonucleotide primer and the lengths of the amplified PCR products. In the following, all PCR-setups used in the scope of this thesis are listed in detail.

3.2.15.1 PCR-Setup for Isolation of the DNA for the Generation of the Targeting Vector

Reaction Mixture		Program		
2.0 µl	Template (genom. DNA)		Time	Temperature
1.0 µl	Sense primer, halfext., 100 µM		[min]	[°C]
1.0 µl	Antisense primer, halfext., 100 µM	Initial denaturation	2:30	95
		40 cycles of		
10.0 µl	5x GoTaq buffer (with $MgSO_4$, Fermentas)	Denaturation	0:30	95
2.0 µl	dNTP-Mix, 2.5 mM each	Hybridization	1:00	62
0.5 µl	GoTaq Flexi® DNA Polymerase (2-3 U/µl)	Extension	2:00	72
2.0 µl	DMSO	Final extension	10:00	72
31.5 µl	UltraPure™ distilled water			

3.2.15.2 PCR Setup for Maintaining the Southern Probe Template

Reaction Mixture		Program		
2.0 μl	Template (genom. DNA, 3.2.3)		Time	Temperature
1.0 μl	Sense primer, halfext., 100 μM		[min]	[°C]
1.0 μl	Antisense primer, halfext., 100 μM	Initial denaturation	2:30	95
		40 cycles of		
10.0 μl	5x GoTaq buffer (with MgSO$_4$, Fermentas)	Denaturation	0:30	95
2.0 μl	dNTP-Mix, 2.5 mM each	Hybridization	1:00	62
0.5 μl	GoTaq Flexi® DNA Polymerase (2-3 U/μl)	Extension	2:00	72
2.0 μl	DMSO	Final extension	10:00	72
31.5 μl	UltraPure™ distilled water			

3.2.15.3 Setup for the Southern Probe for Detection of Targeted ES Cells

For the generation of the radiolabeled probe used for Southern-blot experiments (3´-southern-probe, 2.4) 7 μl of the isolated (QIAquick® Gel Extraction Kit) template (3.2.15.2) was mixed with 3 μl UltraPure™ distilled water, incubated 5 min at 97°C, and then was put immediately on ice for 2 min. Subsequently, random hexamer primer, dNTPs, 5 μl dCTP32, and 2U Klenow fragment of DNA polymeraseI were added (Random Primed DNA Labeling Kit, Roche), and the mixture was incubated for 1 h at 37°C. Afterwards, 30 μl of STE-buffer (10 ml TE, 300 μl 5 M NaCl) were added, and the probes were cleaned up with the ProbeQuant™-Kit according to the manufacturer's recommendations. 15 μl of the flow-through were used for the Southern-blot detection.

3.2.15.4 PCR-Setup for the qPCR-Primer Validation

Reaction Mixture		Program		
1.5 μl	cDNA-template (3.2.14)		Time	Temperature
1.0 μl	Respective "sense" primer, 40 pmol		[min]	[°C]
1.0 μl	Respective "antisense" primer, 40 pmol	Initial denaturation	2:00	95
		40 cycles of		
5.0 μl	5x GoTaq buffer (Fermentas)	Denaturation	0:30	95
0.5 μl	dNTP-Mix, 10 mM	Hybridization	0:30	55
0.5 μl	GoTaq Flexi® DNA Polymerase (2-3 U/μl, Fermentas)	Extension	0:30	72
0.7 μl	MgCl$_2$	Final extension	1:00	72
15 μl	UltraPure™ distilled water			

3.2.15.5 PCR Setup for Expression Analysis by qPCR

SYBRGreen fluorescence signal was monitored using a qPCR cycler (Realplex2 S). Since the CT-value is proportional to the logarithm of the initial concentration of the target gene in the sample, samples measured in parallel can be compared relative to each other. The use of the unspecific fluorescence dye SYBRGreen, instead of gene-specific probes as well as exertion of ubiquitous reaction terms allowed the high-throughput detection of different target sequences, as like this qPCR specificity was determined only by selection of the particular primer sequences.

To optimize qPCR conditions, different template and primer concentrations for the target genes were tested initially in parallel. The sizes of the resulting PCR products for each primer pair were also verified by gel electrophoresis (appendix: **9.2**). Furthermore, efficiencies of reference gene primers coding for *GAPDH* and *β-actin* were determined by dilution curves. Both reference genes were detected, but *β-actin* transcript was expressed slightly more stably and therefore chosen for these analyses.

Extraction of mRNA was carried out from the brain areas frontal cortex, striatum and hippocampus of 3 month old animals. It was essential that the obtained mRNA was free from genomic DNA. Therefore, a DNAse digest was accomplished before extraction was carried out. Integrity of the mRNA was verified through the presence of the two discreet 18S and 28S rRNA bands on agarose gels (appendix: **Figure 45**). After extraction and purification of total RNA (Methods, 3.2.13), cDNA was synthesized from RNA prior to qPCR reaction (Methods, 3.2.14). Data obtained from *ProT $^{-/-}$*- and *ProT $^{+/+}$*-genotypes were finally normalized by the reference gene *β-actin*.

The efficiencies for the primers used for analyses of the genes of interest were not determined explicitly, and were assumed to be amplified with 100% efficiency for calculation (amplification-coefficient was set at 2).

Reaction Mixture		Program		
2.0 μl	cDNA-template (3.2.14)		Time	Temperature
1.0 μl	Respective "sense" primer, 10 pmol		[min]	[°C]
1.0 μl	Respective "antisense" primer, 10 pmol	Initial denaturation	10:00	95
		40 cycles of		
5.0 μl	Jump-Mix (Sigma)	Denaturation	0:30	95
1.0 μl	dNTP-Mix, 2.5 mM each	Hybridization	0:30	59
2.0 μl	UltraPure™ distilled water	Extension	0:30	72
		Final extension	10:00	72

3.2.15.6 PCR Setup for RT-PCR Analysis

Reaction Mixture		Program		
2.0 µl	cDNA-template (3.2.14)		Time	Temperature
1.0 µl	"Sense" primer, Ex5 Forward 100 µM		[min]	[°C]
1.0 µl	"Antisense" primer, Ex9 Reverse resp. Beta-Actin, 100 µM	Initial denaturation	2:00	95
		30 cycles of		
5.0 µl	5x GoTaq PCR buffer (Fermentas)	Denaturation	0:30	94
1.0 µl	dNTP-Mix, 10 mM	Hybridization	0:30	55 resp. 58 (β-Actin)
0.3 µl	GoTaq Flexi® DNA Polymerase (Fermentas)	Extension	0:45	70
	(2-3 U/µl)			
1.0 µl	DMSO	Final extension	2:00	70
12.7 µl	UltraPure™ Distilled water			

3.2.15.7 PCR Setup Genotyping

Presence of wild-type allele was proven by an amplicon of 354 bp, whereas the occurrence of modification of *ProT* gene was shown by the appearance of a PCR product of 430 bp.

Reaction Mixture		Program		
1.0 µl	Isolated genomic DNA (3.2.3)		Time	Temperature
0.5 µl	Respective "sense" primer, 20 µM		[min]	[°C]
0.5 µl	Respective "antisense" primer, 20 µM	Initial denaturation	2:00	95
		30 cycles of		
5.0 µl	5x Taq buffer (Fermentas)	Denaturation	0:30	95
2.0 µl	$MgCl_2$	Hybridization	0:30	59
1.0 µl	dNTP-Mix, 10 mM	Extension	0:30	72
0.3 µl	GoTaq Flexi® DNA Polymerase (5U /µl, Fermentas)			
1.0 µl	DMSO	Final extension	1:00	72
13.7 µl	UltraPure™ distilled water			

3.2.16 Preparation of Plasmamembrane-Enriched Polypeptide-Fractions (P2-Fractions)

Respective brain area samples were transferred into 900 µl of ice-cold sucrose-lysis-buffer (0.32 M Sucrose, 1 mM EDTA, 10 mM Hepes-Tris, pH 7.4) and homogenized with a dounce-type glass homogenizer (20 strokes) on ice. Afterwards, suspensions were spun down (6100 x g, 5 min) at 4°C, the supernatants were transferred in new reaction-tubes and centrifuged (16000 x g, 30 min, 4°C) again. Pellets became resuspended in 500 µl buffer 2

(125 nM NaCl, 5 mM KCl, 1.2 mM CaCl$_2$, 1.3 mM MgSO$_4$, 10 mM Glucose and 25 mM HEPES-TRIS, pH 7.4) and spun down (16.100 x g, 30 min, at 4 °C). Resulting pellets were resuspended in 80 μl of buffer 3 (5 mM Tris/ 1 mM EDTA). Afterwards, suspensions were frozen and stored at –80°C.

3.2.17   Determination of the Protein Content of P2-Fractions

Protein concentrations of P2-Samples were determined based on the method of Bradford with minor modifications (Bradford 1976). In brief, 2 μl of samples were diluted (1:20) with 0.1 M NaOH. A bovine serum albumin (BSA calibration) standard (0 μg/μl - 10 μg/μl BSA) was prepared. 200 μl Bradford Reagent were added to each sample (10 μl/well, triplicates, 96 well plates), and the absorbance was measured after 5 min by use of an ELISA microplate reader (Sunrise-Basic Tecan) at 595 nm. Subsequently, the protein concentrations were calculated according to the calibration graph.

3.2.18   SDS-Polyacrylamide-Gel-Electrophoresis (SDS-PAGE) and Western-Blot Analysis

P2-fraction samples were separated in 6% - 12% SDS-polyacrylamide gels based on the method of Laemmli with minor modifications (Laemmli 1970). In brief, NuPage Sample Reducing Agent (Invitrogen) was added to the sample buffer (NuPage, Invitrogen), and 500 μl NuPage Antioxidant (Invitrogen) were added to the running buffer. Samples (40 μg of protein) were heated 10 minutes at 70°C. 5 μl prestained Kaleidoscope standard (Bio-Rad) and 2.5 μl Magic Marker standard (Invitrogen) were used as molecular weight markers.

The gels were transferred to nitrocellulose membranes (2.13) using a blotting module (XCell II Blot Module, Invitrogen) for 90 min at 30 V in NuPage Transfer Buffer (including 20 % methanol). Nitrocellulose filters were rinsed in PBS (2.6), blocked in Roti Block (2.5) for 1 h at room temperature, and incubated with the respective antibodies in Roti Block, over-night at 4°C. Afterwards, membranes were washed three times (5 min) with washing buffer (PBS + 0.1 % Tween 20). Thereafter, nitrocellulose filters were incubated with the respective secondary antibodies diluted in Roti Block (1h at RT). For detection, enhanced chemoluminescence reagent (GE Healthcare) was used according to the manufactures recommendations, and nitrocellulose filters were scanned by use of DeVision DBOX Detection-System (Decon).

3.2.19 Stripping of Nitrocellulose Filters

Antibodies binding to nitrocellulose filters were removed (stripped) by rotating them in buffer (62.5 mM TRIS-HCl pH 6.8, 2 % SDS, 100 nM ß-mercaptoethanol) at 50°C for 30 minutes. Afterwards, they were washed 6 times (5 min each) in washing buffer (PBS + 0.1 % Tween 20) and subsequently blocked with Roti Block (60 min, RT).

3.2.20 Southern-Blotting

Screening of mouse embryonic stem cell clones for homologous recombination was done by the method of Southern blotting. Digested (*BamHI*) DNA was separated by electrophoresis through 1% agarose gels, and subsequently depurinated (2.7) for 10 min in the gel, followed by denaturation (2.7), and neutralization (30 min each, 2.7). Blotting transfer to nylon membranes was performed in 10x SSC (2.7) over-night as capillary blot. Via UV-crosslinking, the DNA was immobilized on nylon membranes before hybridization with denatured radio-labeled probes at 62°C overnight. Unspecific binding was avoided by prehybridisation with herring sperm DNA (Invitrogen). Thereafter, membranes were incubated once for 10 min in 2x SSC/0.1% SDS at room temperature, followed by final washes in 0.2x SSC/0.1% SDS at 58°C (2 x 10 min). Afterwards, membranes were equilibrated in maleic acid buffer. The results were detected by exposure to a hyperfilm (Amersham Pharmacia) for up to over-night.

3.2.21 L-[^{3}H]-Proline Uptake

After preparation of synaptosome-suspensions [protocol according to preparation of P2-fractions 3.2.16, with the exception that final pellets were resuspended in Krebs-Ringer-Hepes solution (125 mM NaCl resp. LiCl, 5 mM KCl, 1.2 mM CaCl$_2$, 1.3 mM MgSO$_4$, 10 mM glucose, 25 mM Hepes-Tris, pH 7.4)] aliquots of 20 µl were preincubated for 2 min at 37°C. Accumulation of L-proline was initiated by addition of 80 µl of Krebs-Ringer-Hepes solution containing 0.063 µM radiolabeled and 2.437 µM unlabeled L-proline (final concentration 2 µM L-proline), and suspensions were incubated for 2 min with gentle agitation at 37°C. Afterwards, the uptake reaction was terminated by addition of 9 ml of ice cold Krebs-Ringer-Hepes solution, and the suspensions were rapidly filtrated onto nitrocellulose (HAWP02500, 0.45 µm, Millipore). The resulting filters were placed into vials, and radioactivity was determined by scintillation spectrometry.

3.2.22 Nissl Staining

Slides with brain sections were passed through a sequence of baths to obtain cresyl violet stained tissue. First, the slides became incubated for 15 min in 95% ethanol, followed by 1 min of incubation in 70% ethanol and a subsequent bath in 50% ethanol. Afterwards, the

sections were washed twice for 2 min in UltraPure^{TM} distilled water, before they were stained by incubation in cresyl violet solution (1.25 g of cresyl violet acetate, 0.75 ml of glacial acetic acid in 250 ml distilled water) for 2 min. Subsequently, the slides were washed 1 min in 50% ethanol, then 2 min in 70% ethanol, and afterwards 2 min in 95% ethanol. Finally, the sections were washed in ethanol absolute, incubated 5 min in roticlear$^{®}$ (Roth) and covered with moviol and cover-slips.

3.3 Experimental Methods with Animals

Behavioral experiments were conducted at the animal facility "Haus für experimentelle Therapie (HET)"of the University´s Medical Center and at the animal facility of the Max Planck Institute for Brain Research of the University of Frankfurt. The microinjection service of the HET was utilized for the reimplantation of positively targeted ES cells into pseudopregnant foster animals to obtain chimeric mice. The S1 (Sicherheitsstufe 1, §§4-7 GenTSV) animal facilities provided standardized climatic conditions and a 12/12-h light/dark cycle (lights were turned on 7:00 a.m. and off 7:00 p.m., respectively. The described animal experiments and the animal housing were approved by the „Landesamt für Natur, Umwelt und Verbraucherschutz"(LANUV) in NRW. All experimental protocols were performed in compliance with existing national regulations and guidelines (Tierschutzgesetz v. 18.5.2006 (BGBl. I S. 1206, 1313), g v. 18.12.2007 (BGBl. I S. 3001; 2008, 47)). Food and drinking water was supplied *ad libitum*. In case of any behavioral experiment, mice were brought to the testing room and allowed to acclimate for at least 15 min prior to the respective test.

3.3.1 Generation of Chimeric Mice

Chimeric mice were obtained by the method of blastocyst injection. For this purpose cells of a targeted SV129 ES cell line proven by Southern-blot were injected into blastocysts maintained from superovulated 4-6 week old C57BL/6J mice (Charles River). Blastocysts were afterwards retransferred to pseudo-pregnant foster mice. Chimeric animals were assessed by coat color and crossed with the C57BL/6J mouse strain.

3.3.2 Preparation of Nervous Tissue

Mice were sacrificed via cervical dislocation, the skulls were opened and the required brain areas were removed rapidly as described previously (Glowinski et al. 1966) and immediately shock-frozen in liquid nitrogen. Tissue samples were stored at –80°C until further usage.

3.3.3 Hot Plate Test

Sensitivity to thermal nociception was investigated by use of a commercially available hot plate analgesia meter (TSE-Systems), with a metal plate that could be heated to a constant temperature. In the experiments performed in the scope of this thesis, the surface of the plate was heated to a temperature of 50°C, and latency to respond was defined as the time between the moments that the mouse was placed onto the plate and that it started to move away or licked a paw.

3.3.4   Open Field Test

The open field test is an evaluation used to ascertain general activity levels, locomotor activity, and exploration habits of rodents. Confrontation to a novel environment usually implies stress to the animals. Therefore, the explorative behavior of an animal gives information about how well this animal can adapt to a novel situation. The behavioral forces are the curiosity to explore the novel situation opposed by the fear about the new situation, which influences the outcoming behavior coincidently. Assessment took place in a square arena (45 x 45 cm). This arena was mounted within specially designed sound attenuating shells. A mouse was placed in one corner of the open field arena and allowed to freely move for 15-30 minutes while being tracked by an automated infrared-tracking system (Actimot, TSE Systems GmbH) recognizing horizontal as well as vertical activity. Hyperactivity threshold was set to 20 cm /s. At the end of each trial the surface of the arena was cleaned with 70% ethanol. The open field test was conducted with two different illumination conditions, depending on the desired behavioral parameter. With an illumination intensity of 2 lux basic exploration behavior of the mice was studied. By intensive illumination (250 lux intensity) the open field test was additionally used to study emotionality of the mice, since normal behavior in mice is to seek the protection of the periphery (Archer 1973). To minimize the influence of anxiety on spontaneous locomotor activity level, animals were monitored under sound-attenuated conditions without the experimenter being visible. Mice were always placed individually in the arena.

3.3.5   Y-Maze Test

Spontaneous alternation behavior was assessed in a symmetrical Y-shaped runway made of white plastic with walls 28 cm high and open top. Each arm was 48 cm long and 12 cm wide. Mice were tested randomly by placing them individually at the end of one arm of the maze. Animals were allowed to move freely in the three arms of the maze during an observation time of 5 min. The maze was wiped clean with 70% ethanol before another mouse was tested. The sequence of arm entries (with all four feet into any of the arms) was recorded visually. Alternation was defined as multiple entries into different arms on overlapping triplet sets. Percentage of spontaneous alternation was calculated via entries into a new arm, thus by the ratio of the possible alternations, as shown by the following equation:

Alternation (%) = (number of alterations/total arm entries − 2) * 100

3.3.6   Forced Swimming Test

The forced swimming test (FST) is a test to investigate depression like behavior in mode of „behavioral despair". This paradigm was developed and established 1977 by Porsolt and colleagues and examines the behavior of a mouse in a cylinder filled to the half with water (Porsolt et al. 1977). Usually, confrontation with this aversive situation first induces escaping behavior that later on changes to immobility, whereas the mice let themselves float in the water. The time period mice spent in immobility is called the "depression like condition". This immobility time can be drastically reduced in favor of the escaping behavior e.g. by prior application of antidepressant drugs to the mice. The test was carried out in a cylinder (high 35 cm, diameter 18 cm) filled with water (25°C) to the half, so that the mouse was not able to touch the bottom nor to escape from the cylinder. Time of immobility was monitored over 5 minutes and calculated in percentage of total time.

3.3.7   Prepulse Inhibition (PPI)

Prepulse inhibition (PPI) is an indicator of sensorimotor gating, a process that is important for filtering irrelevant sensory information and allows attention to be focused on a given stimulus. PPI is determined with a weak acoustic noise that inhibits the reaction to a subsequent strong startling one. To measure PPI the startle reflex measurement system (TSE-Systems) was used. The test was started by placing a mouse into a small cage, which was put in a sound-attenuated chamber onto a balance to record the startle response elicited by the sound-stimuli. First, the mouse was left undisturbed for 5 min to habituate to the new situation. Background noise level of the chamber was set at 60 dB. The prepulse sounds (0, 65, 70, 75, 78, 80 and 85 dB) of 20 ms were presented for 120 ms before the startle stimulus (110 dB for 40 ms) was given. All pulse combinations were presented in a randomized order. The PPI percentage was calculated using the following equation:

(1 - Average of startle amplitude in trail with prepulse/

Average of startle amplitude in trails without prepulse)*100

3.3.8   Determination of Body Weights

Determination of the body weights was carried out by scaling the mice in a carton on a laboratory balance (Sartorius).

3.3.9   Rotarod Test

The rotarod test was carried out with a rotarod device (TSE-Systems). This test is designed to evaluate motor coordination and balance skills of the mice. Therefore, a mouse was placed on a rotating (5 rpm) rod in orientation opposite to that of its rotation, and the rods accelerated to 25 rpm gradually over 75 seconds. This rotating rod was placed 35 cm above the floor to induce locomotion of the mice by avoidance to fall down. Falling down latencies of the mice were recorded automatically.

4   Results

4.1   Generation of *ProT*-Knockout Mice

In the present section, all experiments related to the generation of the high affinity sodium-dependent L-proline transporter (PROT) deleted mouse line will be described. This comprises the experimental design concerning the strategy of targeting the *ProT* gene, as well as the procedure of creating the artificial DNA construct.

4.1.1   Targeting Strategy

The target gene (*ProT*) encoding the murine PROT (SLC6A7) is located on chromosome 18 and encompasses 14 coding exons (www.ensemble.org), distributed over a genomic DNA-stretch of 18.82 kb (**Figure 4**). Transcription of this gene originates mRNA with a length of 3362 bp (NCBI acc. no. NM 201353.1), and the translated protein consists of 637 amino acids (NCBI acc. no. NP 958741.1).

The strategy for generating the *ProT* gene deleted mouse strain is outlined in **Figure 4**. A region of 1158 bp containing the reading frames for exons 6 and 7 was selected as target for the deletion of *ProT*. This area encodes the central region of the murine PROT, including the transmembrane domain 5, the extracellular loop 3 and the transmembrane domain 6. The transmembrane domain 6 is located in the core of the protein and essential for the transport action of amino acid antiporters (Chang et al. 2010). Therefore, removal of this central region (1158 bp) of the *ProT* gene was thought to disrupt the expression of *ProT* mRNA through disturbance of the gene locus and to break down functionality of the transporter. This deletion should be achieved by replacing the region of 1158 bp with a neomycin resistance gene (*neo*) of 1826 bp under the control of the phosphoglycerate kinase (PGK) promoter.
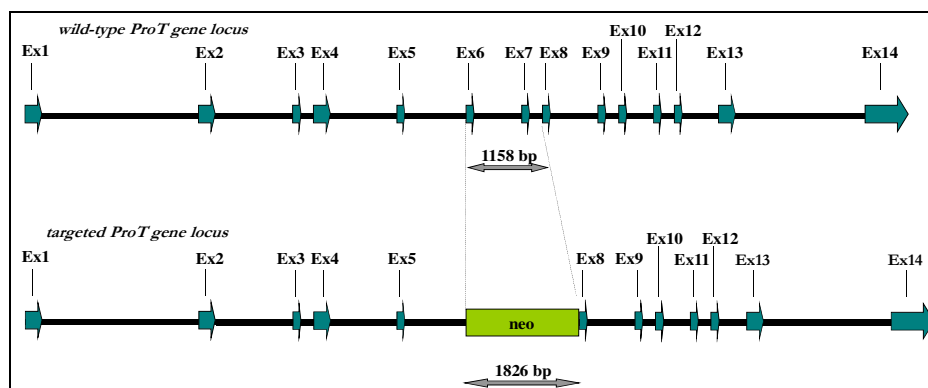
Figure 4 Knockout strategy of *ProT* showing wild-type *ProT* locus and the targeted allele

At the top, the murine wild-type *ProT* gene locus is pictured with exons represented as blue arrows, and the target region for deletion containing exons 6 and 7 (1158 bp) is indicated with a grey arrow. At the bottom, the targeted *ProT* gene locus after effective homologous recombination is depicted. The locus contains the neomycin resistance gene (1826 bp) pictured as a green block (neo) instead of the target region (1158 bp).

4.1.2   Isolation of the *ProT* Gene

A mouse genomic bacterial artificial chromosome (BAC) library was virtually screened (using NCBI clone finder; http://www.ncbi.nlm.nih.gov/projects/mapview) for the genomic sequence of the *ProT* gene (SLC6A7), previously gained from ensembl data base (http://www.ensembl.org). Three identified recombinant *E. coli* clones containing *ProT* genomic DNA were delivered from the Children´s Hospital Oakland Research Institute (CHORI), seeded on LB plates and grown to recover BAC DNA. Southern blot analysis confirmed the presence of the full length SLC6A7 DNA in the three clones (**Figure 5**).
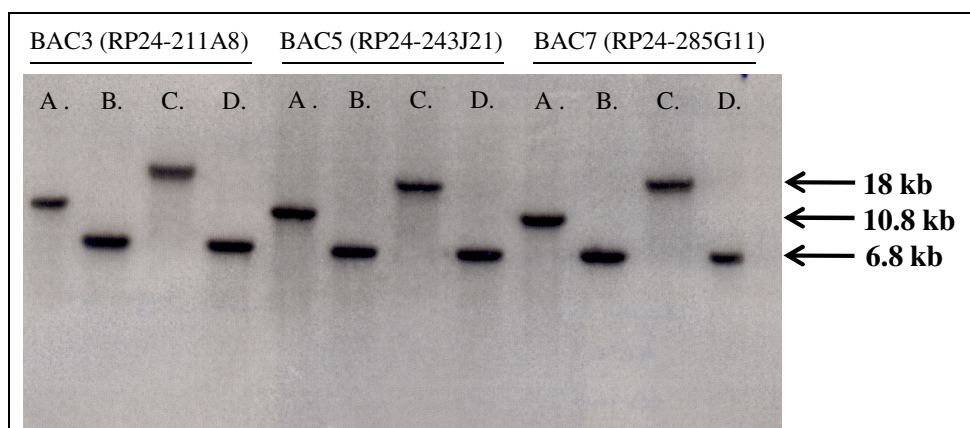
Figure 5 Southern-blot analysis of DNA from BAC clones to prove presence of the full length *ProT* genomic DNA

Pictured are BAC clones 3, 5 and 7 confirming presence of SLC6A7 DNA after cleavage with *KpnI* (A.), *BamHI* (B.), *EcoRI* (C.) as well as double digest with *EcoRI* and *BamHI* (D.). A DNA sequence homologous to exons 3 and 4 was used as a probe. Presence of *ProT* should result in appearance of a fragment of 10.8 kb after *KpnI* cleavage, digestion with *BamHI* would give rise of a 6.8 kb fragment, *EcoRI* restriction should give an 18 kb fragment and *BamHI*/*EcoRI* cleavage would result in a fragment of 6.8 kb. As shown, all analyzed BAC clones could be verified containing SLC6A7 DNA as expected.

4.1.3   Construction of the *ProT* Targeting Vector

The next step was the generation of a targeting vector for homologous recombination. Toward this goal, a 7.3 kb genomic DNA sequence of the murine *ProT* gene, which includes exons 2 to 9, and the XpPNT-vector (appendix: **Figure 41**), containing a gene encoding for neomycin resistance (*neo*) as well as a herpes simplex virus thymidine kinase gene (HSV-TK; 1127 bp), were used.

Insertion of the *neo* gene into the genomic locus of the *ProT* gene was expected to be achieved by homologous recombination in embryonic stem (ES) cells. Therefore, the targeting vector contained DNA sequences, which were 5´ and 3´ homologous to the targeted 1158bp-*ProT*-region that was anticipated to be removed.

For the 5' homologous region, a 5028 bp-fragment from the end of exon 2 up to the beginning of exon 6 (including exons 3, 4 and 5) was chosen. The 3' homologous area comprised an 1131 bp-fragment from the beginning of exon 8 up to the beginning of exon 10 (**Figure 6**). PCR reactions were performed to amplify the 5´ and 3´ homologous region respectively, applying appropriate oligonucleotide primers and the BAC clone RP24-243J21 (BAC5) as genomic DNA template (further information concerning PCR-conditions: 3.2.15.1 and appendix: **Figure 42**). Each fragment was subcloned into pBluescript-vector (pBS) and verified by restriction analysis (appendix: **Figure 43 A** and **Figure 43 B**) and sequencing. The 3' homologous fragment was first inserted into the XpPNT-vector between the *neo* and the *HSV-TK* genes by using *BamHI* and *EcoRI*. Afterwards, the 5' homology fragment was introduced by *NotI* and *XhoI* into the XpPNT-vector.
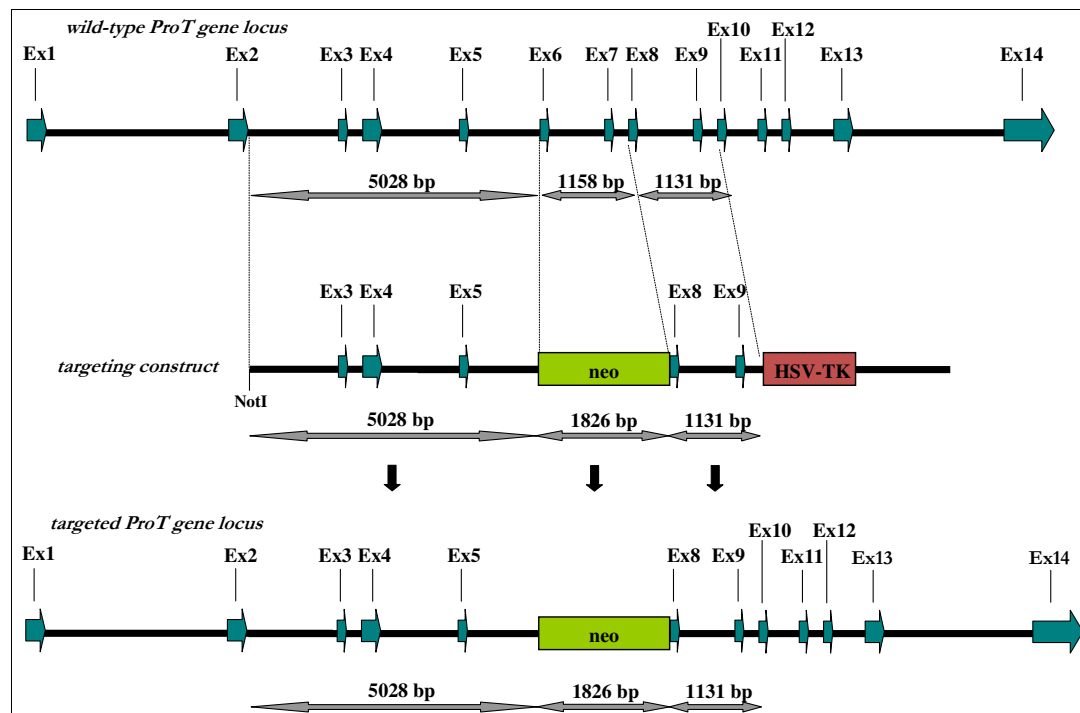
Figure 6 *ProT*-knockout-strategy showing the wild-type *ProT* locus, the cloned targeting construct and the targeted allele

At the top, the murine wild-type *ProT* gene locus is pictured with exons represented as blue arrows. The fragment representing 5' homology (5028 bp, Ex2-Ex6) to the targeting construct, the target region for deletion (1158 bp, Ex6-Ex7) and the fragment representing 3' homology (1131 bp, Ex8-Ex10) are indicated with grey arrows. In the center, the targeting construct containing the 1826 bp neomycin resistance gene for positive selection (neo), pictured as a green block and the truncated herpes simplex virus thymidine kinase gene fragment for negative selection, embodied as a red block (HSV-TK), are shown. At the bottom, the targeted *ProT* gene locus after effective homologous recombination is depicted, showing the exchange of 1826 bp neo gene (neo) for the target region (1158 bp).

4.1.4   Transfection of Mouse Embryonic Stem Cells and Screening by Genomic Southern Blot-Analysis

Next, the targeting vector was linearized at the single *NotI* restriction site previous to transfection by electroporation in HM1-ES cells derived from agouti colored 129/Sv mice (Magin et al. 1992). Electroporated cells were grown in selective media containing the neomycin analog antibiotic G418 and the nucleoside analogue FIAU (3.1.4) in order to select resistant colonies indicative for the presence of the neomycin resistance gene as well as absence of the *HSV-TK* gene, thus identifying those cells that underwent homologous recombination. Upon selection, 106 cell clones were harvested and examined by Southern-blot analysis for proper insertion of the *neo* gene at the *ProT* gene locus. The Southern-blot analysis strategy is described in **Figure 7**.

Finally, out of the 106 harvested cell clones, 10 homologous recombinant ES cell clones were obtained. Exemplary results from Southern-blot analysis for six ES clones after *BamHI*-cleavage are outlined in **Figure 8**. In clones 40, 93, and 105 proper homologous recombinations occurred, as confirmed by the expected genomic DNA restriction patterns.
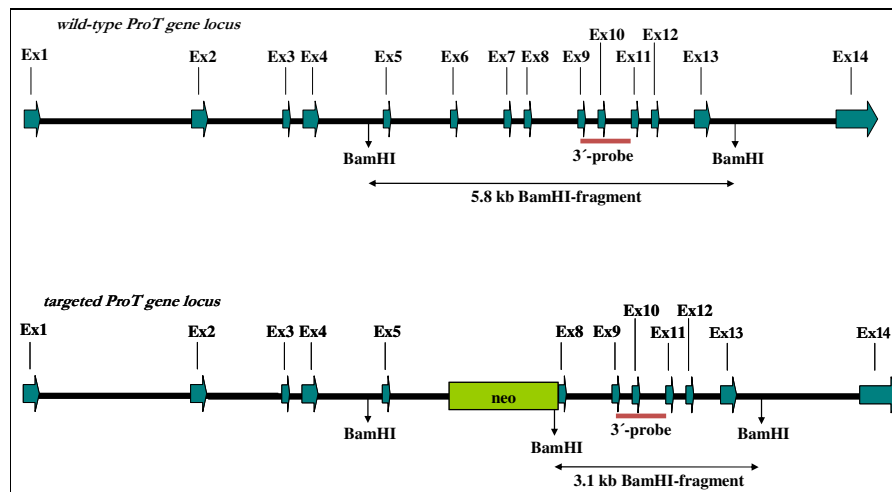
Figure 7 Strategy of Southern-blot analysis of genomic ES cell DNA

The murine wild-type *ProT* gene locus and the *ProT*-deleted locus are indicated, with exons represented as blue arrows. Binding sites for the hybridization probe are outlined in red and sizes of the restriction fragments after *BamHI*-cleavage are indicated as grey arrows. Expected fragment sizes with this probe are 5.8 kb for the wild-type allele (top) and 3.1 kb for the targeted allele (bottom).
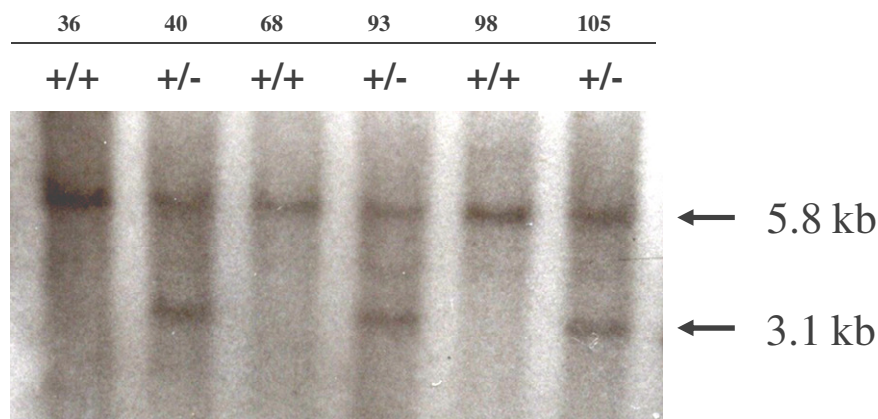
Figure 8 Southern-blot analysis of genomic DNA from ES cells to verify homologous recombination

After cleavage of the genomic DNA with *BamHI,* Southern-blot analysis was carried out using a probe binding 3´ of the knockout-locus (3´-probe, indicated in Figure 7). Results of clones 36, 40, 68, 93, 98 and 105 are shown as exemplary to demonstrate correctly targeted heterozygous ES cells (+/-) and ES cells exhibiting a randomly integrated targeting construct (+/+), respectively. The presence of a single 5.8 kb fragment displays attendance of two wild-type alleles (+/+), and presence of a 5.8 kb and a 3.1 kb fragments indicates attendance of one wild-type allele as well as one *ProT*-deleted allele (+/-), thus reporting a successfully targeted ES cell clone.

4.1.5   Generation of a *ProT* Knockout Mouse Line and Genotyping

Five of the ten positive ES cell clones containing one *ProT*-deleted allele were expanded, injected into blastocysts derived from C57BL/B6J mice and reimplanted into 22 pseudo pregnant foster mice. The independent injection of ES cells derived from clone 105 into six foster animals led to the birth of two highly chimeric male mice (**Figure 9**) out of 11 offsprings (F0 generation).

Figure 9 Highly chimeric mice

Chimeric mice were generated by injection of recombinant ES cell clone 105 (agouti colored 129/Sv) in blastocysts obtained from C57BL/6J mice.

The degree of chimerism was assessed by coat color, as the injected ES cell line was derived from agouti colored 129/Sv mice in contrast to the blastocysts generated from black C57BL/B6J animals. One chimeric male was fertile and further bred with C57BL/B6J females. The agouti coat color of the offspring (F1 generation) indicated the germline transmission.

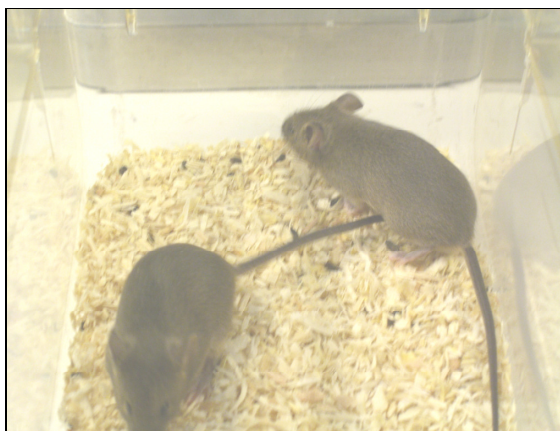Next, to prove that the *ProT*-deleted allele was transmitted to the germline, genomic DNA was prepared from small tail biopsies of the F1 generation litters 4 weeks after birth and subjected to genotype analysis by PCR. The organization of the wild-type and *ProT*-deleted alleles as well as alignment of the PCR primers for the genotype analysis are shown in **Figure 10 A**. To determine the genotypes of the animals, two separate PCRs were used. Each PCR was designed to cover the region containing the insertion site of the neomycin resistance gene. This resulted in PCR fragments of different lengths for the wild-type (430 bp) and *ProT*-deficient (354 bp) allele.

The analyzed F1 offspring generation displayed mice heterozygous for the mutated allele as well as wild-type mice consistent with the Mendelian rules predicting 50% probability. Mice heterozygous for the *ProT* mutant allele (*ProT* +/-) showed undisturbed development and fertility.

Finally, to create mice homozygous for *ProT*-deficiency, heterozygous F1 mice were bred with each other. After genotyping, these matings resulted, as well in agreement with the Mendelian rules, in 50% mice heterozygous for the mutated allele, 25% wild-type mice and 25% homozygous *ProT*-deficient mice, thus indicating that there was no increased embryonic mortality in the mutant animals. An example of the PCRs used in genotype analysis is shown in **Figure 10 B**.
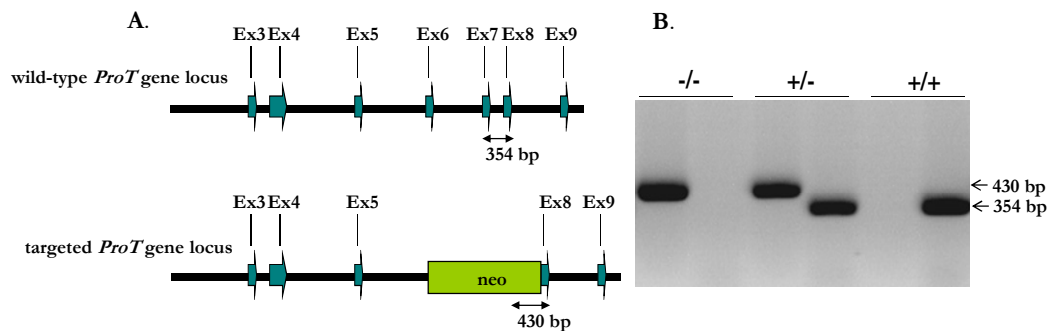
Figure 10 Genotyping of the *ProT* knockout mice

A. Organization of wild-type (top) and *ProT*-deleted (bottom) alleles with alignment of the particular PCR primers. Amplification with primer pair WTSIII 5´ (annealing in Ex7) and WTAS 3´ (annealing in Ex8) results in a 354 bp fragment revealing the presence of the wild-type allele and amplification with the primer pair neoS 5´ (annealing in the neo gene) and WTAS 3´ results in the formation of a 430 bp fragment, showing attendance of a targeted allele. **B**. Agarose gel electrophoresis of PCR products derived from F2 mice. Appearance of a single 430 bp amplicon (-/-) indicates the presence of a knockout animal (left). The attendance of a 430 bp fragment as well as a 354 bp amplicon reveals the presence of a heterozygous (+/-) animal (middle). Appearance of a single 354 bp fragment (+/+) displays the attendance of a wild-type animal (right). For detailed information about PCR conditions refer to materials and methods section 3.2.15.7.

4.2   Verification of the *ProT*-Knockout in Mutant Mice

To confirm that the expression of *ProT* gene is turned off in the knockout mice, PCR and Western blot analysis were performed.

4.2.1   Analysis of the *ProT* mRNA Expression by RT-PCR & qPCR

Examination of mRNA levels by reverse transcription polymerase chain reaction (RT-PCR) and quantitative real time polymerase chain reaction (qPCR) are the most sensitive techniques for detection and quantification of the transcription of a selected gene.

Total mRNA was extracted (see 3.2.13) from different regions of the brain (olfactory bulb, frontal cortex, striatum and hippocampus) of 3 month old animals, and cDNA was synthesized (3.2.14). RT-PCR primers were designed to amplify a specific *ProT* cDNA fragment of 280 bp. The sense primer attaches to exon 7, which is expected not to be present in the deleted allele, and the antisense primer binds to exon 8. RT-PCR results of *ProT* in wild-type (+/+) as well as heterozygous (+/-) and knock-out (-/-) mice are depicted in **Figure 11**.

Presence of the *ProT* mRNA was verified in heterozygous and wild-type mice. Its absence in homozygous mutants clearly demonstrates that in these animals transcription of the *ProT* gene does not take place. The lack of detectable *ProT* mRNA is not due to a poor RNA extraction from the different brain regions of the knockout mice, since equal amounts of *β-Actin* transcript were found in all analyzed tissues of the different genotypes.

Similar results were obtained by qPCR (see 3.2.15.5), showing specific expression levels of *ProT* in different brain regions in wild-type mice, but never in knockout animals (**Figure 12**).
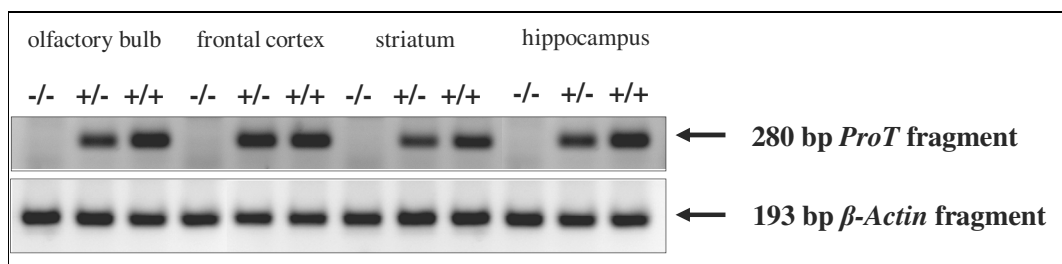
Figure 11 RT-PCR analysis of *ProT* expression in various brain areas

ProT transcript (280 bp) is detected in wild-type animals (+/+) and slightly reduced also in heterozygous mice (+/-), but not in knockout animals (-/-) within all analyzed brain areas, confirming truncation of *ProT* transcription in the knockout mice. As control, *β-Actin* transcripts (193 bp) could be detected in all cases. (For detailed information about PCR conditions, see section 3.2.15.6.)
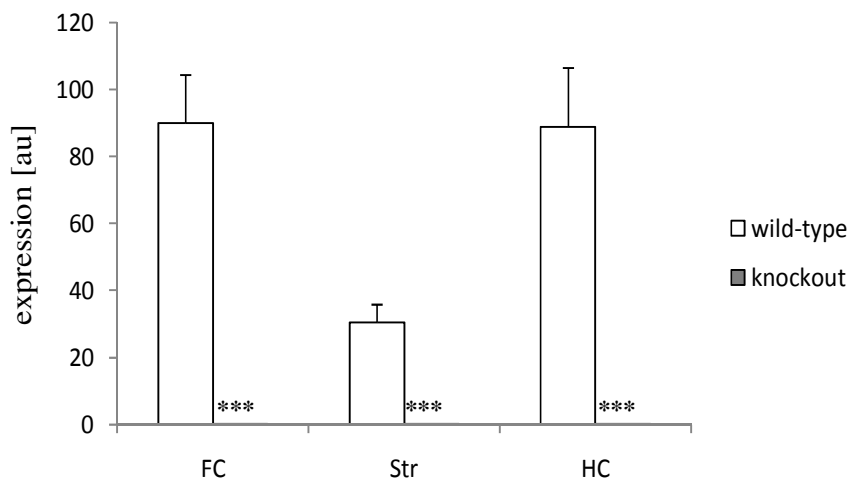
Figure 12 qPCR analysis of *ProT* expression in mutated versus wild-type mice

The diagram shows the expression levels as arbitrary units (au) of *ProT* mRNA in the frontal cortex (FC), striatum (Str) and hippocampus (HC) of wild-type versus knockout mice. mRNA levels were gained from C_T-values of *ProT* transcripts upon normalization with *β-actin* transcripts. Note the absence of *ProT* transcripts in knockout animals. Analyzed animals were 3 month of age. Data are given as means ± SEM (n = 3 for each genotype). Asterisk indicates significantly different expression levels of knockout mice from wild-type mice, p < 0.001 (Student´s t-test). (For detailed information about qPCR conditions and cDNA synthesis, please refer to section 3.2.15.5).

4.2.2 Verification of the Absence of PROT Protein in Knockout Mice

In order to confirm the presence or absence of PROT-expression at protein level in all mouse genotypes, a Western blot analysis was performed. Plasma membrane enriched brain homogenates (P2-fractions) from 2 different brain areas were separated on SDS-polyacrylamide gel electrophoresis, transferred to nitrocellulose and probed with antibodies specifically recognizing the C-terminal domain of PROT (Materials, section 2.2). As shown in **Figure 13**, Western blot analysis showed strong immunoreactivity in samples prepared from wild-type mice (+/+), and reduced immunoreactive labeling in heterozygous animals (+/-), but failed to exhibit immunoreactive polypeptide in PROT-knockout mice (-/-), thus confirming the lack of the PROT protein in the homozygous mutants.
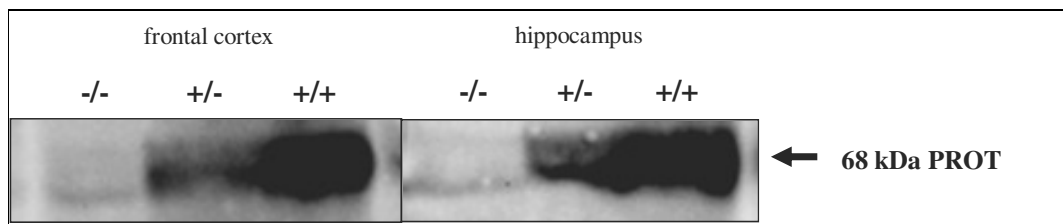
Figure 13 Western blot analysis of PROT polypeptide in hetero- and homozygous PROT-deficient mice and wild-type controls

P2-fractions (60 µg protein/lane) of frontal cortices (A.) and hippocampi (B.) were separated by 8% SDS-polyacrylamide gel electrophoresis, transferred to nitrocellulose and probed with antibodies which specifically recognize the C-terminal domain of PROT. Compared to wild-type mice, expression of PROT was reduced in heterozygotes (+/-) and completely abolished in homozygous (-/-) knockout mice. MagicMark® ladder was applied for size estimations and sample number was n = 3. (For detailed information about Western-blot procedure, refer to section 3.2.18.)

4.3   Analysis of the PROT-deficient Mice

In this section experiments concerning the first analysis of the *ProT* deleted mouse line are illustrated.

4.3.1   Contribution of PROT to the Sodium-dependent High Affinity L-Proline Uptake in Brain

To reveal the functional consequences of *ProT* gene deletion on high-affinity Na^+-dependent uptake of L-proline, crude synaptosomal preparations (P2-fractions) from different brain areas, namely frontal cortex, striatum, hippocampus and olfactory bulbs, were prepared and incubated with L-[^{3}H]-proline for 2 minutes (3.2.21).

Two-way ANOVA revealed that there was an effect of the brain area on L-[^{3}H]-proline uptake ($F_{3,23}$ = 30.74; p-value < 0.001) as well as a strong effect of the genotype on L-[^{3}H]-proline uptake ($F_{2,23}$ = 122.96; p-value < 0.001). In addition, there was an effect of the interaction between genotype and brain area ($F_{6,23}$ = 9.43; p-value < 0.001).

As shown in **Figure 14,** L-[^{3}H]-proline uptake was significantly reduced, by ≥50% in the olfactory bulbs (OB) and ≥75% in the hippocampus (HC), frontal cortex (FC) and striatum (Str) of PROT$^{-/-}$ mice, as compared to wild-type littermates. P2 membrane fractions from heterozygous animals showed intermediate L-[^{3}H]-proline uptake values, consistent with a clear gene dosage effect of PROT expression.

Incubation of membrane fractions from wild-type animals with 2.5 mM sarcosine, an inhibitor of PROT (Fremeau et al. 1992), decreased the uptake of L-[^{3}H]-proline in fractions from wild-type animals to values comparable to the transport activity measured in the PROT-knockout membranes (**Figure 15**). These results indicate that PROT-mediated L-[^{3}H]-proline is totally abolished in the homozygous mutants.
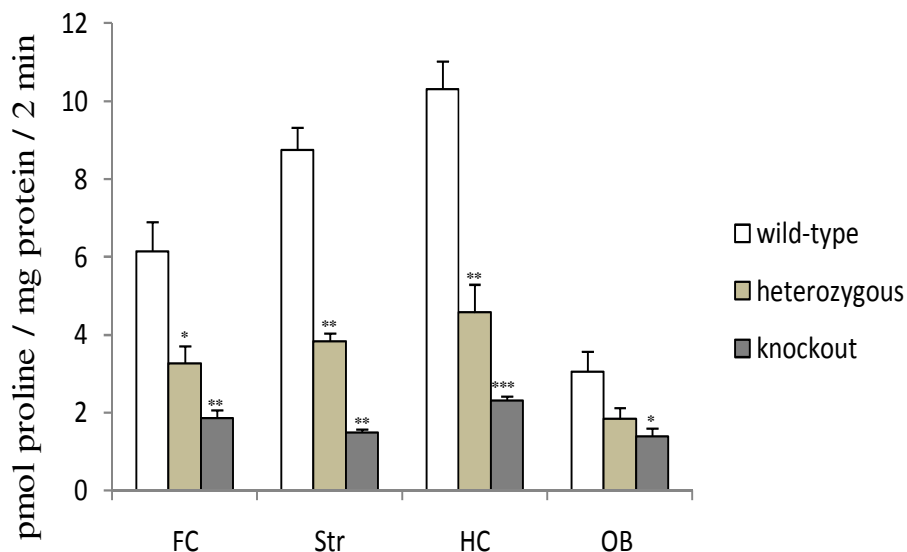
Figure 14 Determination of high-affinity sodium dependent L-[³H]-proline in membrane preparations from different brain areas

Uptake was determined in frontal cortex (FC), striatum (Str), hippocampus (HC) and olfactory bulb (OB) of wild-type, heterozygous and knockout mice. Accumulation of L-[³H]-proline was reduced by half in synaptosomal preparations of heterozygous animals and further reduced in knockout mice. Data are given as means ± SEM (n = 3 for each genotype). Asterisk indicates significant difference from wild-type mice, with p < 0.05: *, p < 0.01: **, p < 0.001: *** (Student´s t-test). (For detailed information about assay procedure refer to section 3.2.21.)
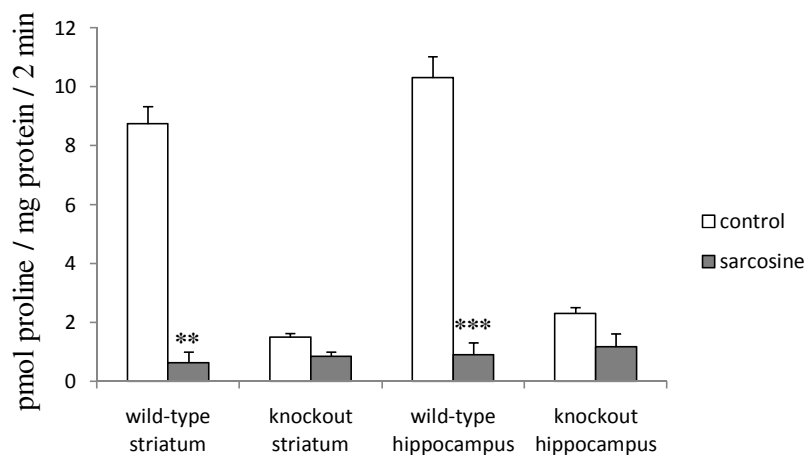
Figure 15 Investigation of Na⁺-dependent accumulation of L-[³H]-proline in two brain areas employing the PROT-specific inhibitor sarcosine (2.5 mM)

Sodium-dependent L-[3H]-proline accumulation of synaptosomal preparations of striati and hippocampi from knockout mice displays a comparable level to L-[³H]-proline uptake from wild-type mice in the presence of the PROT inhibitor sarcosine. Asterisk indicates significantly different from wild-type mouse controls, with p < 0.01: **, p < 0.001: *** (Student´s t-test). (For detailed information about assay procedure, refer to section 3.2.21.)

4.3.2   Analysis of Expression Levels of L-Proline Metabolizing Enzymes

It was observed that the deletion of neuronal PROT protein impairs L-proline clearance capacity (4.3.1), thereby suggesting both an increase of the extracellular L-proline concentration at the synapse and a decrease of this amino acid intracellularly. Therefore, it was examined whether metabolic turnover of L-proline could be affected by alterations of L-proline levels in PROT-deficient brains, analyzing the transcriptional levels of enzymes involved in its metabolic pathways. Expression of the enzyme P5C-synthase (*Pycr*) that catalyzes the NADPH-dependent conversion of Δ^1-pyrroline-5-carboxylate to L-proline, and expression of proline dehydrogenase (*PRODH*), which catalyzes the first step in L-proline catabolism by converting L-proline to Δ^1-pyrroline-5-carboxylate, were determined by qPCR.

Transcriptional levels of *Pycr* were found to be weakly increased in the brains of PROT-deficient animals, but without statistical significance (**Figure 16**). Similarly, expression of L-proline degrading *PRODH* was not found to be significantly changed (**Figure 16**). The investigation of the expression levels of L-proline controlling enzymes demonstrates that neither adaptive enhancement nor reduction of L-proline turnover developed in the knockout animals. This demonstrates that synthesis and degradation of L-proline remains constant in the mutated animals compared to wild-type controls.
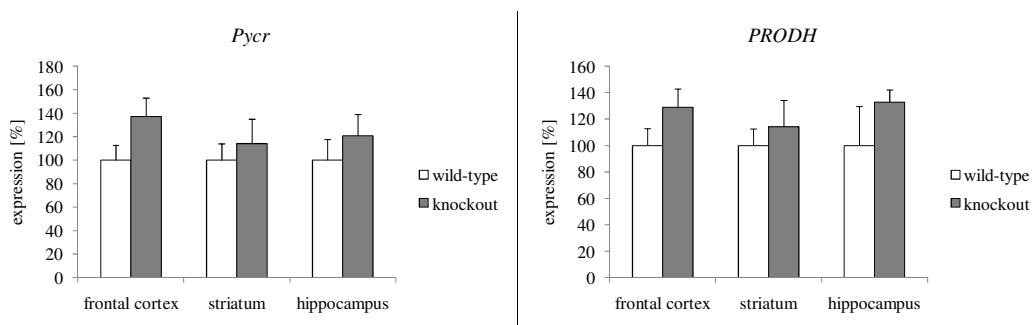
Figure 16 Relative mRNA expression profiling of L-proline metabolizing enzymes

Determination of pyrroline-5-carboxylate reductase (*Pycr*) and proline dehydrogenase (*PRODH*) expression as deduced from the amount of mRNA in different brain areas of *ProT*-deficient mice and wild-type controls revealed no significant differences. Analyzed animals exhibited 3 months of age. Data were normalized to *β-actin* and represent means ± SEM (n = 3 for each genotype).

4.3.3 Determination of Body Weights

Although PROT-deficient mice were normal in appearance, monitoring of body weights of 2-3 months old male mice detected a significant genotype-effect on the growth of mutant mice in contrast to wild-type controls. Body weights of PROT$^{-/-}$ animals were 15% significantly lower (21.6 g $\pm$ 0.5; n = 20, p-value < 0.01) than body weights of PROT$^{+/+}$ mice (25.35 g $\pm$ 0.42; n = 20) of the same age (**Figure 17**). This outcome is surprising because the high affinity L-proline transporter is exclusively expressed in brain and therefore not thought to be involved in L-proline accumulation serving for protein synthesis. Nevertheless, a reduced body weight is a frequent finding of knockout mice strains (Reed et al. 2008) and has been reported as well for other neuronal transporter knockout mice and *PRODH*-deficient mice formerly (Giros et al. 1996; Xu et al. 2000).
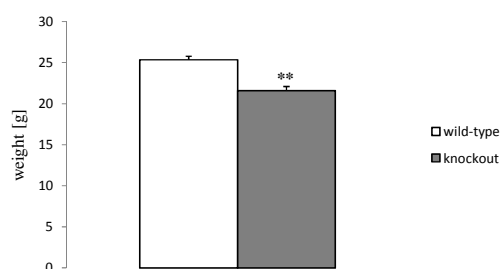
Figure 17 Determined body weights of PROT-deficient and wild-type mice, respectively

PROT$^{-/-}$ mice of 3 months exhibited statistically significant decreased body weights versus wild-type controls. Data are given as means $\pm$ SEM (n = 20 for each genotype). Asterisk indicates significantly different from wild-type mice (p < 0.01 by Students t-test).

4.3.4 Histological Analysis for Detection of Abnormalities in the Brain

In animal experimental models of hyperprolinemia, histological studies revealed degenerative alterations in their brains (Shanti et al. 2004). Because of the broad expression of PROT throughout the CNS, it was required the investigation whether PROT deletion induces gross morphological changes in the knockout brains. Macroscopic comparison of cresyl violet-stained brain sagittal sections of PROT$^{-/-}$ mice versus PROT$^{+/+}$ animals detected no obvious differences, as shown in **Figure 18.**
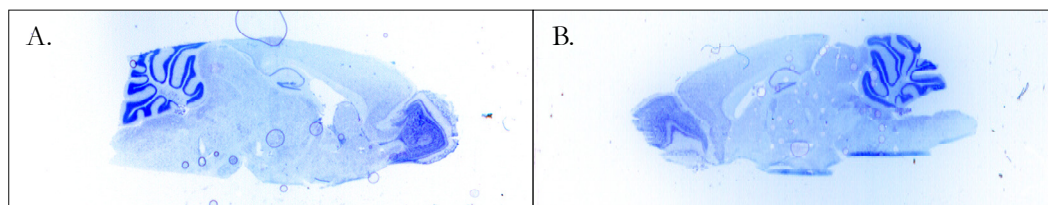
Figure 18 Cresyl-violet stained sagittal sections of wild-type (A.) and knockout (B.) mice

No gross morphological alterations were detected in PROT-deficient mice compared to their wild-type littermates. (For detailed information about staining procedure, refer to section 3.2.22.)

Furthermore, detailed analyses of brain areas that are known to exhibit a high PROT expression, namely the hippocampal formation, striatum and the cerebral frontal cortex, revealed no obvious defects in the number of cells and organization of brain anatomy (**Figure 19**). Therefore, it was concluded that PROT-deficient mice display normal morphological architecture of brain structures. Beyond this observation, PROT-deficient mice were normal in appearance and showed, comparable to their wild-type and heterozygous counterparts, undisturbed development and fertility.
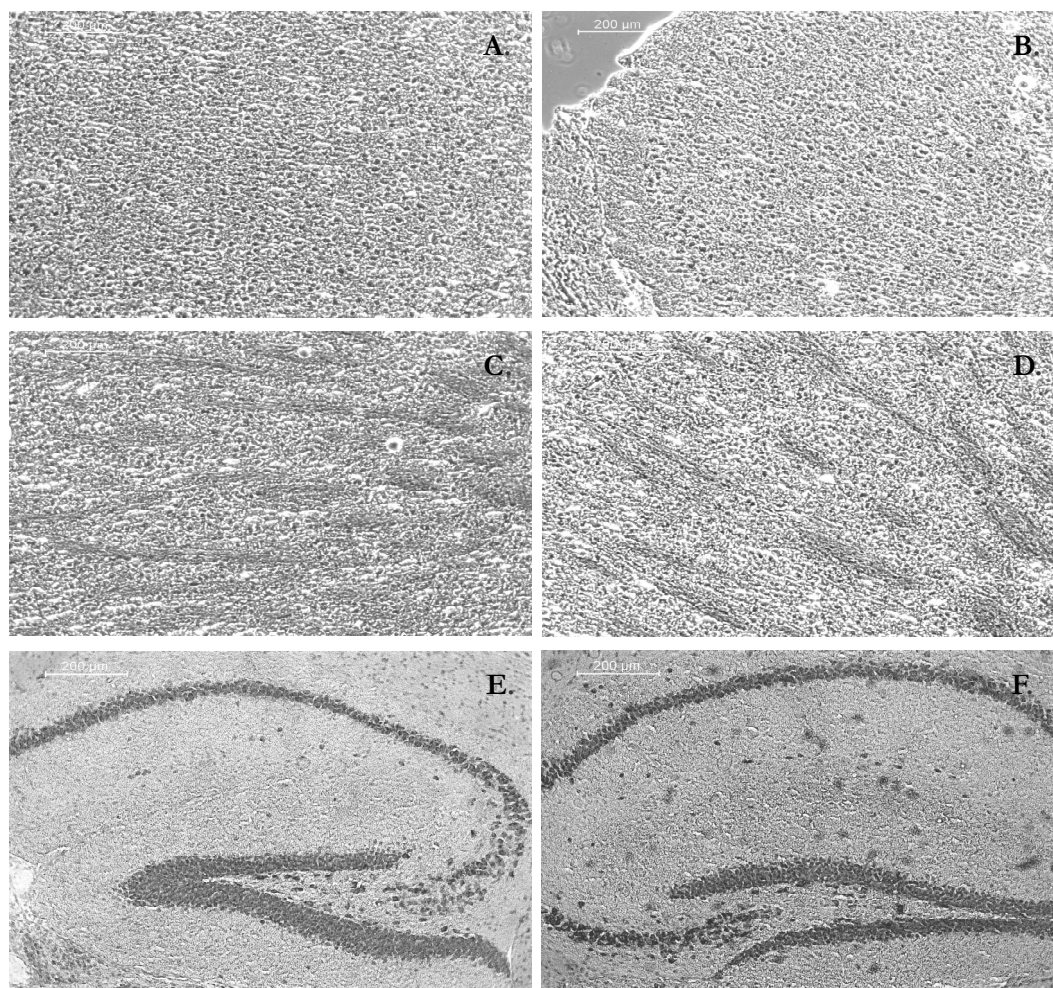
Figure 19 Light microscopy of cresyl-violet stained sagittal sections of frontal cortices (A. and B.), striati (C. and D.) and hippocampal formations (E. and F.) from knockout (A., C., E.) and wild-type (B., D., F.) mice

No alterations in the cellular appearance and tissue formation were observed in PROT-deficient mice compared to wild-type controls. Magnification factor was 10x. (For detailed information about staining procedure, refer to section 3.2.22.)

4.4 Behavioral Phenotyping of PROT-deficient Mice

Given that PROT is a neuronal protein, a comparative investigation of general behaviors of PROT-deficient mice and wild-type controls would be a beneficial way to get insights into putative alterations produced by this mutation. Toward this goal, different behavioral patterns have been examined, including sensorimotor tasks (rotarod and open field), as well as schizophrenia related alterations (PPI-test) and the analysis of nociceptive abilities (hot plate test). All analyses were carried out with 2-3 month old animals.

4.4.1 Nociception - Hot Plate Test

It has previously been proposed that PROT and L-proline might play a role in analgesia, due to the fact that application of enkephalins selectively inhibits transport function of PROT in transfected cells as well as in prepared synaptosomes (Fremeau et al. 1996; Galli et al. 1999). Therefore, it was of interest to study if pain perception is changed in PROT-deficient mice. With the hot plate test sensory, defects in basic pain reception to a thermal stimulus were investigated. For this purpose, the surface of the test plate was heated to a constant temperature of 50°C, mice were then placed on the hot plate, and the latency was measured until the animals started licking a paw or tried to escape. Upon analysis, $PROT^{-/-}$-mice did not demonstrate any genotypical effect with respect to their nociceptive ability's when compared to wild-type control animals. In average, $PROT^{-/-}$ mice displayed a reaction to the thermal stimulus after 2.77±0.1 seconds, whereas $PROT^{+/+}$ mice revealed in mean a reaction time of 2.78±0.07 seconds (n = 20, **Figure 20**). Thus, this result demonstrates that $PROT^{-/-}$ mice have normal sensory capabilities regarding pain perception.
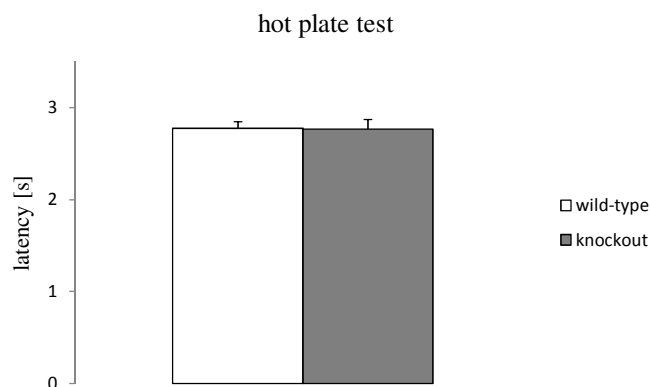
Figure 20 Investigation of sensitivity to nociception

No significant differences were detected in a hot plate test with respect to mean escape latencies for PROT-deficient mice versus wild-type controls. Data are given as means ± SEM (n = 20 for each genotype).

4.4.2 Locomotor Skills - Rotarod Test

It was of interest to examine the locomotor skills of PROT-deficient animals, as it has previously been reported that animals with reduced proline oxidase activity and high plasma L-proline levels exhibit sluggish behavior (Kanwar et al. 1975; Hayward et al. 1993). Therefore, PROT-deficient mice were subjected to the rotarod test, which is an animal test for locomotion skills such as coordination and balance. The animals were placed onto a rod, rotating with an initial speed of 5 rpm that gradually accelerated over 75 seconds to a final speed of 25 rpm. The rotation speed at which the mice could no longer handle walking on the rod was recorded. No significant genotypic effect on the ability of the mice to stay on an accelerating rod was observed (**Figure 21**). In average, the analyzed male PROT$^{-/-}$ mice withstood the forced motor activity to 13.01 ± 1.19 rpm versus on PROT$^{+/+}$ mice that achieved an average performance of 12.62 ± 0.81 rpm. To examine whether locomotor learning was affected by the mutation, both mouse strains were examined 5 minutes later, showing similar increased performance. Here, mutants achieved 14.86 ± 0.84 rpm, compared to PROT$^{+/+}$ mice, achieving 14.28 ± 0.99 rpm (**Figure 21**). In summary, the conducted rotarod analyses demonstrate that PROT$^{-/-}$ mice exhibit normal coordination and balance skills.
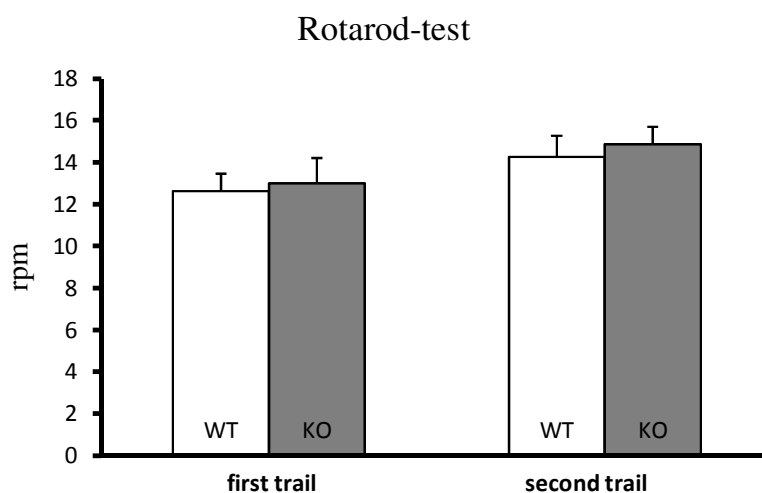
Figure 21 Rotarod analysis of mutants (KO) versus on wild-type (WT) mice

Results are shown from two trails, with the second trail being performed 5 minutes after the first to measure additional locomotor learning abilities. No statistically significant difference in rotarod performance was detected for PROT$^{-/-}$ mice. Data are given as means ± SEM (n = 20 for each genotype). For detailed information about the rotarod protocol used, please refer to section 3.3.9.

4.4.3 Motor Activity - Open Field Test

It was concerned whether PROT might play a role in affecting locomotion, since behavioral studies revealed that mice bearing a mutation in the gene that encodes proline oxidase display high plasma L-proline levels and altered locomotor activity (Moreira et al. 1989; Paterlini et al. 2005). For this reason an analysis of the explorative behavior of the PROT-knockouts was conducted.

The open field test is a standard paradigm to screen for general motor activity and spontaneous explorative behavior, both quantitatively and qualitatively. In this paradigm, mice were individually placed into an open arena and monitored without the experimenter being visible. Then, the distance traveled during 30 minutes under 2 lux illumination intensity was investigated. Total traveled distances of the mutant animals were significantly lower (248.44±14.87 m, n = 14) than those of their wild-type counterparts (313.6±14.94 m, p-value < 0.05), as represented in **Figure 22 A**, hence demonstrating a diminished basic locomotor activity of the PROT-deficient animals. Time course analysis of the traveled distances revealed that PROT-knockout mice were less active during the first 20 minutes of the total 30 minutes observation period (**Figure 22 B**). Two-way ANOVA showed an effect of the genotype on distance moved ($F_{(1,120)}$ = 8.24; p < 0.01) and an effect of the time period on distance moved ($F_{(5,120)}$ = 16.84; p < 0.001).
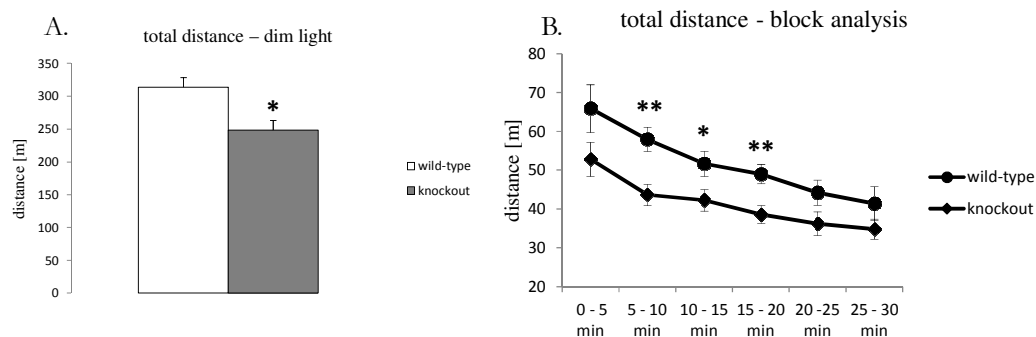
Figure 22 Motor activity test of wild-type and knockout mice

Total distance traveled (**A**) under 2 lux illumination during 30 minutes revealed decreased locomotor activity of PROT$^{-/-}$ mice versus wild-type mice in a novel environment. Time course analysis of total distance traveled (**B**) is presented in intervals (5 min) and displays significantly decreased locomotor activity of PROT$^{-/-}$ mice particularly in the habituation phase to a novel environment. Data are given as means ± SEM (n = 14 for each genotype). Asterisk indicates significant different from wild-type mice, p < 0.05 (Student´s t-test).
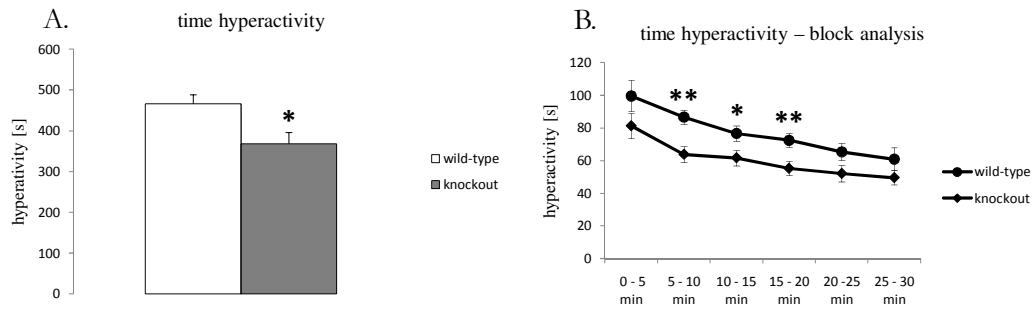
Figure 23 Analysis of time periods spent in hyperactivity

A. Time spent in hyperactivity in a novel environment displays significantly decreased periods for PROT$^{-/-}$ mice particularly in the habituation phase to a novel environment. **B**. Time block analysis in 5 minute intervals display significantly decreased time periods spent in hyperactivity for PROT$^{-/-}$ mice as well particularly in the habituation phase to a novel environment.. Non aversive illumination conditions of 2 lux were used to investigate basic exploration behavior. Data are given as means $\pm$ SEM (n = 14 for each genotype). Asterisk indicates significant difference from wild-type mice, with $p < 0.05$: *, $p < 0.01$: ** (Student´s t-test).

Analysis of time periods in which mice were hyperactive additionally revealed that PROT$^{-/-}$ mice spend in average 368.21$\pm$27.39 seconds in hyperactivity versus on PROT$^{+/+}$ mice spending 466.44$\pm$22.69 seconds (n = 14, p-value < 0.05; **Figure 23 A**). This decrease in high velocity locomotor activity indicates a better attention of the PROT-deficient mice. Furthermore, it shows in agreement to data from the analysis of total traveled distances a lower activity of the mutants in the novel environment. Two-way ANOVA of time course analysis showed an effect of the genotype on time spend in hyperactivity ($F_{(1,120)} = 7.67$; $p < 0.05$) and an effect of the time period spent in the novel environment on time spend in hyperactivity ($F_{(5,120)} = 17.26$; $p < 0.001$). Block analysis (**Figure 23 B**) revealed that the significant difference is only based on the beginning of the open field test and disappears after 20 minutes measurement suggesting as well that the PROT-mutants are more rapidly familiar with the novel environment and therefore exhibit a higher ability to habituate to the test chamber than wild-type controls.

4.4.4 Prepulse Inhibition Test and Acoustic Startle

Prepulse inhibition (PPI) is an indicator of sensorimotor gating both in humans and rodents, a process that is important for filtering irrelevant sensory information and allows attention to be focused on a given stimulus. PPI is determined with a weak acoustic noise (prepulse) that inhibits the reaction to a subsequent strong startling one (pulse). It was of interest to examine the PPI responses of PROT-deficient animals, as mice with an inactivated *PRODH* gene, and thereby exhibiting elevated L-proline levels, show abnormalities in sensorimotor gating (Gogos et al. 1999). Furthermore, it is known that in humans, hyperprolinemia is a risk factor for schizophrenia (Clelland et al. 2011). The PPI test is widely used as a trait marker to diagnose schizophrenia in humans or animals because sensorimotor gating deficits occur in this disease as manifested by a reduction in PPI.

First, an acoustic startle (AS) test was used as a pre-screen for PPI. The acoustic startle response is a protective response, elicited by a sudden and intense acoustic stimulus. Facial and skeletal muscles are activated within a few milliseconds, leading to a whole body flinch in rodents. AS trials were performed to check whether mice were unable to respond to weak prepulse tones whereas they reacted to loud tone pulses. As expected, wild-type and PROT-deficient mice showed no reaction in the presence of the different prepulses presented alone. Interestingly, PROT$^{-/-}$ mice displayed a tendency for higher startle amplitudes, although not statistically significant, than those observed in wild-type animals **Figure 24**. This observation might be due to either better sensory abilities towards acoustic stimuli or an increased anxiety phenotype in PROT-deficient animals.

Notably, a statistically significant genotypical effect showing a higher PPI on prepulse stimuli of 65 db, and 70 db was observed for PROT$^{-/-}$ mice compared with PROT$^{+/+}$ controls (n = 6, p-value < 0.05; **Figure 25**). Prepulse stimuli of 75 db as well revealed a higher degree of PPI but without statistical significance. This indicates that PROT-deficient animals have slightly better sensorimotor gating abilities that could be caused by an enhanced glutamatergic neurotransmission. Based on these results, it can be concluded that PROT-deficiency leads to neuronal adaptions giving rise to better attention abilities.
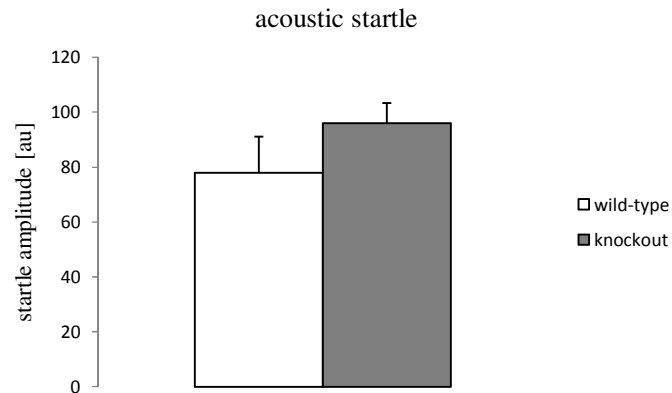
Figure 24 Acoustic startle amplitudes of PROT-knockout mice and wild-type controls.

For PROT mutant mice slightly increased startle amplitudes were observed in comparison to wild-type controls. Data are given as means ± SEM (n = 6 for each genotype, p-value = ns).
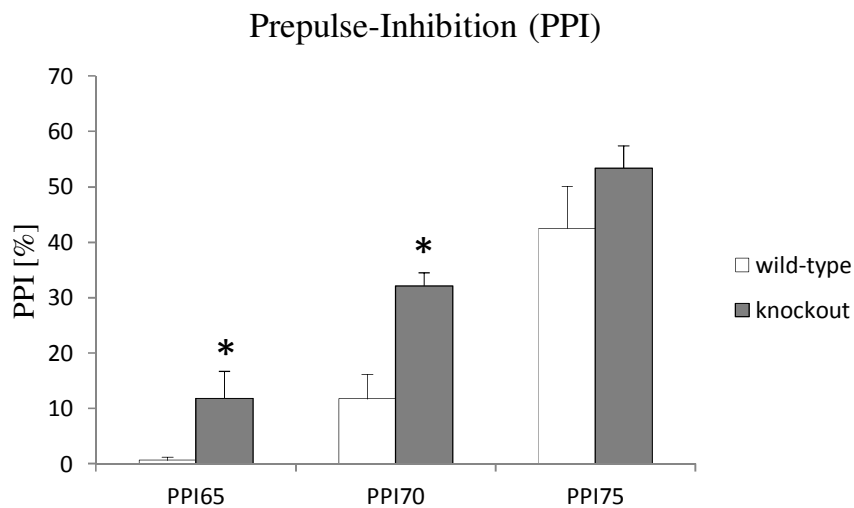
Figure 25 Prepulse inhibition (PPI) of acoustic startle responses of knockout and wild-type mice

Analysis of PPI was conducted at 3 different prepulse intensities as indicated. PPI is expressed as % inhibition of the acoustic startle produced by the main pulse alone. Data are given as means ± SEM (n = 6 for each genotype). Asterisk indicates significant different from wild-type mice, p < 0.05 (Student´s t-test).

4.5   Biochemical Analysis of PROT-deficient Mice

According to literature reports, different knockout experiments point out that inactivation of one gene can modify the expression of related genes. For example, neuronal transporter knockout mice exhibit up- or down-regulations of related synaptic proteins (Xu et al. 2000). To discover the role of PROT protein in neurotransmission in detail and to investigate if its inactivation causes brain biochemical alterations, an examination of the transcriptional expression of several genes by qRT-PCR studies, which are potentially associated with PROT-function, and the quantification of the expression levels of their corresponding polypeptides by Western blotting has been accomplished.

4.5.1   Determination of the Influence of PROT-deficiency on glutamatergic synaptic Biochemistry

As mentioned above (Introduction, 1.3), it is known that PROT is localized primarily at glutamatergic synapses where L-proline produces complex electrophysiological actions. Therefore, it was of interest to investigate possible changes in the expression levels of specific components of glutamatergic neurotransmission, putatively appearing upon deletion of PROT which is thought to increase L-proline concentration in the synaptic cleft.

4.5.1.1 Examination of Possible Alterations Regarding Expression of the Kainate-Receptor

It has been published that high concentrations of L-proline can activate the kainate-subtype of glutamate-receptors in brain slices (Henzi et al. 1992). Furthermore, application of the kainate-receptor inhibitor CNQX was reported to block responses triggered by L-proline (Takemoto 2005). Therefore, in the scope of this thesis, it was investigated whether the absence of PROT has an influence on the expression of kainate-receptors. The amounts of polypeptide expressed in synaptic terminals (P2-fractions) were analyzed by Western-blot, quantified densitometricly (Methods, 3.2.18) and normalized to the reference gene β-tubulin. Due to possible irregular transfer rates over the membrane area, wild-type and knockout samples were loaded alternately.

Upon analysis of the brain universally expressed regulatory KA2 subunit of the kainate-receptor (Herb et al. 1992), no altered expression was observed in frontal cortices of PROT-mutant mice versus wild-type littermates (**Figure 26**). Expression of the presynaptically localized GluR7 subunit was as well detected not to be modified in frontal cortices of PROT-knockout mice (**Figure 26**).

Western-blot analysis of hippocampi revealed a significantly moderate increased expression of GluR7 (+18.9±6.1%, p<0.05) and KA2 (+30.9±6.6%, p<0.01) levels in PROT-deficient mice versus wild-type controls (**Figure 27**). This adaptive increase in expression of KA2 and GluR7 in the hippocampal formation suggests a potentially enhanced sensitivity of neurons containing kainate-receptors towards the transmitter glutamate.
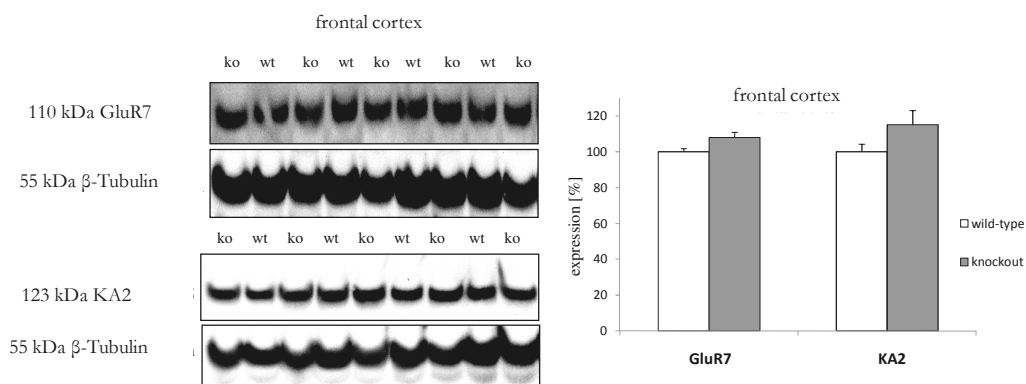
Figure 26 Expression level determination of KA2 and GluR7 subunits in frontal cortices

Left panel: Western-blotting analyses in synaptosomal preparations from frontal cortices of knockout (ko) and wild-type (wt) mice at the age of 3 months. Right panel: Corresponding densitometric quantification of relative GluR7 and KA2 levels in frontal cortices of PROT-knockout and age-matched wild-type animals. Data are given as means ± SEM (n = 4-5 for each genotype).
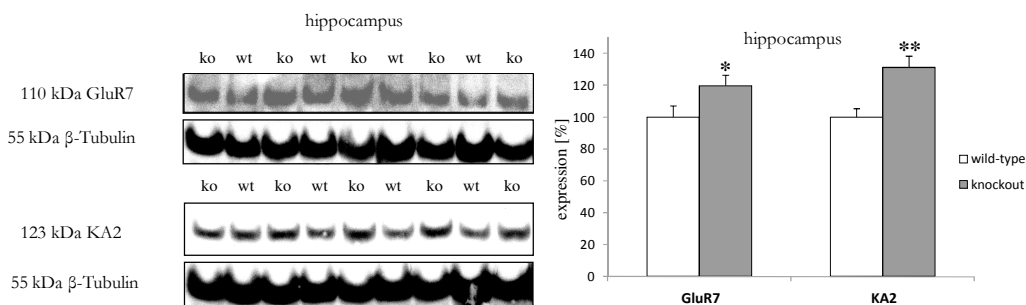
Figure 27 Changes in expression of KA2 and GluR7 subunits in hippocampus

Left panel: Western-blotting analyses of GluR7 and KA2 levels in synaptosomal preparations from hippocampi of knockout (ko) and wild-type (wt) mice at the age of 3 months. Right panel: Corresponding densitometric quantification of relative GluR7 and KA2 levels in hippocampi of PROT-knockout and age-matched wild-type animals. Data are given as means ± SEM (n = 4-5 for each genotype). Asterisk indicates significantly different from wild-type mice, with p < 0.05: *, p < 0.01: ** (Student´s t-test).

4.5.1.2 Analysis of potentially induced Alterations on NMDA-Receptor Expression

Initial examination on the mRNA expression levels of NMDA-receptor components was carried out in mouse samples from frontal cortex, hippocampus and striatum. Analysis was focused on the NMDA-receptor anchoring protein PSD95 and on the NR2A subunit, which is the major regulatory NMDA subunit present in the adult neocortex and hippocampus, regions where as well high PROT expression levels can be found.

Notably, removal of *ProT* significantly induced expression changes of the regulatory NR2A subunit. *ProT* $^{-/-}$ mice exhibited a significantly raised expression of *NR2A* mRNA in frontal cortex (+56.8±18.6%, p<0.05) and hippocampus (+72.9±18.7%, p<0.05), whereas no significant alteration was detected in striatum (**Figure 28**). Interestingly, no expression change was detected on the mRNA levels of the NMDA-receptor anchoring protein PSD95 in any of the analyzed brain areas (**Figure 28**).

To verify that the detected adaptive modifications of mRNA levels upon *ProT*-deletion corresponded to a concomitant increase in the expression of NMDA-receptor polypeptides in synaptic terminals, P2 fractions were prepared and analyzed by Western-blotting. Extraction of proteins was carried out from frontal cortex and hippocampus, previously found by the qPCR analyses to be the brain areas comprising major alterations. In agreement with the mRNA analysis, verification of the NR2A subunit expression by Western-blot analysis detected a significantly, although moderate, increased expression in frontal cortices (+19.7±6.8%, p<0.05; **Figure 29**) as well as a dramatic upregulation in hippocampi (+76.4±7.9%, p<0.01, **Figure 30**) of PROT$^{-/-}$ mutants. In addition, Western-blot analysis also comprised the functionally obligatory NR1 subunit and the regulatory NR2B subunit, which represents the second major NR2 subunits present in the adult neocortex and hippocampus. Investigation of the membrane enriched fractions detected significantly increased levels of the NR1 subunit in frontal cortices (+28.0±4.1%, p<0.05), whereas no significant change in expression was observed in hippocampi, as represented in **Figure 29** and **Figure 30**.

Surprisingly, NR2B expression analysis in PROT-mutant mice revealed an elevation with a sharp increase of this subunit in frontal cortices (+86.3±15.8%, p<0.05; **Figure 29**). Moreover, a significantly upregulated expression of NR2B was observed in hippocampi of PROT-deficient animals (+36.8±10.3%, p<0.01; **Figure 30**). Confirming the qPCR analysis, no genotypical effect was present concerning expression of the NMDA-receptor anchoring protein PSD95 in any of the analyzed brain areas (**Figure 29** and **Figure 30**).
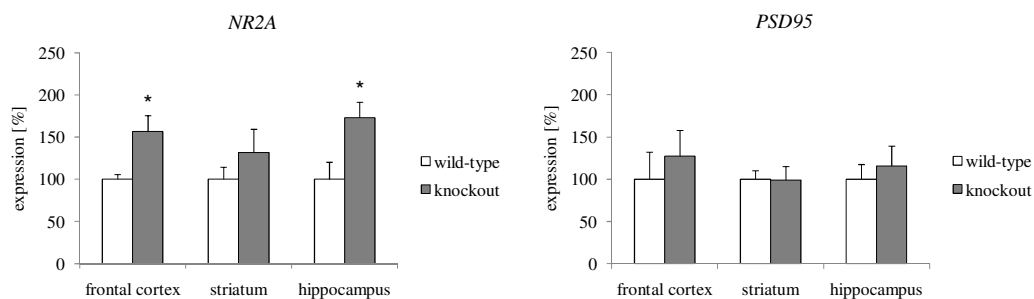
Figure 28 Relative mRNA expression profiling of NMDA-receptor components *NR2A* and *PSD95*

Data were normalized to *β-actin* and represent means ± SEM (n = 3 for each genotype). Asterisk indicates significant difference from wild-type mice, $p < 0.05$ (Student´s t-test).
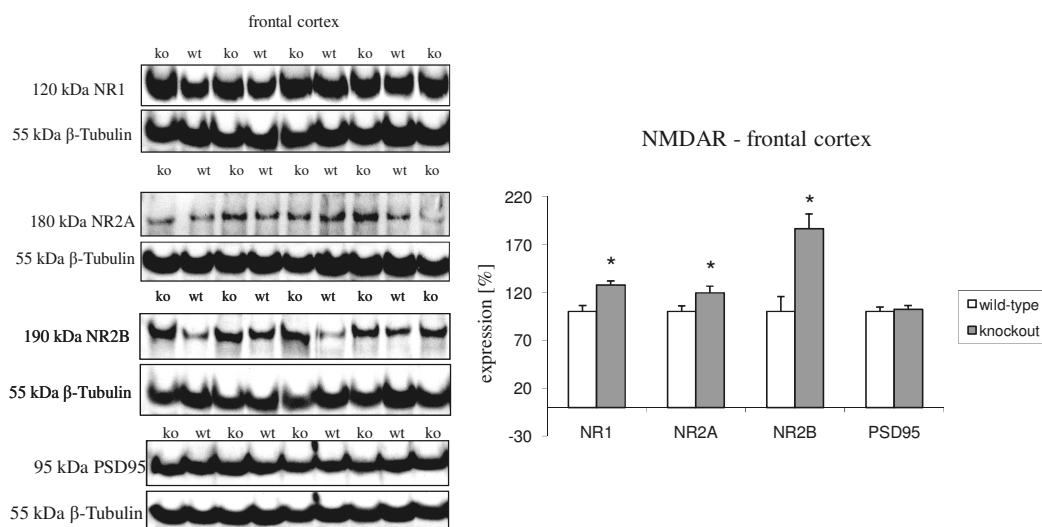
Figure 29 Validation of NMDA-receptor subunit level and -related PSD95 expression in frontal cortices of PROT-knockout and wild-type mice

Left panel: Western-blotting analyses of NR1, NR2A, NR2B and PSD95 levels in synaptosomal preparations (P2-fractions) from frontal cortices of knockout (ko) and wild-type (wt) mice at the age of 3 months. Right panel: Corresponding densitometric quantification of relative levels in frontal cortices of PROT-knockout and age-matched wild-type animals. Data are given as means ± SEM (n = 4-5 for each genotype). Asterisk indicates significant difference from wild-type mice, $p < 0.05$ (Student´s t-test).
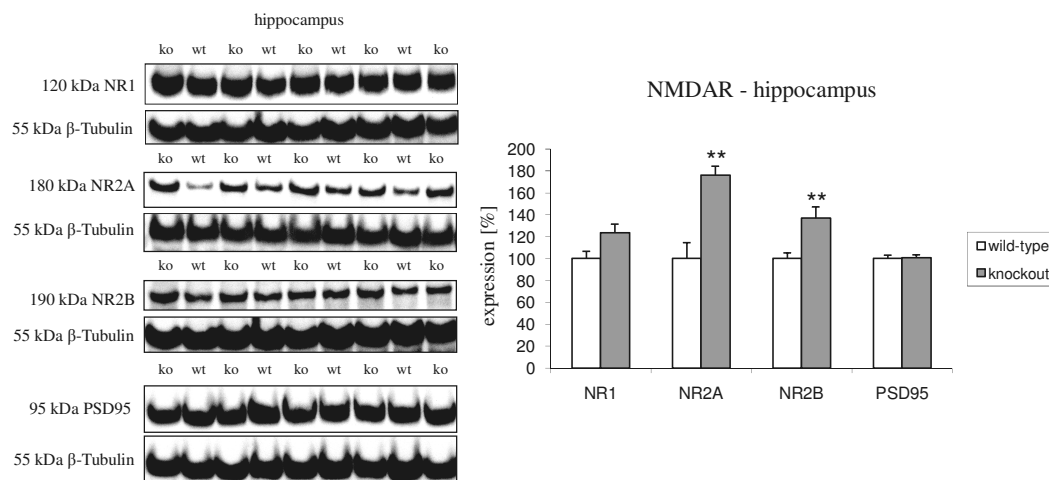
Figure 30 Composition of NMDA-receptor complex in hippocampi of PROT-knockout and wild-type mice

Left panel: Western-blotting analyses of NR1, NR2A, NR2B and PSD95 levels in synaptosomal preparations from hippocampi of knockout (ko) and wild-type (wt) mice at the age of 3 months. Right panel: Corresponding densitometric quantification of relative subunit levels in hippocampi of PROT-knockout and age-matched wild-type animals. Data are given as means ± SEM (n = 4-5 for each genotype). Asterisk indicates significant different from wild-type mice, p < 0.01 (Student´s t-test).

In summary, analysis of NMDA-receptor subunits disclosed that expression levels of subunits were changed after ablation of PROT, thus suggesting a possible alteration in the subunit composition and total number of NMDA-receptors, which could result in changed glutamatergic signaling performance at these brain regions.

4.5.1.3 Investigation of Putative Changes in AMPA-Receptor Expression

AMPA receptors colocalize with NMDA-receptors in many brain areas, and activation of both is necessary to express long-term potentiation (LTP), a molecular basis of learning (for review see Nicoll 2003). As an increase of the NMDA subunits was detected in PROT-knockout mice, and being aware of the fact that application of L-proline at high concentrations activates AMPA-receptors in brain slices (Henzi et al. 1992), it was also of interest to investigate AMPA-receptor expression in *ProT*-deficient mice.

Initial examination of mRNA expression of the ubiquitary expressed *Gria1*, coding for the GluR1 subunit, and *Gria3*, which encodes for the GluR3 subunit, displayed no alterations in both *Gria* transcript levels from PROT-knockout when frontal cortex, hippocampus and striati were analyzed (data not shown).

To investigate whether the *Gria2* gene expression is adaptively modified upon PROT-deficiency, polypeptide expression of the corresponding GluR2 subunit in plasma

membrane enriched fractions of frontal cortices and hippocampi were analyzed by Western-blotting. Similar to *Gria 1 and Gria 3*, polypeptide expression of the GluR2 subunit displayed no change in the cerebral frontal cortex. However, a significantly moderate increase (+20.5% ±4.0 %, p<0.05) was observed in the hippocampal formation (**Figure 31**), thus suggesting a changed glutamatergic excitability by AMPA receptors in this brain region.

Taken together, deletion of PROT induces adaptive changes on glutamate-receptor expression levels in PROT-knockout brains, particularly in hippocampus where expression increase of the regulatory KA2 subunit of the KA-receptor, the regulatory NR2A and NR2B subunits of the NMDA-receptor and the GluR2 subunit of the AMPA-receptor could be observed. Since the hippocampus is a brain area involved in memory function (Milner and Penfield 1955-1956), and activation of AMPA- as well as NMDA-receptors are required for the formation of LTP (O'Connor et al. 1995), these data suggest that PROT-knockout animals might exhibit the prerequisite for better learning abilities in relation to those of wild-types.
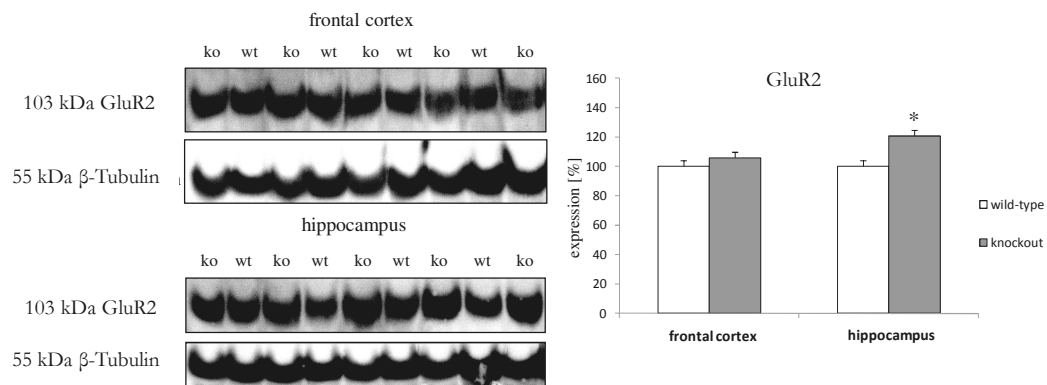
Figure 31 Changes of GluR2 subunit expression in PROT-knockout and wild-type mice

Left panel: Western-blot analysis of GluR2 levels in P2 fractions from frontal cortices and hippocampi of knockout (ko) and wild-type (wt) mice at the age of 3 months. Right panel: Corresponding densitometric quantification of relative GluR2 levels in frontal cortices and hippocampi of PROT-knockout and age-matched wild-type animals. Data are given as means ± SEM (n = 4-5 for each genotype). Asterisk indicates significantly different from wild-type mice, p < 0.05 (Student´s t-test).

### 4.5.2   Examination of Allosteric NMDA-Receptor Modulators

To gain further insights into how PROT-deficiency affects glutamatergic neurotransmission, it was investigated whether expression of genes controlling the allosteric NMDA-receptor modulators glycine and D-serine were changed. It could be envisaged that L-proline could help NMDA-receptors reaching their activated conformation due to the binding to an allosteric site. Evidence came from the observation that high concentrations of L-proline inhibit the binding of [^{3}H]-glycine to the strychnine-sensitive site of NMDA-receptors at the NR1 subunit (Ortiz et al. 1997). If L-proline as well acts as an allosteric enhancer of NMDA-receptor activation, it may be suggested that the level of the other positively allosteric modulating molecules, glycine and D-serine, are adaptively downregulated to protect against increased activation. Therefore, mRNA levels of the D-serine facilitating enzyme serine racemase (*SR*) and the extracellular glycine concentration controlling protein glycine-transporter 1 (*GlyT1*) were studied by qPCR-analysis. As shown in **Figure 32**, no significant decreases in the expression of the mRNA levels of serine racemase or glycine-transporter 1 were detected. The absence of adaptions in the expression of these proteins, controlling the level of allosteric NMDA-receptor modulators, suggests that L-proline does not activate NMDA-receptors by an allosteric mechanism via the NR1 subunit.
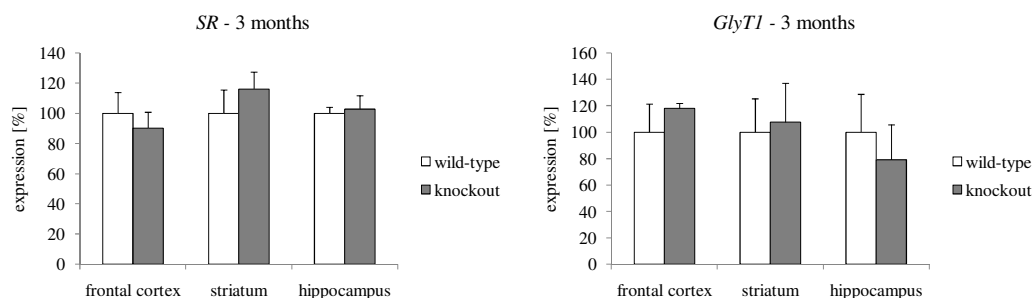
Figure 32 Relative RNA expression profiling of serine racemase (SR) and glycine-transporter 1 (GlyT1) of PROT-knockouts and wild-type mice

Data were normalized to *β-actin* and represent means ± SEM (n = 3 for each genotype).

4.5.3 Investigation of Components of Dopaminergic System

It is known that NMDA-receptors modulate the extracellular levels of dopamine in brain (Araneda and Bustos 1989). Consequently, dopaminergic neurotransmission could be affected as NMDA-receptors are altered in PROT-deficient animals (4.5.1.2). Determination of the expression of the enzyme catechol-O-methyltransferase (*COMT*) mRNA in frontal cortices of *ProT*-deficient animals revealed no significant changes (**Figure 33**). Similarly, no significant change in *COMT* expression was observed in striatum and hippocampus. Examination of the dopamine synthesizing enzyme tyrosine hydroxylase (*TH*) revealed a dramatic, statistically significant upregulation of 144.7±32.6% in frontal cortex of PROT-deficient mice (**Figure 33**). Even though PROT-deficient animals exhibited a moderate upregulation of the dopamine-receptor 1 (*DRD1*) mRNA in frontal cortices of 76.0±20.9 %, it was not statistically significant due to a high variance (**Figure 33**). However, the most potent adaptions on mRNA expression within the dopaminergic system were found for the dopamine-receptor 2 (*DRD2*). Frontal cortices of PROT-deficient mice exhibited a more than six fold increase in *DRD2* mRNA (+573.4±120.5%), and a more than three-fold expression (+241.3±74.0%) of *DRD2* mRNA in hippocampi (**Figure 33**).
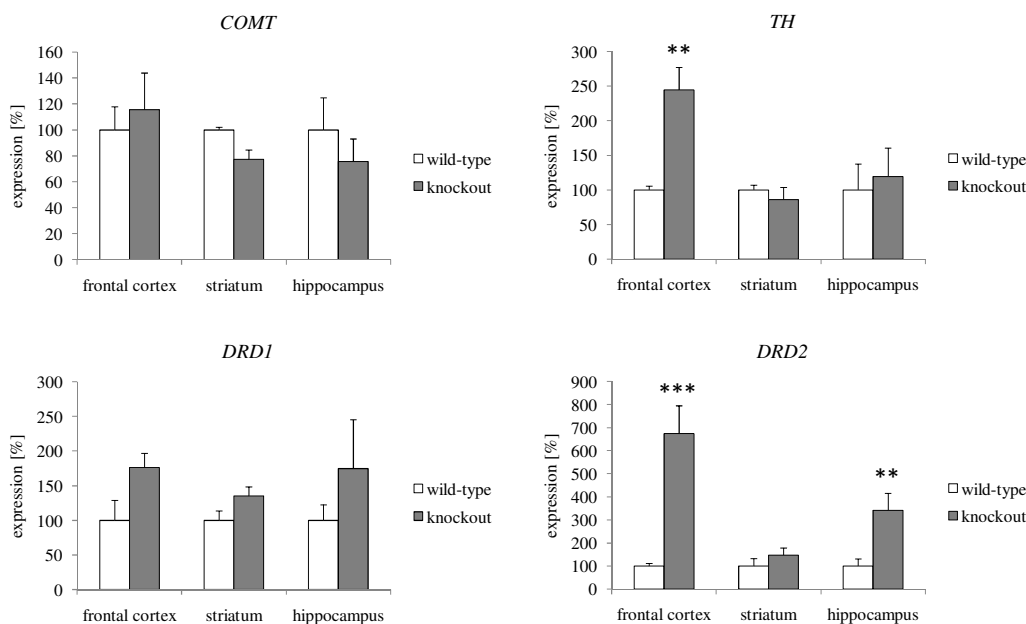
Figure 33 Relative mRNA expression profiling of proteins involved in dopaminergic neurotransmission of PROT-knockouts and wild-type mice

Data were normalized to *β-actin* and represent means ± SEM (n = 3 for each genotype). Asterisk indicates significantly different from wild-type mice, with $p < 0.01$: **, $p < 0.001$: *** (Student´s t-test).

In summary, deletion of PROT results in changes on the expression levels of components of the dopaminergic system, thus suggesting a dysregulation of dopaminergic neurotransmission probably mediated by the persistent glutamatergic alteration previously observed in PROT-knockout mice. Interestingly, a mechanism to enhance working memory has been proposed to be mediated through activation of hippocampal DRD2-receptors (for a review, see Liggins JTP, 2009). Therefore, DRD2 increase in PROT-knockout mice strongly suggests improved performance in memory trials for these animals compared to wild-type mice.

4.6 Further Behavioral Analysis of PROT-Knockout Mice

The finding that PROT-knockout animals displayed an altered expression of synaptic components involved in glutamatergic and dopaminergic neurotransmission prompted us to further investigate potential behavioral abnormalities in these mice. Activation of glutamate-receptors is the molecular basis controlling several behavioral patterns, such as affective and cognitive tasks. Therefore, open field by intensive illumination, forced swim and Y-maze tests were examined next.

4.6.1 Anxiety - Zone Analysis Test

The fact that NR2A knockout mice display reduced anxiety-like behavior (Boyce-Rustay and Holmes 2006), in connection with the NR2A upregulation observed in PROT-deficient animals, proposed an altered anxiety-like behavior in PROT-mutants. In order to prove this hypothesis, open field test analyses with aversive illumination conditions were conducted. By intensive illumination instead of very dim light, the open field test can be used to study emotionality of mice, as normal behavior of mice is to seek the protection of the periphery (Archer 1973). Interestingly, the distances that mice traveled into the center of the open field revealed a significant genotypical effect using 250 lux illumination intensity: $PROT^{-/-}$ mice covered only a small distance of 0.66 ± 0.03 meters compared to $PROT^{+/+}$ animals that traveled 2.0 ± 0.12 meters into the center (**Figure 34).** Although $PROT^{-/-}$ mice exhibit a lower basal locomotor activity, which accounts for a reduction of 20%, the disparity of the traveled distance in the center composes 67% reduction.

A   distance center

B   visits center

C   time center
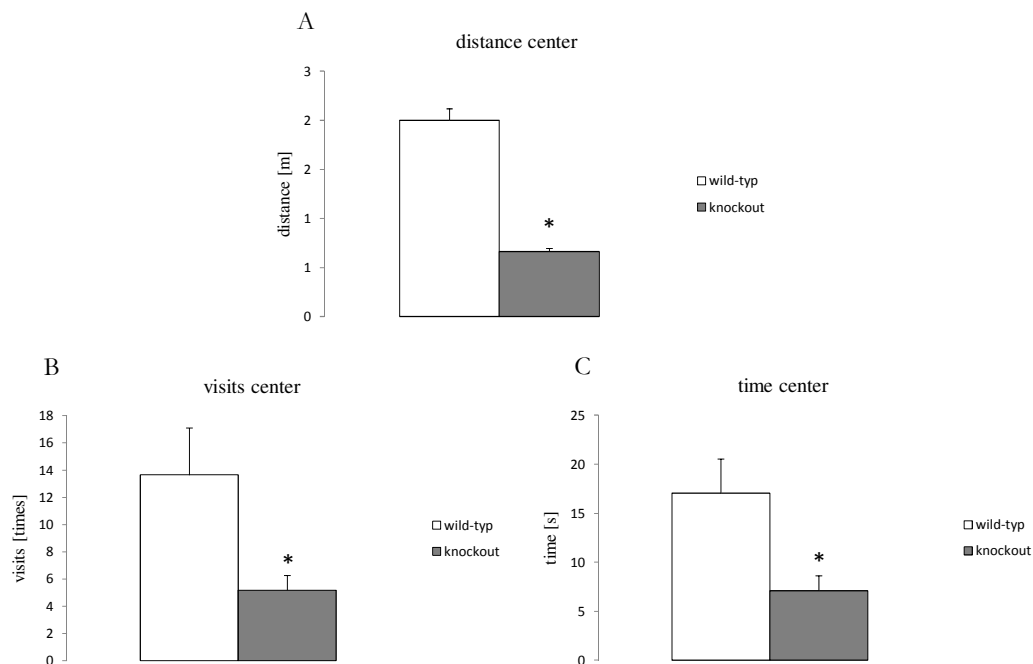
Figure 34 PROT-knockout mice exhibit increased anxiety-like behavior compared to wild-type animals.

PROT-knockout mice traveled significantly less far into the center area of the open field (A) as compared to wild-type controls. Furthermore, PROT mutants made significantly less entries into the center of the open field (B) and spent significantly less time in the center area (C). Data are given as means $\pm$ SEM (n = 20 for each genotype). Asterisk indicates significant different from wild-type mice, $p < 0.05$ (Student´s t-test).

Consistent with the results concerning traveled distances into the center, there was a significant genotypical effect for the total number of visits to the center of the open field: PROT$^{-/-}$ animals entered the center significantly less often (5.18$\pm$1.08, p-value < 0.05) than PROT$^{+/+}$ control mice (13.65$\pm$3.46, n = 17) as represented in **Figure 34**. Accordingly, the average of time PROT$^{-/-}$ mice spend in the center, was 7.09$\pm$1.56 seconds versus 17.04$\pm$3.52 seconds for PROT$^{+/+}$ controls (n = 17, p < 0.05; **Figure 34**). In summary, zone analysis data, using aversive illumination conditions, indicates an increased anxiety phenotype of the mutant mice, by uncovering increased avoidance behavior with respect to numbers of visits to, distance traveled into, and time spend in the center of the open field.

4.6.2   Depression - Forced Swim Test

The increase observed in biochemical analysis with respect to GluR7 expression gave rise to examine depression related behavior, since GluR7 is known to be associated with recurrent major depressive disorder (Schiffer and Heinemann 2007). Additionally, being aware of the finding that PROT-deficient mice exhibit a changed emotionality, namely an increased anxiety-like behavior (4.6.1), further analysis of affective behaviors was accomplished by examining the animals in a forced swim test. The forced swim test, also referred to as Behavioral Despair test, is used to investigate depression related behavior in animals. Mice were put in a cylinder from which they could not escape, and which was filled with water forcing the mice to swim. Information about emotionality is gained from the duration of immobility (or vice versa from the time of swimming). Usually, confrontation with this aversive situation firstly induces escaping behavior that later on changes to immobility, where the mice let themselves float in the water.

Interestingly, a significant genotypical effect on the time period of immobility could be assigned to PROT$^{-/-}$ mice, which spent less time (60.89 $\pm$ 6.97 s resp. 20.3 $\pm$ 2.3%) immobile over a 5 minute period compared to PROT$^{+/+}$ mice (127 $\pm$ 11.41 s resp. 42.3 $\pm$ 3.8%), indicating a behavioral correlation with either positive mood or increased fear due to enhanced escaping behavior (**Figure 35**).
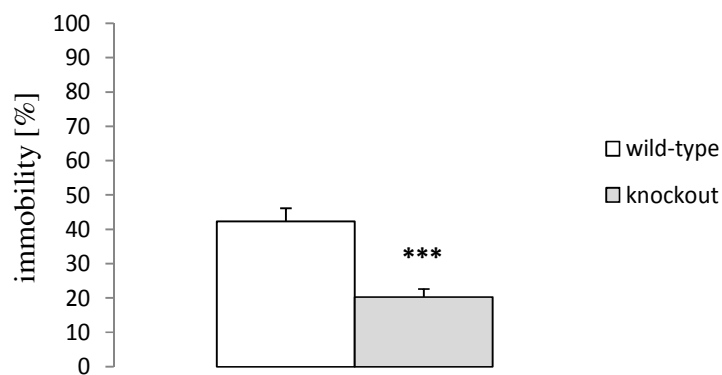
Figure 35 Immobility in the forced swim test of knockout and wild-type mice.

PROT-knockout mice significantly behaved less immobile than wild-type control animals. Data are given as means $\pm$ SEM (n = 10 for each genotype). Asterisk indicates significantly different from wild-type mice, p < 0.0001 (Student´s t-test).

4.6.3   Short Term Memory - Y-Maze Test

It was reported by Bavaresco et al. that chronic hyperprolinemia causes memory deficits (Bavaresco et al. 2005). In addition, biochemical investigations of the present thesis revealed a change in the expression levels of NMDA-receptor subunits of the knockout animals (section 4.5.1.2). On the basis of these findings, it was supposed that the long-term potentiation (LTP) is altered, affecting memory formation in the mutant mice.

To examine this, $PROT^{-/-}$ mice as well as wild-type controls were studied for spontaneous alternation behavior in a Y-maze test. This paradigm is considered to reflect spatial working memory, which belongs to the short term memory. It was monitored whether these animals alternate between the "arms", reflecting if they remember which "arm" they entered last.

Interestingly, a significant genotypical effect was disclosed by the investigation of the spontaneous alternation behavior (**Figure 36**). $PROT^{-/-}$ mice outperformed wild-type controls by entering significantly more often a new "arm" (75.06 ± 2.05 % of the total entries versus on $PROT^{+/+}$ mice, 55.47 ± 2.8 % of the total entries; n = 8, p-value < 0.001). This result indicates that PROT-deficient mice exhibit an enhanced spatial working memory due to the observed better performance in this test.
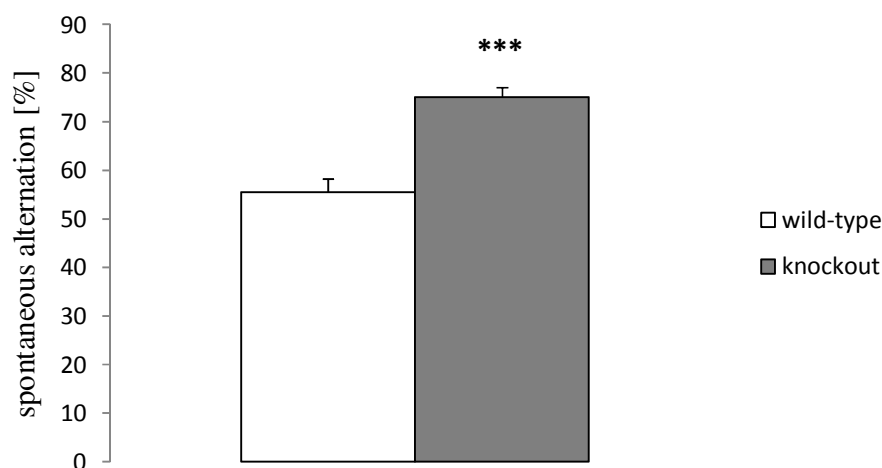
Figure 36 Analysis of spontaneous alternation behavior in the Y-maze test of PROT-knockout and wild-type mice.

PROT-knockout mice performed significantly better in this cognitive task compared to wild-type controls. Data are given as means $\pm$ SEM (n = 8 for each genotype). Asterisks indicate significantly different from wild-type mice, p < 0.001 (Student´s t-test).

Taken together, these results indicate that the alterations detected in synaptic components of PROT-knockout mouse brains are associated with enhanced reaction to aversive stimuli, as demonstrated by two anxiety-related test paradigms, and modifications in memory formation. Our behavioral data are in agreement particularly with the expression increase of NMDA-receptor subunits and DRD2 in hippocampus of PROT-deficient mice, as this brain region is primarily involved in learning and memory, and anxiety-related responses are thought to be mediated by the septohippocampal system in both humans and animals.

4.7   Analysis of Mature PROT-Knockout Mice

Aging is known to influence many physiological processes in the brain, including expression of neurotransmitter receptors, thus resulting in modulation of neurotransmission functionality and behavioral patterns (Clayton et al. 2002a; Clayton et al. 2002b). To discover whether the observed behavioral alterations of PROT-deficient mice increase during the aging process, further analyses were carried out with mature mice.

4.7.1   Behavioral Analysis

4.7.1.1 Open Field Analysis

In agreement with the experimental data gained from the analysis of 3 months old mice, mature 8 months old PROT$^{-/-}$ mice as well covered significantly lower traveled distances (205.44±12.17 m, n = 18) in the open field compared to PROT$^{+/+}$ mice (278.77±13.82 m, p-value < 0.001, **Figure 37 A**). Time course analysis of the traveled distances revealed that PROT-deficient mice were less active during each 5-min interval of the total 30 minutes observation period (**Figure 37 C**). Two-way ANOVA showed a significant effect of the genotype on distance moved ($F_{(1,180)}$ = 15.55; p < 0.001) and of the time period on distance moved ($F_{(5,180)}$ = 38.76; p < 0.001). Therefore, PROT-mutants exhibit a higher ability to habituate to the test chamber than wild-type controls, possibly due to changed signaling abilities of glutamate receptors leading to enhanced long-term-potentiation. For specification, this enhanced effect on locomotor activity with respect to the genotype was observed to be stronger in mature PROT-deficient animals, thus indicating that the adaptive effects of the mutation increase upon aging of the laboratory animals.

In addition to the analysis of the horizontal activity, an even stronger genotypical effect was ascertained with mature 8 months old PROT$^{-/-}$ mice by examination of the time that was spent in hyperactivity. In average, PROT-mutants exhibited significantly lower hyperactive time periods (281.93±19.22 s) in comparison to wild-type controls (420.89±24.23 s, n = 18, p-value < 0.001, **Figure 37 B**). Block analysis confirmed this result by displaying that PROT-knockouts spent less time in hyperactivity during each 5-min interval of the total 30 minutes observation period (**Figure 37 D**). Two-way ANOVA of time course analysis revealed an effect of the genotype on the time spend in hyperactivity ($F_{(1,180)}$ = 19.6; p < 0.001), and additionally an effect of the time period spent in the novel environment, on the time spend in hyperactivity was disclosed ($F_{(5,180)}$ = 35.33; p < 0.001). Via this observed

improved habituation abilities, it could be concluded that PROT ablation induces adaptions that ameliorate attention and learning deficits occurring upon aging.
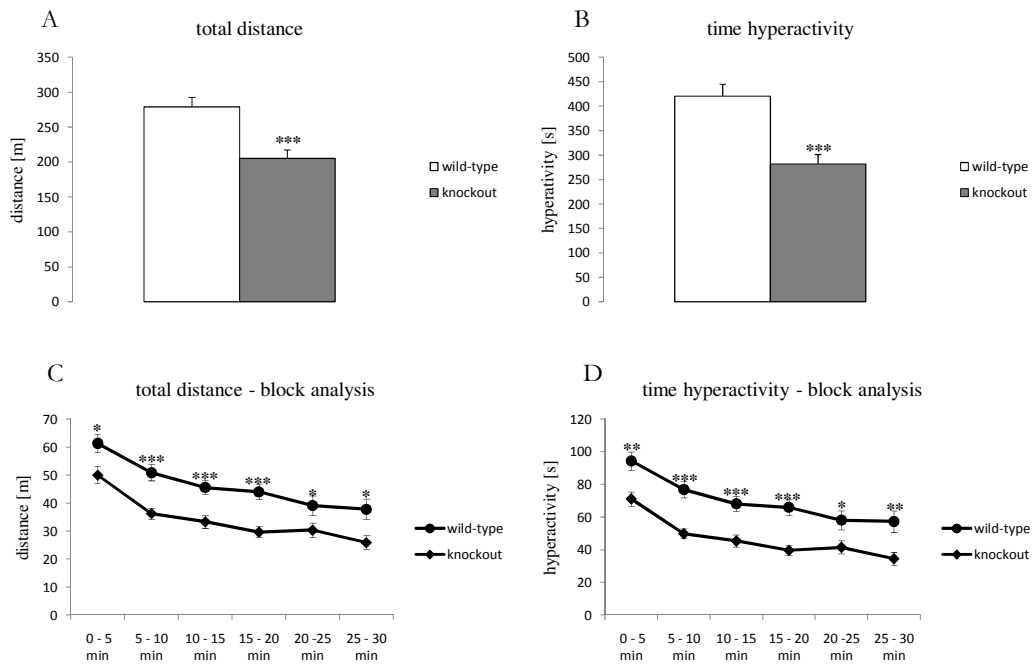
Figure 37 Motor activity test of 8 months old wild-type and knockout mice

A. Investigation of total covered distances (q.v. 4.4.3) revealed a statistically significant decreased locomotor activity of mature PROT$^{-/-}$ mice in a novel environment. **B.** Determination of periods spent in hyperactivity after exposure to a novel environment by 8 months old knockout and wild-type mice shows a significant genotypical effect. Total time spent in hyperactivity over 30 minutes display significantly decreased hyperactivity-time for PROT$^{-/-}$ mice versus control animals under non aversive conditions (2 lux illumination intensity). **C.** Time course analysis of total covered distance shown in intervals of 5 min revealed a particular decreased locomotor activity of PROT$^{-/-}$ mice in the first half phase (habituation phase) of the test. **D.** Block analysis of time spent in hyperactivity in 5 minute intervals (B) display significantly decreased observed hyperactive time periods for PROT$^{-/-}$ mice versus control animals Illumination conditions of 2 lux were used to investigate basal exploration behavior. Data are given as means $\pm$ SEM (n = 14 for each genotype). Asterisk indicates significantly different from wild-type mice, with $p < 0.05$: *, $p < 0.01$: **, $p < 0.001$: *** (Student´s t-test).

4.7.1.2 Y-Maze Test

To investigate retentivity of mature PROT-deficient mice, they were subjected to a Y-maze test. In agreement with the observations obtained by analyses of 3 months old mice, also 8 months old PROT$^{-/-}$ mice entered significantly more frequently a new "arm" of the maze (71.42 $\pm$ 2.34 %, n = 8) than PROT$^{+/+}$ controls (51.39 $\pm$ 2.31 % of the total entries, p-value < 0.001) of this age (**Figure 38**). These data show that mature PROT-deficient mice display a significantly improved spatial working memory in relation to wild-type controls of the same age.
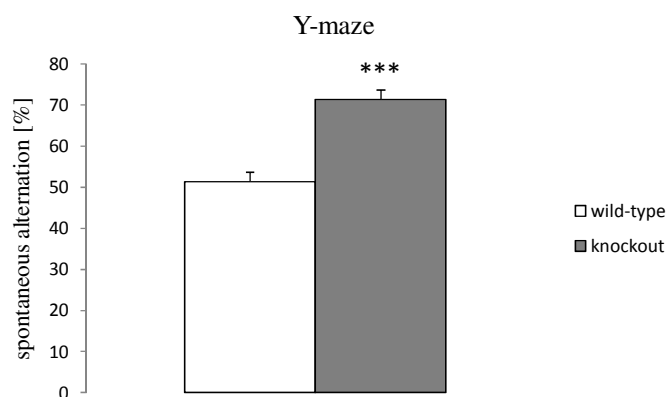
Figure 38 Examination of spontaneous alternation behavior of mature mice in a Y-maze test.
PROT-knockout mice were shown to perform significantly better in this cognitive task than wild-type controls. Data are given as means $\pm$ SEM (n = 8 for each genotype). Asterisk indicates significant different from wild-type mice, p < 0.001 (Student´s t-test).

4.7.2 Analysis of NMDA-Receptor Composition in Mature Mice

Aging is known to be associated with a selective decrease in the expression of NR1, NR2A and NR2B subunits of the NMDA-receptor (Clayton and Browning 2001; Sonntag et al. 2000). To investigate whether the detected alterations in NMDA-receptor expression of PROT-deficient mice vary during aging of the animals, further Western-blot analyses were carried out.

Surprisingly, and in discrepancy to the results from the behavioral analysis of 8 month old PROT-deficient animals, investigation of the amounts of polypeptides expressed in synaptic terminals of 11 months old mice led mainly to the observation that no differences in expression of NMDA-receptor subunits were detectable (**Figure 39**, **Figure 40**). The only exception was the expression of the NR2B subunit in hippocampi, which was still significantly increased in *ProT*-deficient animals (**Figure 40**). These results

indicate a counter regulation to the observed adaptions in the expression of NMDA receptor subunits found for PROT-deficient mice at the age of 3 months.
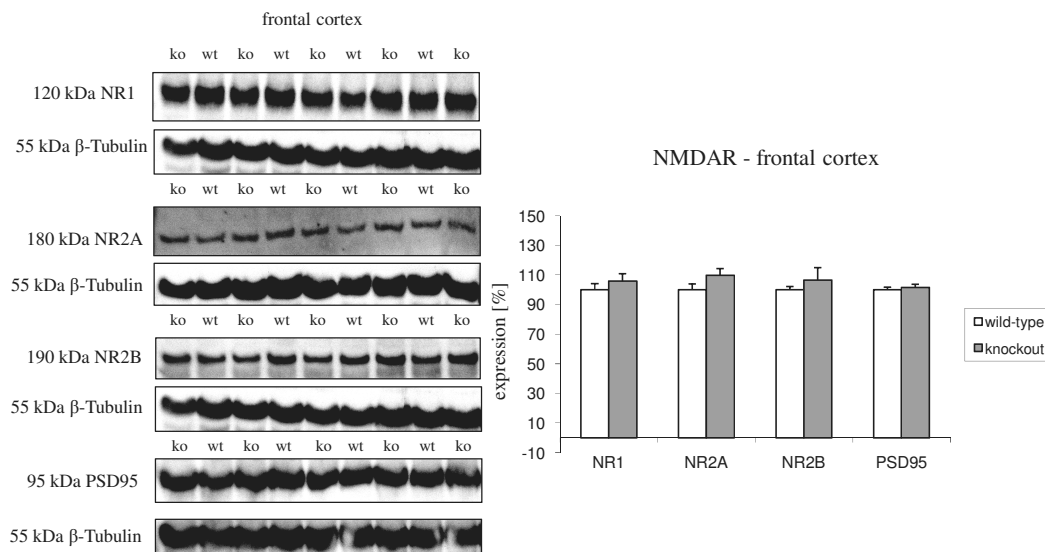
Figure 39 Validation in NMDA-receptor subunit level and -related molecule PSD95 expression

Left panel: Western-blot analyses of NR1, NR2A, NR2B and PSD95 levels in synaptosomal preparations (P2-fractions) from frontal cortices of 11 months old knockout (ko) and wild-type (wt) mice. Right panel: Corresponding densitometric quantification of relative subunit levels in frontal cortices of PROT-knockout and age-matched wild-type animals. Data are given as means ± SEM (n = 4-5 for each genotype). Asterisk indicates significant different from wild-type mice, $p < 0.05$ (Student´s t-test).
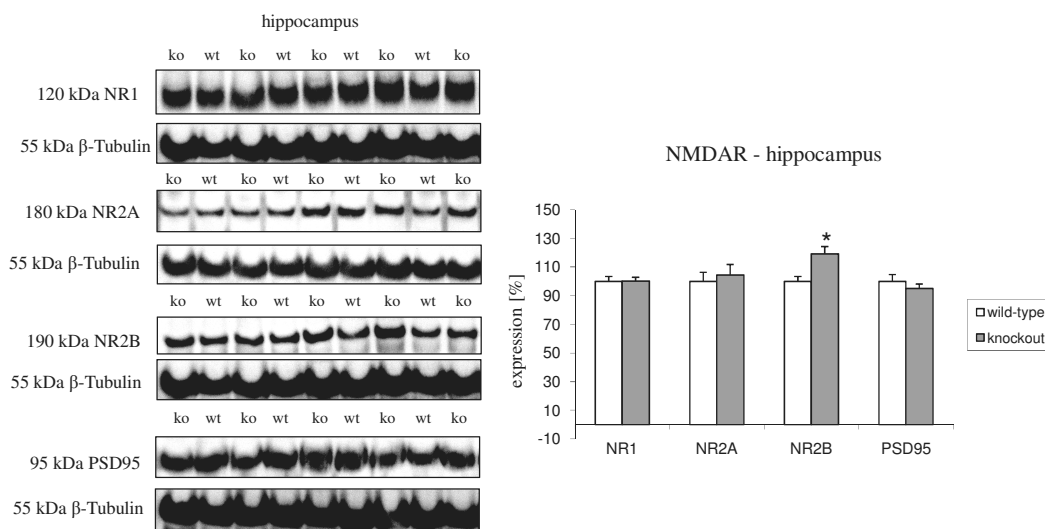
Figure 40 Composition in NMDA-receptor complex in hippocampi of mature PROT-knockout and age-matched wild-type mice

Left panel: Western-blot analyses of NR1, NR2A, NR2B and PSD95 levels in synaptosomal preparations from hippocampi of 11 months old knockout (ko) and wild-type (wt) mice. Right panel: Corresponding densitometric quantification of relative subunit levels in hippocampi of PROT-knockout and age-matched wild-type animals. Data are given as means ± SEM (n = 4-5 for each genotype). Asterisk indicates significant different from wild-type mice, $p < 0.01$ (Student´s t-test)

.

5   Discussion

Within the scope of this thesis the generation of a new mouse model was described. In the generated mouse strain, the expression of a functional murine *ProT* gene was abolished (knockout strain). Furthermore, this mouse strain was analyzed and initial experiments were accomplished. The data derived from these studies will be discussed in this chapter.

5.1   Generation and Validation of the PROT-deficient Mouse Strain

The aim of this thesis was the generation of a mouse line with a mutated *ProT* gene locus and, as a result, the ablation of the expression of a functional PROT protein. This was achieved through the use of established knowledge in genetics and cell biology. Fragments of mutated genomic DNA are introduced into mouse mammalian embryonic stem (ES) cells and can recombine with endogenous homologous sequences via crossing-over events (Thomas et al. 1986). These targeted ES cells can then be used to transfer the manipulated gene into the mouse germline to create a chimeric animal (Robertson 1991). This chimera can then be used to create a manipulated mouse strain through breeding, in case the mutation is not lethal.

In this thesis, a targeting construct was created and subsequently transferred into HM1-ES cells from SV129 origin to mutate the murine *ProT* locus (4.1.3 & 4.1.4). Selection for targeted ES cell clones was performed upon culture in G418 and FIAU containing media. Homologous recombination of the targeting construct was successfully verified by Southern-blot analysis (4.1.4) and yielded ten homologously recombined ES cell clones. The frequency of homologous recombination observed in this experiment was higher (9.4%) in relation to earlier reported homologous recombination frequencies of 1–3% (Capecchi 1989). An exponential relationship has been described between the size of the homologous region and the targeting frequency (Capecchi 1989), meaning that an increase in homology leads to highly elevated recombination frequencies. Moreover, the possibility of a homologous recombination also depends on the state of compaction of the targeted genomic DNA locus (Hasty et al. 1991). As our targeting vector contained DNA sequences comparable in size to other targeting constructs previously used to generate different knockout mouse lines, the high frequency of homologous recombination observed in our experiment could be due to the possibility that the murine *ProT* gene locus is highly accessible for recombination events in ES cells.

The reimplanted blastocysts gained upon injection of the ES cell clone 105 led to the birth of chimeric male mice that were used to transmit the mutation to progeny. It was

successfully verified by PCR analysis that the offspring generated by mating the chimera with C57/B6 mice exhibited the mutation according to the ratios described by Mendel. Similarly, it was confirmed by RT-PCR and by qPCR (4.2.1) that the mutation of the *ProT* gene locus led to decreased *ProT* transcript in heterozygous animals and to total abortion of *ProT* mRNA expression in homozygous mice. Moreover, a decreased PROT polypeptide content in isolated synaptosomes could be determined in preparations of heterozygous PROT-knockouts and the analysis of homozygous PROT-deficient mice proved the complete absence of PROT polypeptide (4.2.2). Taken together, the generation of the PROT-knockout mouse line could be therefore successfully verified.

5.2   Characterization of PROT-deficient Mice

PROT-knockout mice were normal in appearance and showed, similar to their wild-type and heterozygous counterparts, undisturbed development and fertility. In addition, they display normal morphological architecture of brain structures (4.3.4). Furthermore, no significant expression differences of the L-proline metabolizing enzymes were detected, indicating unchanged L-proline metabolism. Therefore, the PROT-deficient mouse strain represents a valuable tool for the analysis of PROT-function *in vivo*.

5.2.1   Contribution of PROT to Sodium-dependent High Affinity L-Proline Uptake in Brain

Synaptosomal preparations of PROT-deficient mice compared to wild-type animals revealed a significant reduction in high-affinity Na^+-dependent uptake of L-proline of different brain areas. The contribution of PROT to the total Na^+-dependent high affinity L-proline uptake was observed to be more than 80% in hippocampus, 54% in olfactory bulbs, ~70% in frontal cortex, and ~80% in striatum (4.3.1). These results are consistent with the expression pattern of PROT determined by Northern-blot analysis, which displayed high expression levels in hippocampus, lower in cortex, and low expression levels in olfactory bulb (Fremeau et al. 1992). The discrepancy between the observations that striatum exhibit high levels of L-proline transport (**Figure 14**) but only low levels of *ProT* mRNA (**Figure 12**) is possibly due to the fact that PROT is synthesized in glutamatergic pyramidal cells in frontal cortex and transported to axon terminals of descending pathways into the striatum.

Addition of sarcosine, an inhibitor of PROT (Fremeau et al. 1992), decreased the uptake of L-proline in synaptosomal preparations of wild-type to similar levels as in the knockout mice (4.3.1). Notably, sodium-dependent L-proline accumulation in knockout mice was also further slightly inhibited by the addition of sarcosine. Thus, this inhibited L-proline accumulation in the knockout mice might be due to any transporter different from PROT, for instance, a low affinity metabolic amino acid transporter like the v7-3 transporter (Drgonova et al. 2007). Taken together, these experiments revealed that PROT mainly contributes to the high-affinity Na^+-dependent L-proline uptake in brain. Therefore, it can be concluded that a physiologically effective knockout of the *ProT* gene is present in the PROT-knockout mouse strain.

5.2.2   Influence of PROT-Deletion on Glutamatergic Neurotransmission

Previous studies have revealed that application of L-proline to brain slices can activate glutamate-receptors of the NMDA-, KA-, and AMPA-type (Henzi et al. 1992; Martin et al. 1992), thus suggesting that PROT is involved in glutamatergic neurotransmission. In addition, it is known that other neuronal transporter knockout mice display molecular adaptive mechanisms, up- or down-regulating related synaptic proteins (Xu et al. 2000). Given that the neuronal L-proline transporter is absent upon embryogenesis in PROT-deficient mice, it could be envisaged that similar compensatory conditions could also occur in these animals, modifying the expression profile of glutamate-receptors.

Within the scope of this thesis, densities of the KA-receptor subunits, KA2 and GluR7, have been found to be upregulated in hippocampus of PROT-knockout mice (4.5.1.1). Since the presynaptic action of KA-receptors is lost in GluR7-knockout mice (Pinheiro et al. 2007), this subunit is suggested to exhibit an exclusively presynaptic localization. On the other hand, the KA2 subunit is mainly localized at postsynaptic sites (Darstein et al. 2003). Thus, KA-receptors are localized pre- and postsynaptically, and are able to regulate transmission of information and excitability in a synapse-specific manner (Lerma et al. 2001). The size of postsynaptic KA-receptor-mediated currents is 10-fold smaller than AMPA-mediated currents, but exhibits a longer duration with a consequently longer integration time (Lerma et al. 2001). Therefore, the adaptive increase in expression of KA2 in the hippocampal formation could result in enhanced sensitivity to the transmitter glutamate. Altogether, the increased expression of both pre- and postsynaptic subunits suggests a different arrangement of KA-receptors in PROT-deficient mice, which could result in altered glutamatergic signaling.

Upon analysis of the expression of the AMPA-receptor subunits, moderate upregulation of GluR2 polypeptide was also observed in the hippocampal formation of PROT-knockout mice (4.5.1.3). AMPA-receptors are heterotetramers composed of maximum two different subunits, with GluR2 being a key subunit for the formation of functional receptors (Mansour et al. 2001). The GluR2 subunit is localized at postsynaptic elements (Hampson et al. 1992). A change in synaptosomal GluR2 therefore likely reflects an alteration in AMPA-receptor availability in dendritic spines, which would result in changed glutamatergic neurotransmission in PROT-deficient hippocampus.

In addition, it was ascertained that PROT-deficient mice exhibit an increase in NMDA-receptor expression compared to wild-type control animals (4.5.1.2). In hippocampus, Western-blot analysis showed a significant high expression increase of the NR2A and

NR2B subunits (+76.36±7.93% and +36.84±10.32%, respectively). Similarly, frontal cortices also displayed an increase of NR2A and NR2B subunit levels (+19.7±6.8% and +86.3±15.8%, respectively). Moreover, a significant upregulation of the NR1 subunit was likewise observed in frontal cortex of PROT-knockout animals. These data suggest that an altered composition (subunit-shift) of the different NMDA-receptor subunits could be present in the postsynaptic density of these particular brain areas. At first sight, these findings could appear controversial as the obligatory NR1 subunit was not observed to be upregulated in the same extend as the NR2 subunits. However, the NR1 subunit has been shown to be highly expressed, allowing a considerable dynamic range in the formation of functional NMDA-receptors (Zhong et al. 1994).

NMDA-receptors are tetramers composed of one NR1-dimer and two NR2 subunits (Laube et al. 1998; Schorge and Colquhoun 2003). Although the NR1 subunit exhibits all properties of the NMDA-receptor channel complex, the assembly of NR2 subunits with the NR1-dimer potentiates or rather ascertains the receptor mediated currents. NMDA-receptors containing NR2B as a partner for NR1 exhibit a prolonged duration of channel opening time compared with receptors built of NR1 and NR2A (Vicini et al. 1998). Therefore, NR2A containing NMDA-receptors mediate faster neurotransmission than those containing NR2B (Cull-Candy et al. 2001). The observed upregulation of NR2A subunits in the hippocampus of PROT-deficient mice could be explained as a counter regulation to the totally increased NMDA-receptor density, attenuating the putatively enhanced NMDA-receptor transmission by shortening the duration of the channel opening time. Thereby, the hippocampal formation would be protected from glutamatergic excitotoxicity arising by an increased glutamate release.

Taken together, our analyses in PROT-knockout mice showed a modified expression profile for several glutamatergic receptor subunits, particularly in hippocampus, which is the brain area primarily involved in learning and memory. The expression elevations of the KA2 and GluR7 subunits of the KA-receptors, GluR2 subunit of the AMPA-receptor, and the regulatory NR2 subunits of the NMDA-receptor strongly indicate changes in hippocampal glutamatergic neurotransmission.

According to the literature, activation of NMDA-receptors increases the surface expression of AMPA-receptor subunits (Li et al. 2009), what is consistent with the detected increase of GluR2 expression in PROT-deficient mice. Activation of AMPA- and NMDA-receptors are required for the formation of long-term potentiation (LTP), a molecular basis of learning (Nicoll 2003), and activity-dependent synaptic maturation (O'Connor et al. 1995).

Therefore, the present data indicate that ablation of PROT induces adaptive changes that might give rise to molecular basis for better learning abilities.

Further investigations are required to verify the mechanism that PROT utilizes to contribute to NMDA-receptor transmission. The amount of NMDA-receptors localized on the cell surface should be analyzed into more detail to ensure that despite the observed total increase, an increased number of receptors are ready to effect signal transduction. Furthermore, it should be determined, e.g. by electrophysiological investigations, whether the overexpression of the NMDA-receptors in PROT-knockout mice translates into enhanced NMDA-receptor mediated synaptic currents.

5.2.3   Contribution of PROT on Dopaminergic Neurotransmission

In this work it was studied if the detected upregulations of glutamate-receptors in PROT-deficient mice leads to a secondary dysregulation of the dopaminergic neurotransmission. Evidence came from the observation that NMDA-receptors regulate the release of dopamine (Araneda and Bustos 1989). Assuming that PROT-deficient mice have enhanced glutamatergic neurotransmission (5.2.2), secondary alterations within the dopaminergic neurotransmission were considered to be possible as well. Moreover, PRODH-knockout mice lacking the L-proline metabolizing enzyme proline-dehydrogenase (*PRODH*) display increased levels of L-proline in the brain and exhibit adaptive changes in the expression of proteins involved in dopaminergic neurotransmission (Paterlini et al. 2005). Since ablation of *ProT* gene is also expected to result in increased levels of L-proline in brain synapses, adaptions in expression of genes belonging to the dopaminergic system were anticipated. Paterlini et al. found a 25% upregulation of the enzyme catechol-O-methyltransferase (*COMT)* in a cohort of frontal cortices of *PRODH*-deficient mice. COMT inactivates biologically active catechols, including the neurotransmitters dopamine, noradrenaline and adrenalin, which are suggested to be involved in physiological as well as pathophysiological processes (Levy 2009). In contrast to the literature, frontal cortices of PROT-knockouts, examined in the present thesis, exhibited no significant expression change of *COMT* mRNA. Furthermore, Paterlini et al. reported that *PRODH*-deficient mice exhibit a significant downregulation ($\sim$35%) of dopamine-receptor D_1 (*DRD1)* mRNA in frontal cortices (Paterlini et al. 2005). However, no significant changes in DRD1 expression were detected in PROT-deficient animals. The most striking adaptions on mRNA expression within the dopaminergic system of PROT-knockout mice were found for dopamine-receptor D_2 (*DRD2*), which was shown to have a slightly reduced expression in *PRODH*-deficient animals (Paterlini et al. 2005). In contrast, here it was shown that

frontal cortices of PROT-deficient mice exhibited a six-fold increase in *DRD2* mRNA, whereas a three-fold increase was also ascertained in hippocampus. Furthermore, in frontal cortices the dopamine synthetizing enzyme tyrosine hydroxylase (TH) was dramatically upregulated, indicating an elevation in dopamine synthesis and thereby suggesting also an increased release of dopamine in frontal cortices of PROT-deficient animals.

The observed alterations within these components of the dopaminergic system are suggested to be due to the elevated NMDA-receptor expression found in PROT-knockout mice (4.5.1.2), since it was demonstrated that NMDA-receptor activation can control dopamine release (Jedema and Moghddam 1996; Del and Mora 2001). It has previously been reported that dopamine transporter (DAT) knockout mice display increased extracellular levels of dopamine, leading to compensatory decreased expression levels of TH- and dopamine receptors in order to dampen dopaminergic responsiveness (Jaber et al. 1997; Jaber et al. 1999). Therefore, it can be suggested that the detected upregulation of TH and dopamine receptors in PROT-deficient mice indicates adaptive changes in dopaminergic neurons in attempt to increase dopaminergic responsiveness, in order to compensate a putative decreased extracellular level of dopamine.

Taken together, the analysis of PROT-knockout mice displayed no comparable adaptions like those of PRODH-knockouts, which counterfeit the disease hyperprolinemia, probably due to different compensatory mechanisms in the dopaminergic system aroused in these different knockouts. Thus, the phenotype of PROT-deficient mice is not comparable to hyperprolinemia. However, in order to completely understand the contribution of PROT on dopaminergic neurotransmission, further more detailed studies are necessary.

5.2.4 PROT-Deficient Mice Exhibit Changed Behavioral Profiles

5.2.4.1 Altered Locomotor Activity in PROT-Deficient Animals

In the course of this work it was shown that PROT-deficient animals display a significantly reduced locomotor activity when they are exposed to a novel environment in the open field test (4.4.3). These lower levels of exploratory locomotor activity of PROT-knockout mice were especially prominent during the first 20 min of the 30-min-test and disappeared by the end of the test session.

Rotarod analysis of PROT-knockout mice confirmed that the detected hypolocomotion is not due to motor impairments of these animals, as PROT-mutants did not exhibit differences in this task compared to wild-type littermates (4.4.2). A second explanation for the decreased locomotion would be due to nonspecific locomotor hypoactivity. However,

the observation that PROT-deficient mice in general possess a significant reduced locomotor activity mainly in the first 20 min of the test (4.4.3) argues against this consideration. In fact, it seems more likely that the reduced locomotor activity arises from an improved ability to judge the familiarity of the recently visited spatial locations, so this paradigm gives information about how well the animals can adapt to a novel situation.

Within the open field test two different and opposite forces govern the behavioral pattern of the animals. These forces are on the one hand the curiosity to explore the novel situation, which is on the other hand opposed by the fear about the new situation. The outcoming behavior is thereby influenced coincidently. In order to reduce the fear-like behavior, open field test analyses with non-aversive illumination conditions were performed. Therefore, the reduced explorative behavior of the PROT-knockout mice indicating a reduced curiosity maybe due to an increased positive mood and better learning abilities in these animals. This would be consistent with the data gained by examining the learning performance of these mice (4.6.3) as well as with the biochemical investigations exhibiting upregulated NMDA-receptor densities in hippocampus (4.5.1.2), suggesting changed signaling abilities, and possibly causing enhanced long-term-potentiation (LTP). Interestingly, it has been reported that NR2A-knockout mice exhibit an opposite phenotype compared to PROT-knockouts when studied in the open field test, with increased locomotor activity compared to wild-type littermates (Boyce-Rustay and Holmes 2006). The biochemical analysis of PROT-deficient animals displayed adaptive elevated NR2A protein levels. This leads to the consideration that the expressed amount of NR2A subunits correlates with this behavioral condition. The concluding hypothesis that an enhanced NMDA-receptor transmission leads to the observed hypolocomotion of PROT-deficient mice is further supported by a study investigating the effects of D-amino acid oxidase (DAO) knockout mice (Almond et al. 2006). These animals display elevated D-serine levels with consequently enhanced NMDA-receptor transmission, demonstrated by enhanced LTP and improved spatial learning abilities. Moreover, this mouse model exhibits as well a reduced locomotor activity when studied in the open field test. The authors hypothesize that an increased glutamatergic neurotransmission augments tonic GABAergic inhibition of nucleus accumbens dopamine release. This could be considered as well to happen in PROT-deficient animals. A decreased dopamine release with subsequent lowered activation of dopamine-receptors is known to result in a decreased locomotor activity (Beaulieu and Gainetdinov 2011; Jackson and Westlind-Danielsson 1994; Jackson et al. 1994) and could thereby contribute to the hypolocomotion of PROT-knockout mice. This hypothesis would be consistent with the data gained by examining the

expression of key proteins involved in dopaminergic neurotransmission within PROT-knockout mice (4.5.3), since the increased expression of tyrosine hydroxylase and dopamine-receptors suggests a compensatory response to reduced dopamine release.

Clearly, it would be interesting to perform further experiments. Clarification of the contribution of NMDA-receptors to the observed differences in locomotor activity of PROT-knockouts and wild-type animals would be beneficial. Application of NMDA-receptor antagonists before examining the performance of PROT-knockout mice in an open field tests, would be also valuable. Thereby, it could be examined if PROT-lacking animals are at least partially protected from the locomotion enhancing effects of NMDA-receptor antagonists.

5.2.4.2 Increased Learning Abilities of PROT Mutant Mice

Within the scope of this thesis, it could be shown by analysis of spontaneous alternation behavior that PROT-deficient mice display a significantly improved spatial working memory (4.6.3). This result demonstrating better learning abilities of PROT-lacking animals is in agreement with the open field analysis (4.4.3) that detected better habituation performances to a novel environment, since habituation represents non-associative learning.

One possible reason for the better learning abilities of PROT-deficient mice could be the observed increase in glutamate-receptor density (4.5.1). It has been shown that NMDA-receptor antagonists reduce spontaneous alternation behavior (Rubaj et al. 2003). Furthermore, it is well established that glutamate-receptors are important for long-term plasticity of synaptic transmission, which represents a cellular basis of learning processes (Martin et al. 2000). NMDA-receptors are critical for the induction of both long-term depression (LTD) and long-term potentiation (LTP) (Dudek and Bear 1992; Clayton et al. 2002b). NMDA-receptors containing NR2B as partner for NR1 exhibit a prolonged duration of channel opening time compared with receptors built of NR1 and NR2A (Tovar et al. 2000). Consequently, the density of NMDA-receptors built with NR2B subunits is important for a better spatial working memory, what could be impressively verified with conditional NR2B-knockout mice showing reduced level of spontaneous alternation behavior, thus demonstrating a short-term spatial working memory deficit for recently visited places (von Engelhardt-Jakob et al. 2008). In addition, improved learning abilities in mice overexpressing NR2B clearly indicate the important role of this NMDA-receptor subunit in spatial learning (Tovar et al. 2000; Tang et al. 1999). PROT-knockouts in young as well as in mature age display enhanced NR2B levels within the hippocampus, a structure

important for learning processes (MILNER and PENFIELD 1955-1956). Therefore, it could be concluded that the detected upregulation of the NR2B subunit is responsible for the significantly improved spatial working memory of PROT-deficient mice.

Furthermore, the increased learning abilities of PROT-knockouts could be partially due to the significantly increased GluR2 expression detected in the hippocampal formation. According to literature, spatial and non-spatial learning performance was disrupted in GluR2-mutant mice (Gerlai et al. 1998). Moreover, activation of AMPA-receptors is required for the formation of LTP, besides the activation of NMDA-receptors (O'Connor et al. 1995). Thus, it seems likely that augmentation of GluR2 expression, reflecting an increased AMPA-receptor number, and NR2B expression in PROT deficient mice facilitates the formation of improved LTP as a molecular basis for increased learning abilities.

Taken together, the present results strongly suggest that PROT plays an important role within learning, possibly by regulating NMDA-receptors, which are the key receptors underlying synaptic plasticity. Therefore, it could be considered that PROT function is important for synaptic plasticity, which is relevant to behavioral and cognitive alterations with respect to learning abilities.

5.2.4.3 Improved Sensorimotor Gating in PROT-Knockout Mice

In the present work it was determined that PROT-knockout mice exhibit improved prepulse inhibition (PPI). PPI is an indicator for sensorimotor gating abilities, a process important for filtering irrelevant sensory information from the environment and thereby allowing attention to be focused on a given stimulus. This process is mediated by a neuronal system in which the brainstem receives modulatory input from the nucleus accumbens that in turn is innervated by the frontal cortex and hippocampus (Schmajuk and Larrauri 2005).

Mice with an inactivated *PRODH* gene and thereby harboring elevated L-proline levels showed abnormalities in sensorimotor gating, ascertained by a ~15% lowered PPI (Gogos et al. 1999). Moreover, it is known that human hyperprolinemia is a risk factor for schizoaffective disorders (Jacquet et al. 2005). PPI is disrupted in patients suffering from schizophrenia or schizoaffective disorders (Grillon et al. 1992). Therefore, it was suggested that deletion of PROT could lead to a comparable phenotype of PRODH-knockout animals and moreover to a schizophrenia-related phenotype. However, the improved PPI of PROT-deficient mice (4.4.4) seems to be in discrepancy to the observations gained with PRODH-knockout animals. Assuming that the better PPI performance of PROT-mutants

is not due to improved auditory abilities caused by PROT-deficiency, variations in synaptic L-proline levels of PRODH- and PROT-knockout mice, which would lead to different compensatory mechanisms, could be responsible for this divergent PPI behavior.

Another aspect to be considered is the common association of lowered PPI performance with schizophrenia. It could be envisaged that inhibition of PROT function could be an effective treatment of the schizophrenic disorder. To prove this hypothesis, it would be interesting to study the effects on PPI deficits induced by NMDA-receptor antagonists in PROT-deficient animals compared to wild-type controls. Thereby, it could be examined if PROT-lacking animals are at least partially protected from the PPI disrupting effects of NMDA-receptor antagonists.

Taken together, the surprising finding of increased PPI in PROT-knockouts indicates that these animals display a slightly better attention performance than wild-type mice. Another conclusion, as mentioned above (5.2.3), is that although PROT-deficient mice and PRODH-knockouts are expected to exhibit increased L-proline levels in brain, both mice strains do not display similar phenotypes.

5.2.4.4 Altered Emotionality in PROT-Knockout Mice

The analysis of PROT-deficient mice in an open field test using aversive conditions gave evidence for an increased anxiety-like phenotype of the PROT mutants (4.6.1). By intensive illumination, the open field test can be used to study emotionality of the mice (Archer 1973), as normal behavior in mice is to seek the protection of the periphery, suppressing the locomotion enhancing curiosity-drive to explore the novel environment. Therefore, the reductions in time spent in the center, in distances traveled in the center area, and in number of visits to the center of the open field by PROT-knockouts, indicate an increased response to the anxiety-related component of the intensive illuminated open field test. This finding is supported by the outcome of the acoustic startle test (4.4.4) used as prescreen for the PPI-analysis. The tendency in PROT-knockouts to a higher reaction caused by a loud tone suggests that these animals exhibit increased anxiety-like behavior.

Anxiolytic-like effects have been demonstrated through application of AMPA-receptor antagonists (Kotlinska and Liljequist 1998), as well as reduced anxiety was reported for GluR2-knockout mice (Mead et al. 2006). Moreover, NR2A-knockout mice also exhibit anxiolytic-like effects (Boyce-Rustay and Holmes 2006). Upon biochemical analysis of PROT-deficient mice, it was observed that these animals display an adaptive increase of NR2A and GluR2 protein levels. Therefore, this receptor upregulations in PROT-deficient mice could be a reasonable molecular basis for their detected increased anxiety-like

behavior. Indeed, mediation of emotion by NMDA neurotransmission is a growing body of evidence and discussed in several studies. Supporting evidence comes from studies where NMDA-receptor antagonist treatment showed also anxiolytic effects in rodents (Martinez et al. 2002; Wiley et al. 1995).

In the scope of this thesis, it was observed that PROT-mutants display significantly reduced time of immobility in the forced swimming test (FST), also referred to as behavioral despair test (4.6.2), indicating antidepressant-like or positive mood behavior. The reduced time of immobility in the FST was not due to a generalized increase in activity, as indicated by the lower basic locomotor activity of the mutants in the standard open field test (4.4.3). It is known that forced swimming causes stress, which is reflected in altered neurotransmitter release and changed cellular signaling (Sakakibara et al. 2005). Central administration of L-proline attenuates induced stress in chicks (Hamasu et al. 2010), which is quenched by co-injection of the NMDA-receptor antagonist MK-801, giving further evidence for the impact of NMDA-receptor density upon emotional state. Interestingly, it has been demonstrated that radio-ligand binding to NMDA-receptors is altered in suicide victims (Nowak et al. 1995), what is consistent with the hypothesis that NMDA-receptors are furthermore involved in the pathophysiology of depression (Trullas and Skolnick 1990). Therefore, the observed NMDA-receptor upregulation in PROT-deficient mice could be a reasonable molecular basis for the decreased behavioral despair upon FST analysis. In addition, it is also known that during stress dopamine release is reduced by activation of glutamate-receptors (Del and Mora 2001), which results in increased expression levels of DRD2. Likewise, consistent with the interpretation that increased swimming times indicate antidepressant-like behavior is the observation that PROT-knockout mice display elevated expression of *DRD2* mRNA (4.5.3), as chronic antidepressant treatment increases DRD2-signaling (Collu et al. 1997). Therefore, it seems possible that PROT-deficient mice, in contrast to their wild-type counterparts, experience less stress in the FST leading to subsequent decreased behavioral despair.

In summary, PROT-deficient mice display altered emotionality that could be explained by adaptive changes in glutamate-receptor expression. Nevertheless, future experiments are necessary to precisely analyze PROT mechanisms governing emotionality.

5.2.5   Alterations in Mature PROT-Knockout Mice

In general, aging is known to be associated with increased glutamate release (Freeman and Gibson 1987), decreased expression of NMDA-receptors (Clayton and Browning 2001) and deficits in activity dependent NMDA-receptor cell surface regulation (Clayton et al. 2002a), consequently resulting in a decreased synaptosomal plasticity. The investigation of mature PROT-deficient mice revealed that these animals exhibit significantly lowered spontaneous locomotion in an novel environment (4.7.1.1) and outperforming spatial learning abilities (4.7.1.2), confirming the results gained by the analysis of 3 months old PROT-knockouts (4.4.3 and 4.6.3). However, analysis of the NMDA-receptor expression revealed no expression differences comparing PROT-mutants with age-matched wild-type controls apart from the significantly increased expression of the NR2B subunit in hippocampus (4.7.2). As mentioned above, analysis of conditional NR2B-knockout mice as well as mice overexpressing NR2B gave evidence that particularly the NR2B subunit plays an important role in spatial learning (Tovar et al. 2000; Tang et al. 1999). Interestingly, it has been reported that a knock-down of the NR2B subunit expression, especially in the hippocampus, can mimic age-related changes in LTP and spatial learning (Clayton et al. 2002b). The better spatial learning abilities of mature PROT-deficient mice could be thereby due to the observed increased expression of NR2B in hippocampus (4.7.2). In addition, as previously discussed, a reduced locomotor activity could arise from an improved ability to judge the familiarity of the recently visited spatial locations. This would as well implicate better learning abilities of the mutant mice and could also be due to the increased hippocampal NR2B expression in the mature PROT-deficient animals.

Additionally, the open field analysis displayed a stronger behavioral phenotype for 8 months old PROT-deficient animals (4.7.1.1) compared to 3 month old mutants (4.4.3), although within these young mice more adaptive changes in protein expression were present (4.5). Thus, the stronger behavioral phenotype of the 8 months old PROT-deficient mice could be a result of increased receptor function in addition to the increased NR2B expression. Enhancement of NMDA-receptor function is known to be mediated by protein kinase C (PKC) and tyrosine kinase activation, which leads to rapid recruitment of NMDA-receptors to the cell surface (Huang et al. 2001; Lu et al. 1999). Furthermore, phosphorylation is known to regulate trafficking of NMDA-receptors (Chung et al. 2004). Therefore, the phosphorylation state of the respective NMDA-receptors subunits and their plasma membrane location levels should be determined in further experiments. Moreover,

to clarify the role of the increased expression of NR2B on synaptic transmission, additional comparative electrophysiological investigations of 8 month old PROT-deficient mice and wild-type littermates would be valuable.

5.3   Benefits from the PROT-Knockout Mouse Line

The generation and analysis of mice lacking the expression of a functional PROT-protein clearly provided deeper insights into the *in vivo* modulatory role of the high affinity transport of L-proline by PROT. The question how L-proline and PROT influence glutamatergic neurotransmission within the normal brain will be further outlined and discussed here. Even though only speculative, some evidence about the physiological relevance can be hypothesized.

First, L-proline has been shown to enhance NMDA-receptor transmission in low concentrations (Cohen and Nadler 1997b). Why should this not be due to the binding to an allosteric site and thereby cause facilitation of NMDA-receptors to reach their activated conformation? In the present thesis it could be shown that the expression level of proteins controlling the allosteric NMDA-receptor modulators glycine and D-serine were not changed in PROT-deficient animals (4.5.2). If L-proline additionally facilitated NMDA-receptor activation through binding to an allosteric site, it could be concluded that the level of the other positively allosteric modulating molecules glycine and D-serine should be adaptively downregulated to protect against increased activation. Therefore, these data would reason against the hypothesis that L-proline is as well a positive allosteric modulator of NMDA-receptors. Moreover, since it was reported that L-proline in high concentrations can activate NMDA-, AMPA- and KA-receptors (Henzi et al. 1992), it could be envisaged that L-proline binds, maybe with low affinity, to orthosteric sites of these receptors and thereby causes their activation. This hypothesis cannot be ruled out, since it is not known whether some glutamate-receptors, with a specific subunit combination, may exhibit an affinity for L-proline. However, it has to be concerned that if glutamate-receptors are activated to a great extent, the physiological problem of glutamate-receptor excitotoxicity arises, and therefore evolution would not favor such a "second low affinity agonist" for glutamate-receptors.

Albeit specific sodium-independent binding of radiolabeled L-proline to rodent brain synaptic membranes was reported (Greene et al. 1986; Cordero et al. 1991), so far no specific high-affinity receptor has been found for L-proline. However, some orphan receptors exist for which no ligand has been described in the literature so far. Since PROT is expressed in glutamate pathway fibers (Nadler et al. 1992), it can be suggested that a high-affinity L-proline specific receptor would be localized in their adjacency. This hypothetical receptor could be expressed by glutamatergic neurons in order to depolarize

the respective cells upon activation via L-proline and thereby simulate the reported potentiation of glutamatergic neurotransmission by L-proline (Cohen and Nadler 1997b).

It is a common knowledge that the number of receptors present at the postsynaptic membrane determines the response to the neurotransmitter released from the presynaptic terminal. How can modulation of the expression of glutamate-receptors upon PROT-knockout be explained? The neurobiological reasons of these alterations are only speculative, but some evidence can be hypothesized.

It is well known that glutamate-receptor amounts can be modulated by chronic increase or decrease of agonist activation (Resink et al. 1996; Follesa and Ticku 1996). Chronic treatment with agonists and subsequent stimulation of the receptor can lead to downregulation of the corresponding receptor through an increase of receptor degradation (Luttrell and Lefkowitz 2002). Agonist-induced downregulation has been reported for NMDA-receptors (Resink et al. 1996), AMPA-receptors (Feligioni et al. 2006), and KA-receptors (Martin et al. 2008), suggesting that these glutamate-receptors are regulated by the same mechanisms. On the other hand, chronic exposure to antagonists can lead to a compensatory increase in glutamate-receptor density with a subsequent supersensitivity towards the corresponding agonist (Williams et al. 1992). It has been suggested that endogenous extracellular L-proline maintains NMDA-receptor containing synapses in a partially potentiated state, as application of L-proline to brain slices, in concentrations normally present in cerebrospinal fluid, potentiates NMDA-receptor transmission (Cohen and Nadler 1997b). Therefore, at least the upregulation of NMDA-receptor amounts could be explained as follows:

Since L-proline is released in a Ca^{2+}-dependent manner from neurons upon depolarization (Mulder and Snyder 1974), the ablation of PROT, which leads to a slower clearance of L-proline (4.3.1), should permanently increases the extracellular level of L-proline (only low affinity transport of L-proline by metabolic carriers is still possible) in distinct synaptic clefts, where PROT usually is situated. According to the literature, enhanced extracellular concentrations of L-proline induce an inhibition of glutamate release (Cohen and Nadler 1997a). Moreover, it has been reported that treatment with NMDA-receptor antagonists induces an upregulation of the density of NMDA-receptors *in vitro* and *in vivo* (McDonald et al. 1990; Williams et al. 1992). Therefore, it is possible that the respective glutamatergic cells react against the chronically lowered agonist-concentration in turn with an increased expression of the NMDA-receptors to maintain excitability of the

respective glutamatergic synapses. This regulation could be triggered by the same cellular mechanisms like chronically treatment with antagonists, which induces a compensatory upregulation of NMDA-receptors (McDonald et al. 1990; Williams et al. 1992).

Alternatively, the increased NMDA-receptor expression is possibly due to increased NMDA-receptor activation in PROT-knockout mice. Ablation of PROT should lead to increased extracellular L-proline levels and, according to the literature, this amino acid should potentiate and, in high concentrations, activate NMDA-receptors, (Cohen and Nadler 1997b; Henzi et al. 1992; Martin et al. 1992). It has been reported that activation of NMDA-receptors increases the expression of both NMDA- and AMPA-receptors. Furthermore, it has been shown that induction of LTP (which prerequisites the activation of NMDA-receptors) does not alter AMPA-receptors, but also increases the expression of NMDA-receptors (Grosshans et al. 2002; Li et al. 2009). Therefore, enhanced NMDA-receptor expression in PROT-deficient mice could be also explained by increased NMDA-function and enlarged LTP.

Besides these speculations, it should be mentioned that the different NMDA-receptor subunits are encoded by different genes (Monyer et al. 1994) and it is uncertain whether these genes are equally regulated upon PROT-knockout. Alterations in the neuronal biochemistry of PROT-deficient mice could lead to unspecific different regulations of the respective transcription factors or influence the promoter accessibilities.

Knockout mice can be highly informative about the discovery of protein function. In addition, it has been shown previously that phenotypes of knockout mice correlate well with the therapeutic effects of a high number of best-selling pharmaceutical drugs (Zambrowicz and Sands 2003). Phenotypical screening of these animals can be used to delineate valuable new drug targets and furthermore help in the determination of the potential on-target side effects associated with a given target. Consequently, PROT-knockout mice provide the advantage that they can be used to model the physiological significance of PROT-inhibitors in a therapeutically relevant manner. Typically, neurotransmitter transporters were thought to function only as terminators of synaptic transmission by active transport of the respective neurotransmitters back into neuronal cells (or into glial cells). However, the findings presented in this thesis indicate that the function of this transporter is more than pure reuptake of L-proline released upon depolarization. The present results show that absence of PROT affects glutamatergic synaptic components and causes behavioral alterations, suggesting that the *in vivo*

physiological role of PROT is, at least in part, to control glutamatergic synaptic transmission. Inhibitors of PROT could be used to ameliorate memory and attention, as well as to improve sensorimotor gating. Moreover, the adaptive changes in the expression of key proteins as well as manifested behavioral alterations observed in PROT-deficient mice within this thesis differ from the adaptive changes found within hyperprolinemia animal models. Therefore, the knockout of PROT is not comparable with the disorder hyperprolinemia. However, further experiments are required to elucidate more precise molecular and cell biological mechanisms to fully uncover the complete relevance of PROT within neurotransmission.

6   Conclusion

The essential outcome of the present study was the successful generation of a mouse strain deficient in the expression of the murine *ProT* gene, encoding for the putative neurotransmitter transporter PROT. Successful deletion of PROT was demonstrated by Southern-blot on ES-cell level, and by PCR-analysis as well as Western-blot technique in the generated animals. Knockout mice were viable, displayed no morphological abnormalities in brain, and exhibited unchanged expression of L-proline metabolizing enzymes, indicating unaffected L-proline metabolism. Therefore, the PROT-deficient mouse strain represented a valuable tool for both elucidation of *in vivo* PROT-function and analysis of adaptive processes in the expression of CNS genes appearing upon PROT inactivation. First, it was shown that PROT contributes to a main extent to the high affinity sodium-dependent L-proline uptake in the brain regions hippocampus, cortex and striatum. Since PROT-function is assumed to affect CNS glutamate neurotransmission, putative alterations within associated elements of glutamatergic synapse were investigated. For this purpose, expression levels of glutamate-receptor subunits were examined using Western-blot technique and mRNA analysis by quantitative real time polymerase chain reaction. Within the scope of this thesis, significantly increased levels of the NMDA-receptor subunits, but unchanged PSD95 expression, were detected in different brain regions of PROT-knockout mice. A predominant upregulation of NR2B could be ascertained in frontal cortices and hippocampi, whereas predominantly increased NR2A levels were found only in hippocampi of PROT-lacking mice, suggesting region specific alterations in NMDA-receptor signaling. Moreover, raised expression of AMPA- and KA-receptor subunits was observed in the hippocampal formation of PROT-deficient animals. Taken together, these findings indicate that ablation of PROT induces adaptive changes in glutamate-receptor expression that could result in alterations of glutamatergic neurotransmission in these mutant animals. In addition, it was assumed that modulation of NMDA-receptor signaling could induce a secondary dysregulation in dopamine neurotransmission. Therefore, dopaminergic system associated proteins like catechol-O-methyltransferase (COMT), tyrosine hydroxylase (TH) and dopamine-receptor D_1 and D_2 (DRD1, DRD2) were also analyzed by qPCR-analysis, disclosing an upregulation of *TH* and *DRD2* mRNA, which suggest far-reaching changes in general CNS neurotransmission in PROT-knockout mice.

Finally, it was investigated whether PROT deletion has an impact on the behavior of PROT-deficient mice. It could be shown that these animals display significantly reduced

levels of exploratory locomotor activity and increased anxiety like behavior. Furthermore, a better performance of PROT-deficient animals compared to their wild-type littermates in memory test was observed. The detected alterations in glutamate-receptor levels might explain the changed behavioral phenotypes of PROT-knockout mice. Since augmented expression levels of NMDA-receptors previously have been associated with improved memory function, the observed increase of NMDA-receptor expression in PROT-deficient animals is consistent with their better performance in memory tests. Moreover, mediation of emotion by glutamatergic neurotransmission could also explain the altered emotionality in PROT-deficient animals. Increased glutamatergic neurotransmission is similarly associated with reduced locomotor activity, as also observed in PROT$^{-/-}$ mice.

Collectively, these studies describe a mouse model that helps to clarify some particular physiological functions of PROT. Nevertheless, further experiments are required to elucidate more precise molecular and cell biological mechanisms to fully uncover the complete relevance of PROT within neurotransmission. Ongoing experiments using this new mouse model will provide new insights into the precise role of this exceptional transporter.

7   List of Abbreviations

ad	(Lt.) up to
bp	Base pairs
cDNA	copy DNA
C°	Celsius
CMV	Cytomegalovirus
CNS	Central nervous system
dH$_2$O	Demineralized water
DMEM	Dulbecco´s modified Eagel´s Medium
DMSO	Dimethyl sulfoxid
DNA	Deoxyribonucleic acid
dNTP	Deoxynucleotidetriphosphate
E.coli	*Escherichia coli*
EDTA	Ethylene diamine tetraacetic acid
e.g.	Exempli gratia *(for example)*
ES cell	Embryonic stem cell
f.c.	Final concentration
FCS	Fetal calf serum
FIAU	Fialuridine
g	Acceleration by gravity
g	Gram
G418	Geneticin
GABA	γ-Aminobutyric acid
h	Hour(s)
HBSS	Hank´s balanced salt solution
HEPES	N-(2-Hydroxyethyl)piperazine-N-ethanesulforinic acid
HET	Haus für experimentelle Therapie
HSV-TK	Herpes simplex virus thymidine kinase
IgG	Immunoglobulin G
KA	Kainate
kb	Kilo base(s)
LIF	Leukemia inhibitory factor
LTD	Long term depression
LTP	Long term potentiation
M	Molar concentration (mol/liter)
m	Murine / mouse

MEF	Mouse embryonic fibroblast
min	Minute(s)
ml	Milliliter
mRNA	messenger RNA
ms	Millisecond
μl	Microliter
μM	Micromolar
n	Number
neo	Neomycin
nm	Nanometer
nM	Nanomolar
NMDA	N-methyl-D-aspartic acid
ns	Non-significant
N-terminus	Amino terminus
OD	Optical density
ORF	Open reading frame
PBS	Phosphate buffered saline
PCR	Polymerase chain reaction
RNA	Ribonucleic acid
rpm	Rounds per minute
RT	Room temperature
RT-PCR	Reverse transcription polymerase chain reaction
s	Second(s)
SDS	Sodium dodecyl sulfate
SEM	Standard error of mean
TE	Tris EDTA
TM	Transmembrane
Tris	Tris(hydroxymethyl)aminomethane
U	Unit
UTR	Untranslated region
UV	Ultraviolet
V	Volt
WT	Wild-type

8 References

Adams, E. (1970): Metabolism of proline and of hydroxyproline. In: *Int Rev Connect Tissue Res* 5, S. 1–91.

Almond, S. L.; Fradley, R. L.; Armstrong, E. J.; Heavens, R. B.; Rutter, A. R.; Newman, R. J. et al. (2006): Behavioral and biochemical characterization of a mutant mouse strain lacking D-amino acid oxidase activity and its implications for schizophrenia. In: *Mol Cell Neurosci* 32 (4), S. 324–334.

Amara, S. G.; Kuhar, M. J. (1993): Neurotransmitter transporters: recent progress. In: *Annu Rev Neurosci* 16, S. 73–93.

Angulo, M. C.; Rossier, J.; Audinat, E. (1999): Postsynaptic glutamate receptors and integrative properties of fast-spiking interneurons in the rat neocortex. In: *J Neurophysiol* 82 (3), S. 1295–1302.

Araneda, R.; Bustos, G. (1989): Modulation of dendritic release of dopamine by N-methyl-D-aspartate receptors in rat substantia nigra. In: *J Neurochem* 52 (3), S. 962–970.

Archer, J. (1973): Tests for emotionality in rats and mice: a review. In: *Anim Behav* 21 (2), S. 205–235.

Ault, B.; Wang, C. M.; Yawn, B. C. (1987): L-proline depolarizes rat spinal motoneurones by an excitatory amino acid antagonist-sensitive mechanism. In: *Br J Pharmacol* 92 (2), S. 319–326.

Balcar, V. J.; Johnston, G. A.; Stephanson, A. L. (1976): Transport of L-proline by rat brain slices. In: *Brain Res* 102 (1), S. 143–151.

Bavaresco, CarenSerra; Streck, EmilioLuiz; Netto, CarlosAlexandre; Wyse, AngelaTerezinhadeSouza (2005): Chronic hyperprolinemia provokes a memory deficit in the Morris water maze task. In: *Metab Brain Dis* 20 (1), S. 73–80.

Baxter, C. F.; Baldwin, R. A.; Davis, J. L.; Flood, J. F. (1985): High proline levels in the brains of mice as related to specific learning deficits. In: *Pharmacol Biochem Behav* 22 (6), S. 1053–1059.

Beaulieu, Jean-Martin; Gainetdinov, RaulR (2011): The physiology, signaling, and pharmacology of dopamine receptors. In: *Pharmacol Rev* 63 (1), S. 182–217.

Boyce-Rustay, JanelM; Holmes, Andrew (2006): Genetic inactivation of the NMDA receptor NR2A subunit has anxiolytic- and antidepressant-like effects in mice. In: *Neuropsychopharmacology* 31 (11), S. 2405–2414.

Bradford, M. M. (1976): A rapid and sensitive method for the quantitation of microgram quantities of protein utilizing the principle of protein-dye binding. In: *Anal Biochem* 72, S. 248–254.

Capecchi, M. R. (1989): Altering the genome by homologous recombination. In: *Science* 244 (4910), S. 1288–1292.

Chang, Shan; Hu, Jian-ping; Lin, Pi-yuan; Jiao, Xiong; Tian, Xu-hong (2010): Substrate recognition and transport behavior analyses of amino acid antiporter with coarse-grained models. In: *Mol Biosyst* 6 (12), S. 2430–2438.

Cherkin, A.; Eckardt, M. J.; Gerbrandt, L. K. (1976): Memory: proline induces retrograde amnesia in chicks. In: *Science* 193 (4249), S. 242–244.

Chung, HeeJung; Huang, YanHua; Lau, Lit-Fui; Huganir, RichardL (2004): Regulation of the NMDA receptor complex and trafficking by activity-dependent phosphorylation of the NR2B subunit PDZ ligand. In: *J Neurosci* 24 (45), S. 10248–10259.

Clayton, D. A.; Browning, M. D. (2001): Deficits in the expression of the NR2B subunit in the hippocampus of aged Fisher 344 rats. In: *Neurobiol Aging* 22 (1), S. 165–168.

Clayton, DanielA; Grosshans, DavidR; Browning, MichaelD (2002a): Aging and surface expression of hippocampal NMDA receptors. In: *J Biol Chem* 277 (17), S. 14367–14369.

Clayton, DanielA; Mesches, MichaelH; Alvarez, Enriquez; Bickford, PaulaC; Browning, MichaelD (2002b): A hippocampal NR2B deficit can mimic age-related changes in long-term potentiation and spatial learning in the Fischer 344 rat. In: *J Neurosci* 22 (9), S. 3628–3637.

Clelland, C. L.; Read, L. L.; Baraldi, A. N.; Bart, C. P.; Pappas, C. A.; Panek, L. J. et al. (2011): Evidence for association of hyperprolinemia with schizophrenia and a measure of clinical outcome. In: *Schizophr Res*.

Cohen, S. M.; Nadler, J. V. (1997a): Proline-induced inhibition of glutamate release in hippocampal area CA1. In: *Brain Res* 769 (2), S. 333–339.

Cohen, S. M.; Nadler, J. V. (1997b): Proline-induced potentiation of glutamate transmission. In: *Brain Res* 761 (2), S. 271–282.

Cohen, S. M.; Nadler, J. V. (1997c): Sodium-dependent proline and glutamate uptake by hippocampal synaptosomes during postnatal development. In: *Brain Res* 100 (2), S. 230–233.

Collingridge, G. L.; Lester, R. A. (1989): Excitatory amino acid receptors in the vertebrate central nervous system. In: *Pharmacol Rev* 41 (2), S. 143–210.

Collu, M.; Poggiu, A. S.; Devoto, P.; Serra, G. (1997): Behavioural sensitization of mesolimbic dopamine D2 receptors in chronic fluoxetine-treated rats. In: *Eur J Pharmacol* 322 (2-3), S. 123–127.

Cordero, M. L.; Negron, A. E.; Ortiz, J. G.; Blanco, C.; Santiago, G. (1991): Inhibition of high-affinity L-proline binding to rat brain membranes by 2-amino-7-phosphonoheptanoic acid. In: *Eur J Pharmacol* 208 (2), S. 179–181.

Cull-Candy, S.; Brickley, S.; Farrant, M. (2001): NMDA receptor subunits: diversity, development and disease. In: *Curr Opin Neurobiol* 11 (3), S. 327–335.

Darstein, Melanie; Petralia, RonaldS; Swanson, GeoffreyT; Wenthold, RobertJ; Heinemann, StephenF (2003): Distribution of kainate receptor subunits at hippocampal mossy fiber synapses. In: *J Neurosci* 23 (22), S. 8013–8019.

Davis, J. L.; Pico, R. M.; Flood, J. F. (1987): Differences in learning between hyperprolinemic mice and their congenic controls. In: *Behav Neural Biol* 48 (1), S. 128–137.

Del, ArcoA; Mora, F. (2001): Dopamine release in the prefrontal cortex during stress is reduced by the local activation of glutamate receptors. In: *Brain Res Bull* 56 (2), S. 125–130.

Dingledine, R.; Borges, K.; Bowie, D.; Traynelis, S. F. (1999): The glutamate receptor ion channels. In: *Pharmacol Rev* 51 (1), S. 7–61.

Drgonova, Jana; Liu, Qing-Rong; Hall, FScott; Krieger, RachaelM; Uhl, GeorgeR (2007): Deletion of v7-3 (SLC6A15) transporter allows assessment of its roles in synaptosomal proline uptake, leucine uptake and behaviors. In: *Brain Res* 1183, S. 10–20.

Dudek, S. M.; Bear, M. F. (1992): Homosynaptic long-term depression in area CA1 of hippocampus and effects of N-methyl-D-aspartate receptor blockade. In: *Proc Natl Acad Sci U S A* 89 (10), S. 4363–4367.

Evans, M. J.; Kaufman, M. H. (1981): Establishment in culture of pluripotential cells from mouse embryos. In: *Nature* 292 (5819), S. 154–156.

Feligioni, Marco; Holman, David; Haglerod, Camilla; Davanger, Svend; Henley, JeremyM (2006): Ultrastructural localisation and differential agonist-induced regulation of AMPA and kainate receptors present at the presynaptic active zone and postsynaptic density. In: *J Neurochem* 99 (2), S. 549–560.

Felix, D.; Kunzle, H. (1974): Iontophoretic and autoradiographic studies on the role of proline in nervous transmission. In: *Pflugers Arch* 350 (2), S. 135–144.

Flynn, M. P.; Martin, M. C.; Moore, P. T.; Stafford, J. A.; Fleming, G. A.; Phang, J. M. (1989): Type II hyperprolinaemia in a pedigree of Irish travellers (nomads). In: *Arch Dis Child* 64 (12), S. 1699–1707.

Follesa, P.; Ticku, M. K. (1996): NMDA receptor upregulation: molecular studies in cultured mouse cortical neurons after chronic antagonist exposure. In: *J Neurosci* 16 (7), S. 2172–2178.

Freeman, G. B.; Gibson, G. E. (1987): Selective alteration of mouse brain neurotransmitter release with age. In: *Neurobiol Aging* 8 (2), S. 147–152.

Fremeau, RTJr; Caron, M. G.; Blakely, R. D. (1992): Molecular cloning and expression of a high affinity L-proline transporter expressed in putative glutamatergic pathways of rat brain. In: *Neuron* 8 (5), S. 915–926.

Fremeau, RTJr; Velaz-Faircloth, M.; Miller, J. W.; Henzi, V. A.; Cohen, S. M.; Nadler, J. V. et al. (1996): A novel nonopioid action of enkephalins: competitive inhibition of the mammalian brain high affinity L-proline transporter. In: *Mol Pharmacol* 49 (6), S. 1033–1041.

Galli, A.; Jayanthi, L. D.; Ramsey, I. S.; Miller, J. W.; Fremeau, RTJr; DeFelice, L. J. (1999): L-proline and L-pipecolate induce enkephalin-sensitive currents in human embryonic kidney 293 cells transfected with the high-affinity mammalian brain L-proline transporter. In: *J Neurosci* 19 (15), S. 6290–6297.

Garcia, Rene (2002): Stress, synaptic plasticity, and psychopathology. In: *Rev Neurosci* 13 (3), S. 195–208.

Gerlai, R.; Henderson, J. T.; Roder, J. C.; Jia, Z. (1998): Multiple behavioral anomalies in GluR2 mutant mice exhibiting enhanced LTP. In: *Behav Brain Res* 95 (1), S. 37–45.

Giros, B.; Jaber, M.; Jones, S. R.; Wightman, R. M.; Caron, M. G. (1996): Hyperlocomotion and indifference to cocaine and amphetamine in mice lacking the dopamine transporter. In: *Nature* 379 (6566), S. 606–612.

Glowinski, J.; Axelrod, J.; Iversen, L. L. (1966): Regional studies of catecholamines in the rat brain. IV. Effects of drugs on the disposition and metabolism of H3-norepinephrine and H3-dopamine. In: *J Pharmacol Exp Ther* 153 (1), S. 30–41.

Gogos, J. A.; Santha, M.; Takacs, Z.; Beck, K. D.; Luine, V.; Lucas, L. R. et al. (1999): The gene encoding proline dehydrogenase modulates sensorimotor gating in mice. In: *Nat Genet* 21 (4), S. 434–439.

Greene, W. M.; Wang, A.; Nadler, J. V. (1986): Sodium-independent binding of L-proline to hippocampal synaptic membranes. In: *Eur J Pharmacol* 130 (3), S. 333–336.

Grillon, C.; Ameli, R.; Charney, D. S.; Krystal, J.; Braff, D. (1992): Startle gating deficits occur across prepulse intensities in schizophrenic patients. In: *Biol Psychiatry* 32 (10), S. 939–943.

Grosshans, D. R.; Clayton, D. A.; Coultrap, S. J.; Browning, M. D. (2002): LTP leads to rapid surface expression of NMDA but not AMPA receptors in adult rat CA1. In: *Nat Neurosci* 5 (1), S. 27–33.

Hamasu, K.; Haraguchi, T.; Kabuki, Y.; Adachi, N.; Tomonaga, S.; Sato, H. et al. (2009): L-proline is a sedative regulator of acute stress in the brain of neonatal chicks. In: *Amino Acids* 37 (2), S. 377–382.

Hamasu, K.; Shigemi, K.; Tsuneyoshi, Y.; Yamane, H.; Sato, H.; Denbow, D. M.; Furuse, M. (2010): Intracerebroventricular injection of L-proline and D-proline induces sedative and hypnotic effects by different mechanisms under an acute stressful condition in chicks. In: *Amino Acids* 38 (1), S. 57–64.

Hampson, D. R.; Huang, X. P.; Oberdorfer, M. D.; Goh, J. W.; Auyeung, A.; Wenthold, R. J. (1992): Localization of AMPA receptors in the hippocampus and cerebellum of the rat using an anti-receptor monoclonal antibody. In: *Neuroscience* 50 (1), S. 11–22.

Hasty, P.; Rivera-Perez, J.; Bradley, A. (1991): The length of homology required for gene targeting in embryonic stem cells. In: *Mol Cell Biol* 11 (11), S. 5586–5591.

Hayward, D. C.; Delaney, S. J.; Campbell, H. D.; Ghysen, A.; Benzer, S.; Kasprzak, A. B. et al. (1993): The sluggish-A gene of Drosophila melanogaster is expressed in the nervous system and encodes proline oxidase, a mitochondrial enzyme involved in glutamate biosynthesis. In: *Proc Natl Acad Sci U S A* 90 (7), S. 2979–2983.

Henzi, V.; Reichling, D. B.; Helm, S. W.; MacDermott, A. B. (1992): L-proline activates glutamate and glycine receptors in cultured rat dorsal horn neurons. In: *Mol Pharmacol* 41 (4), S. 793–801.

Herb, A.; Burnashev, N.; Werner, P.; Sakmann, B.; Wisden, W.; Seeburg, P. H. (1992): The KA-2 subunit of excitatory amino acid receptors shows widespread expression in brain and forms ion channels with distantly related subunits. In: *Neuron* 8 (4), S. 775–785.

Hu, Chien-AnA; Bart, WilliamsD; Zhaorigetu, Siqin; Khalil, Shadi; Wan, Guanghua; Valle, David (2008): Functional genomics and SNP analysis of human genes encoding proline metabolic enzymes. In: *Amino Acids* 35 (4), S. 655–664.

Huang, Y.; Lu, W.; Ali, D. W.; Pelkey, K. A.; Pitcher, G. M.; Lu, Y. M. et al. (2001): CAKbeta/Pyk2 kinase is a signaling link for induction of long-term potentiation in CA1 hippocampus. In: *Neuron* 29 (2), S. 485–496.

Jaber, M.; Dumartin, B.; Sagne, C.; Haycock, J. W.; Roubert, C.; Giros, B. et al. (1999): Differential regulation of tyrosine hydroxylase in the basal ganglia of mice lacking the dopamine transporter. In: *Eur J Neurosci* 11 (10), S. 3499–3511.

Jaber, M.; Jones, S.; Giros, B.; Caron, M. G. (1997): The dopamine transporter: a crucial component regulating dopamine transmission. In: *Mov Disord* 12 (5), S. 629–633.

Jackson, D. M.; Westlind-Danielsson, A. (1994): Dopamine receptors: molecular biology, biochemistry and behavioural aspects. In: *Pharmacol Ther* 64 (2), S. 291–370.

Jackson, D. M.; Johansson, C.; Lindgren, L. M.; Bengtsson, A. (1994): Dopamine receptor antagonists block amphetamine and phencyclidine-induced motor stimulation in rats. In: *Pharmacol Biochem Behav* 48 (2), S. 465–471.

Jacquet, H.; Demily, C.; Houy, E.; Hecketsweiler, B.; Bou, J.; Raux, G. et al. (2005): Hyperprolinemia is a risk factor for schizoaffective disorder. In: *Mol Psychiatry* 10 (5), S. 479–485.

Jacquet, Helene; Raux, Gregory; Thibaut, Florence; Hecketsweiler, Bernadette; Houy, Emmanuelle; Demilly, Caroline et al. (2002): PRODH mutations and hyperprolinemia in a subset of schizophrenic patients. In: *Hum Mol Genet* 11 (19), S. 2243–2249.

Jayanthi, L. D.; Wilson, J. J.; Montalvo, J.; DeFelice, L. J. (2000): Differential regulation of mammalian brain-specific proline transporter by calcium and calcium-dependent protein kinases. In: *Br J Pharmacol* 129 (3), S. 465–470.

Jedema, H. P.; Moghddam, B. (1996): Characterization of excitatory amino acid modulation of dopamine release in the prefrontal cortex of conscious rats. In: *J Neurochem* 66 (4), S. 1448–1453.

Kamiya, H.; Ozawa, S. (2000): Kainate receptor-mediated presynaptic inhibition at the mouse hippocampal mossy fibre synapse. In: *J Physiol* 523 Pt 3, S. 653–665.

Kanner, B. I. (1989): Ion-coupled neurotransmitter transport. In: *Curr Opin Cell Biol* 1 (4), S. 735–738.

Kanwar, Y. S.; Krakower, C. A.; Manaligod, J. R.; Justice, P.; Wong, P. W. (1975): Biochemical, morphological and hybrid studies in hyperprolinemic mice. In: *Biomedicine* 22 (3), S. 209–216.

Kotlinska, J.; Liljequist, S. (1998): The putative AMPA receptor antagonist, LY326325, produces anxiolytic-like effects without altering locomotor activity in rats. In: *Pharmacol Biochem Behav* 60 (1), S. 119–124.

Laemmli, U. K. (1970): Cleavage of structural proteins during the assembly of the head of bacteriophage T4. In: *Nature* 227 (5259), S. 680–685.

Laube, B.; Kuhse, J.; Betz, H. (1998): Evidence for a tetrameric structure of recombinant NMDA receptors. In: *J Neurosci* 18 (8), S. 2954–2961.

Lerma, J.; Paternain, A. V.; Rodriguez-Moreno, A.; Lopez-Garcia, J. C. (2001): Molecular physiology of kainate receptors. In: *Physiol Rev* 81 (3), S. 971–998.

Lerma, Juan (2006): Kainate receptor physiology. In: *Curr Opin Pharmacol* 6 (1), S. 89–97.

Levy, Florence (2009): Dopamine vs noradrenaline: inverted-U effects and ADHD theories. In: *Aust N Z J Psychiatry* 43 (2), S. 101–108.

Li, G. H.; Jackson, M. F.; Orser, B. A.; Macdonald, J. F. (2009): Reciprocal and activity-dependent regulation of surface AMPA and NMDA receptors in cultured neurons. In: *Int J Physiol Pathophysiol Pharmacol* 2 (1), S. 47–56.

Liggins, J.T.P. (2009). The Roles of Dopamine D1 and D2 Receptors in Working Memory Function. In MSURJ • Volume 4, Issue 1

Lu, W. Y.; Xiong, Z. G.; Lei, S.; Orser, B. A.; Dudek, E.; Browning, M. D.; Macdonald, J. F. (1999): G-protein-coupled receptors act via protein kinase C and Src to regulate NMDA receptors. In: *Nat Neurosci* 2 (4), S. 331–338.

Luttrell, LouisM; Lefkowitz, RobertJ (2002): The role of beta-arrestins in the termination and transduction of G-protein-coupled receptor signals. In: *J Cell Sci* 115 (Pt 3), S. 455–465.

Magin, T. M.; McWhir, J.; Melton, D. W. (1992): A new mouse embryonic stem cell line with good germ line contribution and gene targeting frequency. In: *Nucleic Acids Res* 20 (14), S. 3795–3796.

Mansour, M.; Nagarajan, N.; Nehring, R. B.; Clements, J. D.; Rosenmund, C. (2001): Heteromeric AMPA receptors assemble with a preferred subunit stoichiometry and spatial arrangement. In: *Neuron* 32 (5), S. 841–853.

Martin, D.; Ault, B.; Nadler, J. V. (1992): NMDA receptor-mediated depolarizing action of proline on CA1 pyramidal cells. In: *Eur J Pharmacol* 219 (1), S. 59–66.

Martin, G. R. (1981): Isolation of a pluripotent cell line from early mouse embryos cultured in medium conditioned by teratocarcinoma stem cells. In: *Proc Natl Acad Sci U S A* 78 (12), S. 7634–7638.

Martin, K. C.; Barad, M.; Kandel, E. R. (2000): Local protein synthesis and its role in synapse-specific plasticity. In: *Curr Opin Neurobiol* 10 (5), S. 587–592.

Martin, Stephane; Bouschet, Tristan; Jenkins, EmmaL; Nishimune, Atsushi; Henley, JeremyM (2008): Bidirectional regulation of kainate receptor surface expression in hippocampal neurons. In: *J Biol Chem* 283 (52), S. 36435–36440.

Martinez, Gabriel; Ropero, Claudia; Funes, Andrea; Flores, Erica; Blotta, Carina; Landa, AdrianaI; Gargiulo, PascualA (2002): Effects of selective NMDA and non-NMDA blockade in the nucleus accumbens on the plus-maze test. In: *Physiol Behav* 76 (2), S. 219–224.

McDonald, J. W.; Silverstein, F. S.; Johnston, M. V. (1990): MK-801 pretreatment enhances N-methyl-D-aspartate-mediated brain injury and increases brain N-methyl-D-aspartate recognition site binding in rats. In: *Neuroscience* 38 (1), S. 103–113.

Mead, A. N.; Morris, H. V.; Dixon, C. I.; Rulten, S. L.; Mayne, L. V.; Zamanillo, D.; Stephens, D. N. (2006): AMPA receptor GluR2, but not GluR1, subunit deletion impairs emotional response conditioning in mice. In: *Behav Neurosci* 120 (2), S. 241–248.

MILNER, B.; PENFIELD, W. (1955-1956): The effect of hippocampal lesions on recent memory. In: *Trans Am Neurol Assoc* (80th Meeting), S. 42–48.

Mitsubuchi, Hiroshi; Nakamura, Kimitoshi; Matsumoto, Shiro; Endo, Fumio (2008): Inborn errors of proline metabolism. In: *J Nutr* 138 (10), S. 2016S-2020S.

Monyer, H.; Burnashev, N.; Laurie, D. J.; Sakmann, B.; Seeburg, P. H. (1994): Developmental and regional expression in the rat brain and functional properties of four NMDA receptors. In: *Neuron* 12 (3), S. 529–540.

Moreira, J. C.; Wannmacher, C. M.; Costa, S. M.; Wajner, M. (1989): Effect of proline administration on rat behavior in aversive and nonaversive tasks. In: *Pharmacol Biochem Behav* 32 (4), S. 885–890.

Mulder, A. H.; Snyder, S. H. (1974): Potassium-induced release of amino acids from cerebral cortex and spinal cord slices of the rat. In: *Brain Res* 76 (2), S. 297–308.

Nadler, J. V. (1987): Sodium-dependent proline uptake in the rat hippocampal formation: association with ipsilateral-commissural projections of CA3 pyramidal cells. In: *J Neurochem* 49 (4), S. 1155–1160.

Nadler, J. V.; Bray, S. D.; Evenson, D. A. (1992): Autoradiographic localization of proline uptake in excitatory hippocampal pathways. In: *Hippocampus* 2 (3), S. 269–278.

Nadler, J. V.; Wang, A.; Hakim, A. (1988): Toxicity of L-proline toward rat hippocampal neurons. In: *Brain Res* 456 (1), S. 168–172.

Nakanishi, S. (1992): Molecular diversity of glutamate receptors and implications for brain function. In: *Science* 258 (5082), S. 597–603.

Nickolson, V. J. (1982): "On" and "off" responses of K+-induced synaptosomal proline release: involvement of the sodium pump. In: *J Neurochem* 38 (1), S. 289–292.

Nicoll, RogerA (2003): Expression mechanisms underlying long-term potentiation: a postsynaptic view. In: *Philos Trans R Soc Lond B Biol Sci* 358 (1432), S. 721–726.

Nowak, G.; Ordway, G. A.; Paul, I. A. (1995): Alterations in the N-methyl-D-aspartate (NMDA) receptor complex in the frontal cortex of suicide victims. In: *Brain Res* 675 (1-2), S. 157–164.

O'Connor, J. J.; Rowan, M. J.; Anwyl, R. (1995): Tetanically induced LTP involves a similar increase in the AMPA and NMDA receptor components of the excitatory postsynaptic current: investigations of the involvement of mGlu receptors. In: *J Neurosci* 15 (3 Pt 1), S. 2013–2020.

Ortiz, J. G.; Cordero, M. L.; Rosado, A. (1997): Proline-glutamate interactions in the CNS. In: *Prog Neuropsychopharmacol Biol Psychiatry* 21 (1), S. 141–152.

Ozawa, S.; Kamiya, H.; Tsuzuki, K. (1998): Glutamate receptors in the mammalian central nervous system. In: *Prog Neurobiol* 54 (5), S. 581–618.

Paterlini, Marta; Zakharenko, StanislavS; Lai, Wen-Sung; Qin, Jie; Zhang, Hui; Mukai, Jun et al. (2005): Transcriptional and behavioral interaction between 22q11.2 orthologs modulates schizophrenia-related phenotypes in mice. In: *Nat Neurosci* 8 (11), S. 1586–1594.

Phang, J. M.; Downing, S. J.; Yeh, G. C.; Smith, R. J.; Williams, J. A. (1979): Stimulation of the hexose-monophosphate pentose pathway by delta 1-pyrroline-5-carboxylic acid in human fibroblasts. In: *Biochem Biophys Res Commun* 87 (2), S. 363–370.

Pinheiro, PauloS; Perrais, David; Coussen, Francoise; Barhanin, Jacques; Bettler, Bernhard; Mann, JeffreyR et al. (2007): GluR7 is an essential subunit of presynaptic

kainate autoreceptors at hippocampal mossy fiber synapses. In: *Proc Natl Acad Sci U S A* 104 (29), S. 12181–12186.

Porsolt, R. D.; Le, PichonM; Jalfre, M. (1977): Depression: a new animal model sensitive to antidepressant treatments. In: *Nature* 266 (5604), S. 730–732.

Reed, DanielleR; Lawler, MaureenP; Tordoff, MichaelG (2008): Reduced body weight is a common effect of gene knockout in mice. In: *BMC Genet* 9, S. 4.

Renick, S. E.; Kleven, D. T.; Chan, J.; Stenius, K.; Milner, T. A.; Pickel, V. M.; Fremeau, RTJr (1999): The mammalian brain high-affinity L-proline transporter is enriched preferentially in synaptic vesicles in a subpopulation of excitatory nerve terminals in rat forebrain. In: *J Neurosci* 19 (1), S. 21–33.

Resink, A.; Villa, M.; Benke, D.; Hidaka, H.; Mohler, H.; Balazs, R. (1996): Characterization of agonist-induced down-regulation of NMDA receptors in cerebellar granule cell cultures. In: *J Neurochem* 66 (1), S. 369–377.

Robertson, E. J. (1991): Using embryonic stem cells to introduce mutations into the mouse germ line. In: *Biol Reprod* 44 (2), S. 238–245.

Rodriguez-Moreno, A.; Herreras, O.; Lerma, J. (1997): Kainate receptors presynaptically downregulate GABAergic inhibition in the rat hippocampus. In: *Neuron* 19 (4), S. 893–901.

Rubaj, Andrzej; Zgodzinski, Witold; Sieklucka-Dziuba, Maria (2003): The influence of adenosine A3 receptor agonist: IB-MECA, on scopolamine- and MK-801-induced memory impairment. In: *Behav Brain Res* 141 (1), S. 11–17.

Sakakibara, Hiroyuki; Ishida, Kaori; Izawa, Yuki; Minami, Yuko; Saito, Satomi; Kawai, Yoshichika et al. (2005): Effects of forced swimming stress on rat brain function. In: *J Med Invest* 52 Suppl, S. 300–301.

Schiffer, H. H.; Heinemann, S. F. (2007): Association of the human kainate receptor GluR7 gene (GRIK3) with recurrent major depressive disorder. In: *Am J Med Genet B Neuropsychiatr Genet* 144B (1), S. 20–26.

Schmajuk, NestorA; Larrauri, JoseA (2005): Neural network model of prepulse inhibition. In: *Behav Neurosci* 119 (6), S. 1546–1562.

Schmitz, D.; Mellor, J.; Nicoll, R. A. (2001): Presynaptic kainate receptor mediation of frequency facilitation at hippocampal mossy fiber synapses. In: *Science* 291 (5510), S. 1972–1976.

Schorge, Stephanie; Colquhoun, David (2003): Studies of NMDA receptor function and stoichiometry with truncated and tandem subunits. In: *J Neurosci* 23 (4), S. 1151–1158.

Shafqat, S.; Velaz-Faircloth, M.; Henzi, V. A.; Whitney, K. D.; Yang-Feng, T. L.; Seldin, M. F.; Fremeau, RTJr (1995): Human brain-specific L-proline transporter: molecular cloning, functional expression, and chromosomal localization of the gene in human and mouse genomes. In: *Mol Pharmacol* 48 (2), S. 219–229.

Shanti, NDesai; Shashikumar, K. C.; Desai, P. V. (2004): Influence of proline on rat brain activities of alanine aminotransferase, aspartate aminotransferase and acid phosphatase. In: *Neurochem Res* 29 (12), S. 2197–2206.

Shastry, B. S. (1994): More to learn from gene knockouts. In: *Mol Cell Biochem* 136 (2), S. 171–182.

Snyder, S. H.; Young, A. B.; Bennett, J. P.; Mulder, A. H. (1973): Synaptic biochemistry of amino acids. In: *Fed Proc* 32 (10), S. 2039–2047.

Sonntag, W. E.; Bennett, S. A.; Khan, A. S.; Thornton, P. L.; Xu, X.; Ingram, R. L.; Brunso-Bechtold, J. K. (2000): Age and insulin-like growth factor-1 modulate N-methyl-D-aspartate receptor subtype expression in rats. In: *Brain Res Bull* 51 (4), S. 331–338.

Sprengel, R.; Single, F. N. (1999): Mice with genetically modified NMDA and AMPA receptors. In: *Ann N Y Acad Sci* 868, S. 494–501.

Sukharev, S. I.; Klenchin, V. A.; Serov, S. M.; Chernomordik, L. V. (1992): Electroporation and electrophoretic DNA transfer into cells. The effect of DNA interaction with electropores. In: *Biophys J* 63 (5), S. 1320–1327.

Takemoto, Yumi (2005): Depressor responses to L-proline microinjected into the rat ventrolateral medulla are mediated by ionotropic excitatory amino acid receptors. In: *Auton Neurosci* 120 (1-2), S. 108–112.

Takemoto, Yumi; Semba, Reiji (2006): Immunohistochemical evidence for the localization of neurons containing the putative transmitter L-proline in rat brain. In: *Brain Res* 1073-1074, S. 311–315.

Tang, Y. P.; Shimizu, E.; Dube, G. R.; Rampon, C.; Kerchner, G. A.; Zhuo, M. et al. (1999): Genetic enhancement of learning and memory in mice. In: *Nature* 401 (6748), S. 63–69.

Thomas, K. R.; Folger, K. R.; Capecchi, M. R. (1986): High frequency targeting of genes to specific sites in the mammalian genome. In: *Cell* 44 (3), S. 419–428.

Tovar, K. R.; Sprouffske, K.; Westbrook, G. L. (2000): Fast NMDA receptor-mediated synaptic currents in neurons from mice lacking the epsilon2 (NR2B) subunit. In: *J Neurophysiol* 83 (1), S. 616–620.

Trullas, R.; Skolnick, P. (1990): Functional antagonists at the NMDA receptor complex exhibit antidepressant actions. In: *Eur J Pharmacol* 185 (1), S. 1–10.

Tsien, J. Z.; Huerta, P. T.; Tonegawa, S. (1996): The essential role of hippocampal CA1 NMDA receptor-dependent synaptic plasticity in spatial memory. In: *Cell* 87 (7), S. 1327–1338.

Velaz-Faircloth, M.; Guadano-Ferraz, A.; Henzi, V. A.; Fremeau, RTJr (1995): Mammalian brain-specific L-proline transporter. Neuronal localization of mRNA and enrichment of transporter protein in synaptic plasma membranes. In: *J Biol Chem* 270 (26), S. 15755–15761.

Vicini, S.; Wang, J. F.; Li, J. H.; Zhu, W. J.; Wang, Y. H.; Luo, J. H. et al. (1998): Functional and pharmacological differences between recombinant N-methyl-D-aspartate receptors. In: *J Neurophysiol* 79 (2), S. 555–566.

von Engelhardt-Jakob; Doganci, Beril; Jensen, Vidar; Hvalby, Oivind; Gongrich, Christina; Taylor, Amy et al. (2008): Contribution of hippocampal and extra-hippocampal NR2B-containing NMDA receptors to performance on spatial learning tasks. In: *Neuron* 60 (5), S. 846–860.

Watkins, J. C.; Evans, R. H. (1981): Excitatory amino acid transmitters. In: *Annu Rev Pharmacol Toxicol* 21, S. 165–204.

Wiley, J. L.; Cristello, A. F.; Balster, R. L. (1995): Effects of site-selective NMDA receptor antagonists in an elevated plus-maze model of anxiety in mice. In: *Eur J Pharmacol* 294 (1), S. 101–107.

Williams, K.; Dichter, M. A.; Molinoff, P. B. (1992): Up-regulation of N-methyl-D-aspartate receptors on cultured cortical neurons after exposure to antagonists. In: *Mol Pharmacol* 42 (1), S. 147–151.

Willis, Alecia; Bender, HansUli; Steel, Gary; Valle, David (2008): PRODH variants and risk for schizophrenia. In: *Amino Acids* 35 (4), S. 673–679.

Wyse, A. T.; Netto, C. A. (2011): Behavioral and neurochemical effects of proline. In: *Metab Brain Dis*.

Xu, F.; Gainetdinov, R. R.; Wetsel, W. C.; Jones, S. R.; Bohn, L. M.; Miller, G. W. et al. (2000): Mice lacking the norepinephrine transporter are supersensitive to psychostimulants. In: *Nat Neurosci* 3 (5), S. 465–471.

Yoneda, Y.; Roberts, E. (1982): A new synaptosomal biosynthetic pathway of proline from ornithine and its negative feedback inhibition by proline. In: *Brain Res* 239 (2), S. 479–488.

Zambrowicz, BrianP; Sands, ArthurT (2003): Knockouts model the 100 best-selling drugs--will they model the next 100? In: *Nat Rev Drug Discov* 2 (1), S. 38–51.

Zhong, J.; Russell, S. L.; Pritchett, D. B.; Molinoff, P. B.; Williams, K. (1994): Expression of mRNAs encoding subunits of the N-methyl-D-aspartate receptor in cultured cortical neurons. In: *Mol Pharmacol* 45 (5), S. 846–853.

9   Annex

9.1   Targeting Vector Map and Generation of the Targeting Vector

The vector XpPNT (**Figure 41**) (Thomas et al. 1986) was developed for gene knock-out experiments in mammalian cells by double homologous recombination (Fiau and neo selection) and used for the construction of the targeting vector for homologous recombination of the murine *ProT* gene locus. Therefore, the plasmid contains a neomycin resistance gene (*neo)* of 1826 bp under the control of the mouse phosphoglycerate kinase 1 (PGK) promoter, as well as a herpes simplex virus thymidine kinase gene (HSV-TK) of 1127 bp. The neomycin resistance gene contains some modifications at the start region of the coding sequence as compared to the wild-type gene. As a third selection marker the plasmid contains an ampicillin resistance gene (*amp*) for featuring introduction and maintenance in bacterial hosts. The origin of replication from *E. coli* allows amplification of the plasmid.
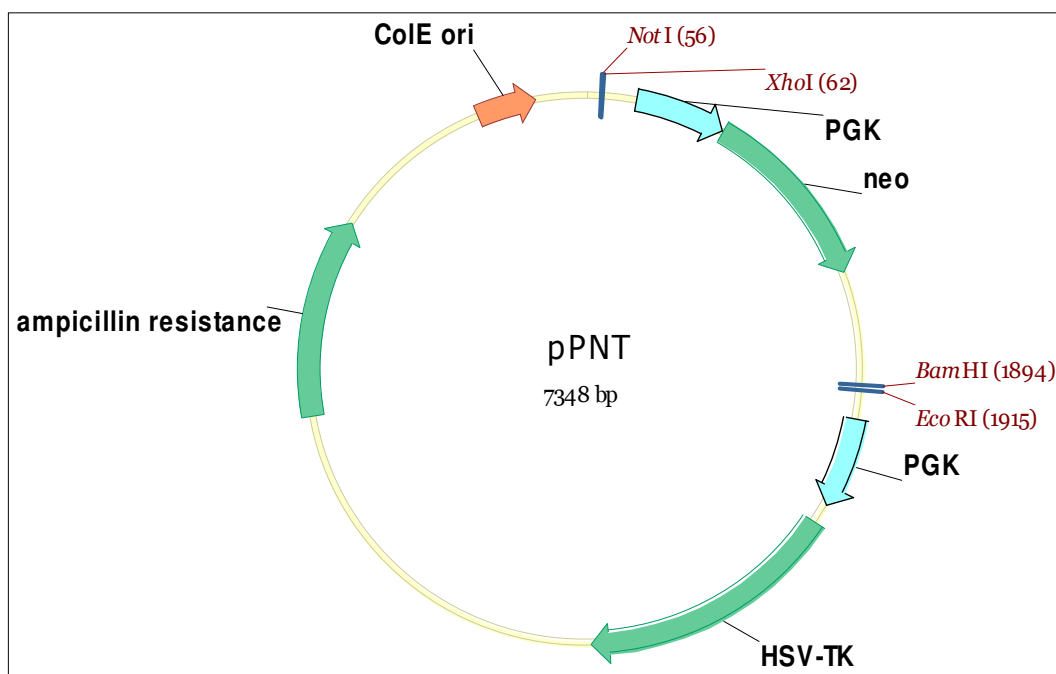

Figure 41 Vector-map of pPNT for gene knockout experiments in mammalian cells

The depicted plasmid-map was designed by the use of the bioinformatics software Vector NTI. Indicated are:
Mouse phosphoglycerate kinase 1 promoter (PGK1), neomycin positive selection marker (neo), replicon of *E. coli* plasmid ColE1 origin (ColE ori), ampicillin selection marker for amplification in bacteria (ampicillin resistance), negative selection marker (HSV-TK) as well as the endonuclease restriction sites used for cloning (*NotI, XhoI, Bam*HI and *EcoRI*) and linearization (*NotI).*

In order to achieve homologous recombination in ES cells the targeting vector had to contain homologous genomic DNA fragments, 5´ and 3´ to the *ProT* central region (1158 bp) that was anticipated to be removed. For the 5' homology region a fragment of 5028bp (long arm) from the end of exon 2 up to the beginning of exon 6 (including exons 3, 4 and 5) were selected and the 3' homology area (short arm) comprised a fragment of 1131bp from the beginning of exon 8 up to the beginning of exon 10. In order to maintain this genomic DNA fragments PCR reactions were performed (**Figure 42**) to amplify the 5´ and 3´ homologous regions by use of appropriate oligonucleotide primers and the BAC clone RP24-243J21 (BAC5) as DNA template. The primers used to amplify the 5' homologous DNA fragment were designed to add artificial endonuclease restriction sites to the amplicons next to amplification of the desired sequence (2.4). To the 5' homologous DNA fragment 5´ a *NotI* site and 3´ an *XhoI* site were added in order to finally allow insertion into the XpPNT- vector by standard cloning techniques. Likewise, endonuclease restriction sites were added to the 3' homologous DNA fragment. 5´ of the short arm a *BamHI* site and 3´ an *EcoRI* site were attached to finally allow insertion into vector. The amplification products of the PCR reactions (**Figure 42**), were purified by agarose gel electrophoresis and isolated by subsequent gel extraction.
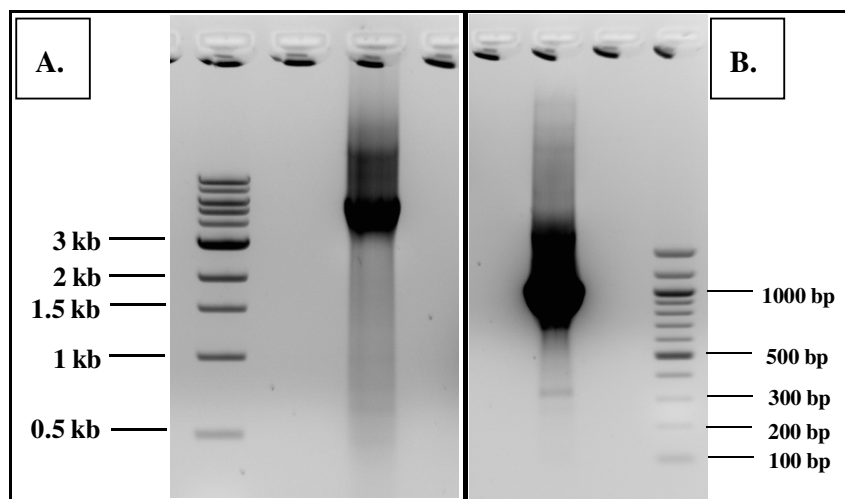

Figure 42 Images of agarose gel electrophoresed PCR products displaying the 5' homologous fragment (A.) and the 3' homologous fragment (B.) detected by use of ethidium bromide under UV-light

PCR amplicons were flanked by artificially introduced restriction sites to finally allow insertion into the vector XpPNT. 5´a *NotI* site and 3´ an *XhoI* site were added to the 5' homologous DNA fragment (A.). The 3´homologous fragment maintained a 5´ *BamHI* site and a 3´ *EcoRI* site. For size estimations a 1kb DNA ladder (2.1) was applied.

Prior to insertion into the vector XpPNT both fragments were subcloned into the vector pBS in order to ensure the correct sequence. Verification was accomplished by restriction analyses (**Figure 43 A**. & **Figure 43 B**.) and sequencing (GATC Biotech AG, Konstanz).
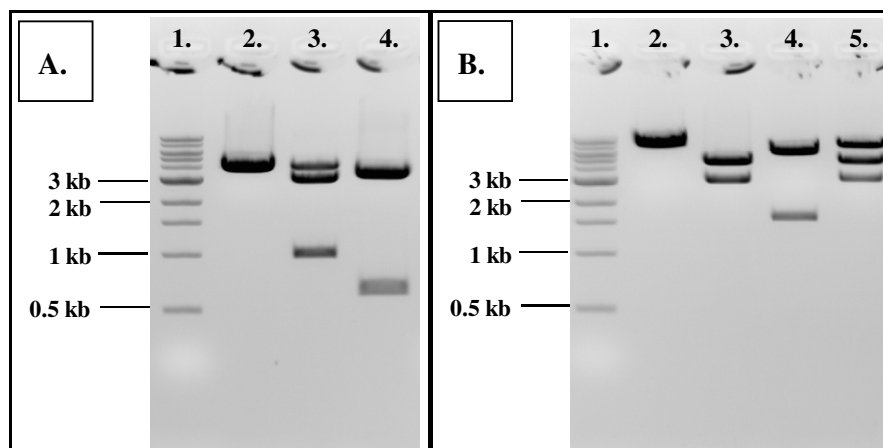

Figure 43 Agarose gel analysis of restriction endonuclease cleavages in order to verify introduction of the 3' homologous fragment (A.) into vector pBS and the 5' homology fragment (B.) in vector pBS envisaged with ethidium bromide under UV-light

  A. Restriction cleavage of the 3' homologous fragment was confirmed by the expected genomic DNA restriction patterns:
     EcoRI cleavage (2.) was expected to result in a linearized DNA fragment of 4423 bp
     NheI and *EcoRI* treatment (3.) should reveale fragments of 3281 bp as well as 1142 bp (additionally partially cut fragment of 4423 bp is visible)
     SpeI cleavage (4.) shows the expected fragments of 3725 bp and 698 bp
     For size estimations a 1kb DNA ladder (1.) was applied.
  B. The 5' homologous fragment was as well verified by the expected restriction patterns:
     Linearization at the single *XhoI* site (2.) resulted into the expected fragment of 8320 bp
     EcoRI and *XhoI* cleavage (3.) revealed fragments of 5110 bp as well as of 3210 bp
     BamHI and *XhoI* cleavage (4.) shows the expected fragments of 6690 bp and 1630 bp
     XbaI and *XhoI* cleavage (5.) was expected to result in the expected fragments of 5040 bp and 3280 bp
     A 1kb DNA ladder (1.) was applied for size estimations.

Finally, the homologous sequences became inserted into the pPNT-vector to accomplish construction of the targeting vector for homologous recombination of the murine *ProT* gene locus. The 3' homologous fragment was first inserted with *BamHI* and *EcoRI* between the *neo* gene and the *HSV-TK* gene. Afterwards the 5' homologous fragment was introduced into the vector XpPNT by *NotI* and *XhoI*. The correctness of this vector was further proven by restriction enzyme analyses (**Figure 44**).
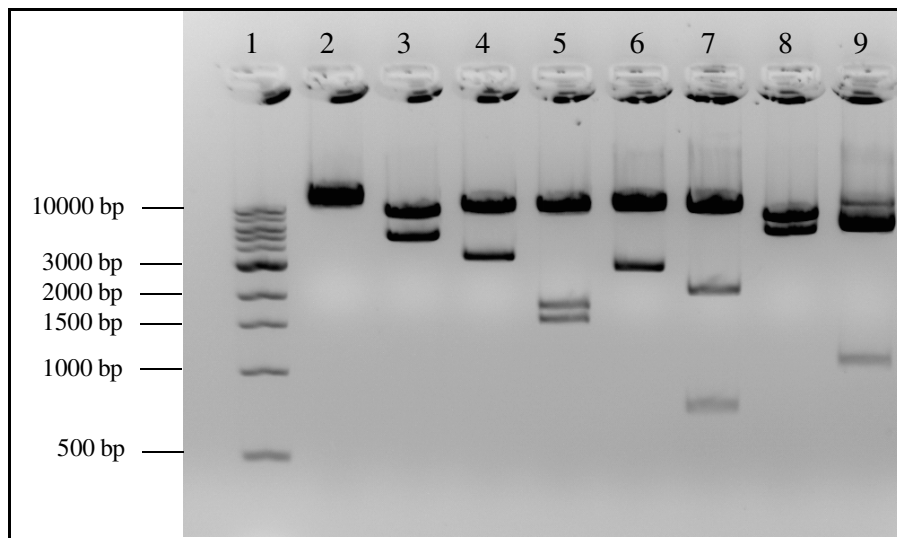
Figure 44 Gel electrophoresis of restriction mapping to confirm the final *ProT*-pPNT targeting vector

Pictured are the expected restriction patterns after cleavage with the particular enzymes to verify the integrity of the final targeting construct. Applied enzymes and expected patterns were: (2) *ProT*-pPNT after *NotI* cleavage resulting in a linearized fragment of ~13.5 kb, (3) fragments of ~5 kb & ~8.5 kb after restriction of the targeting vector with *NotI* and *XhoI*, (4) *ProT*-pPNT after *BamHI* cleavage generating two fragments of ~3.4 kb and ~10 kb, (5) 10 kb, 1.8 kb 1.6 kb fragments after *XhoI* & *BamHI* cleavage of *ProT*-pPNT, (6) 10.5 & 2.9 kb fragments after *HindIII* restriction*,* (7) *SpeI* resulting in 10.5 & 2.2 & 0.8 kb fragments, (8) *ProT*-pPNT after *EcoRI* cleavage resulting in 7.8 + 5.7 kb fragments, (9) 1.1 + 5.9 + 6.3 kb fragments after *XbaI* treatment, as well 1kb-ladder (1)

9.2   qPCR-Setup

Initially integrity of the extracted and purified mRNA was verified through presence of the two discreet 18S and 28S rRNA bands visible after agarose gel electrophoresis (**Figure 45**). It was essential that the obtained mRNA was free from genomic DNA. Therefore, a DNase digest was accomplished before the extraction was carried out. After purification cDNA was synthesized from the mRNA prior to qPCR reaction. To optimize the qPCR conditions, different template concentrations as well as different primer concentrations were tested in parallel.
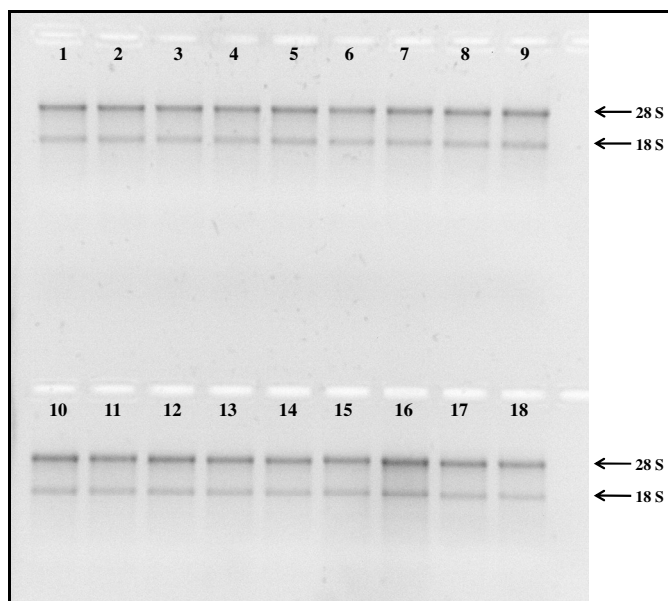
Figure 45 Exemplary depiction of the control of mRNA integrity in a number of different areas of the brain by agarose gel electrophoresis, visible by use of ethidium bromide under UV-light

Agarose gel electrophoresed RNA (each 0.5μg) displaying discrete 18S and 28S rRNA bands detected with ethidium bromide under UV-light. Loaded were:

1 = frontal cortex knockout 1	10 = frontal cortex wild-type 2
2 = striatum knockout 1	11 = striatum wild-type 2
3 = hippocampus knockout 1	12 = hippocampus wild-type 2
4 = frontal cortex wild-type 1	13= frontal cortex knockout 3
5 = striatum wild-type 1	14 = striatum knockout 3
6 = hippocampus wild-type 1	15 = hippocampus knockout 3
7 = frontal cortex knockout 2	16 = frontal cortex wild-type 3
8 = striatum knockout 2	17 = striatum wild-type 3
9 = hippocampus knockout 2	18 = hippocampus wild-type 3

Moreover, the sizes of the resulting PCR products for each primer pair have been verified by gel electrophoresis to ascertain fitting to their respective theoretical calculations (**Figure 46** and **Figure 47**).
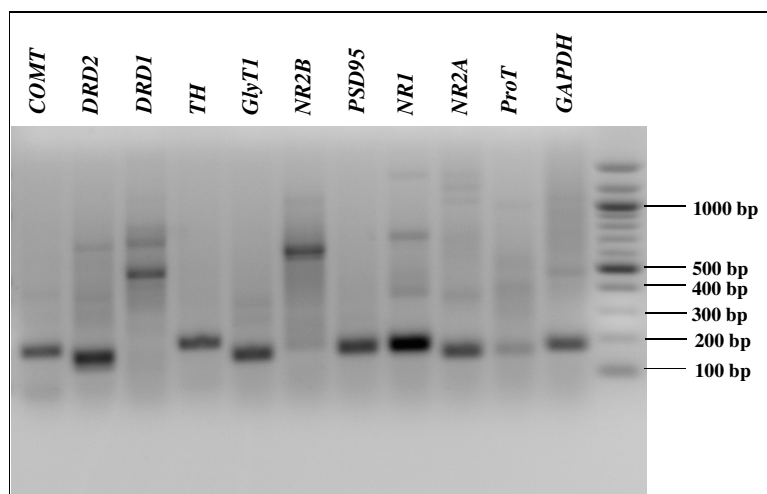
Figure 46 Agarose gel electrophoresis of PCR products displaying amplicons of the respectively indicated primer pairs detected by use of ethidium bromide under UV-light

Figure 47 Agarose gel electrophoresis of PCR products displaying amplicons of the respectively indicated primer pairs detected by use of ethidium bromide under UV-light
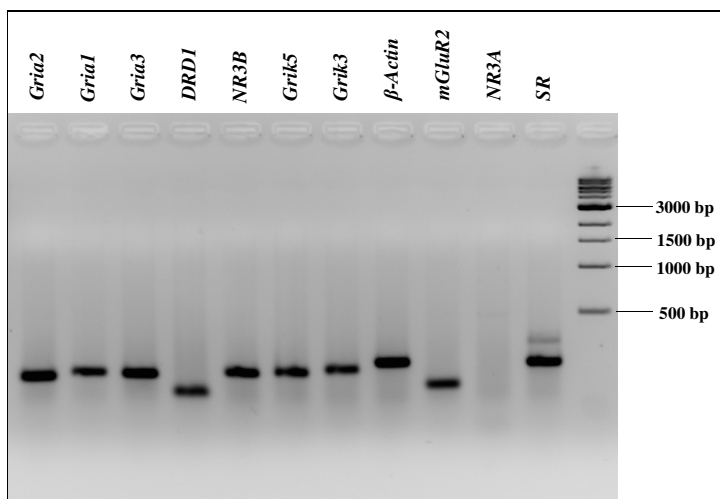
Efficiencies of reference gene primers were determined by dilution curves. Both reference genes *GAPDH* as well as *β-Actin* were stably expressed, but *β-actin* was slightly better expressed and therefore chosen for the analysis. The efficiencies for the primer pairs used for analyses of the genes of interest were not determined and for calculation assumed to be 100% efficient.

To permanently control amplification products and exclude false fluorescence signals (primer-dimer) of the respective reaction, a melting curve was recorded subsequently to each experiment (**Figure 48**).
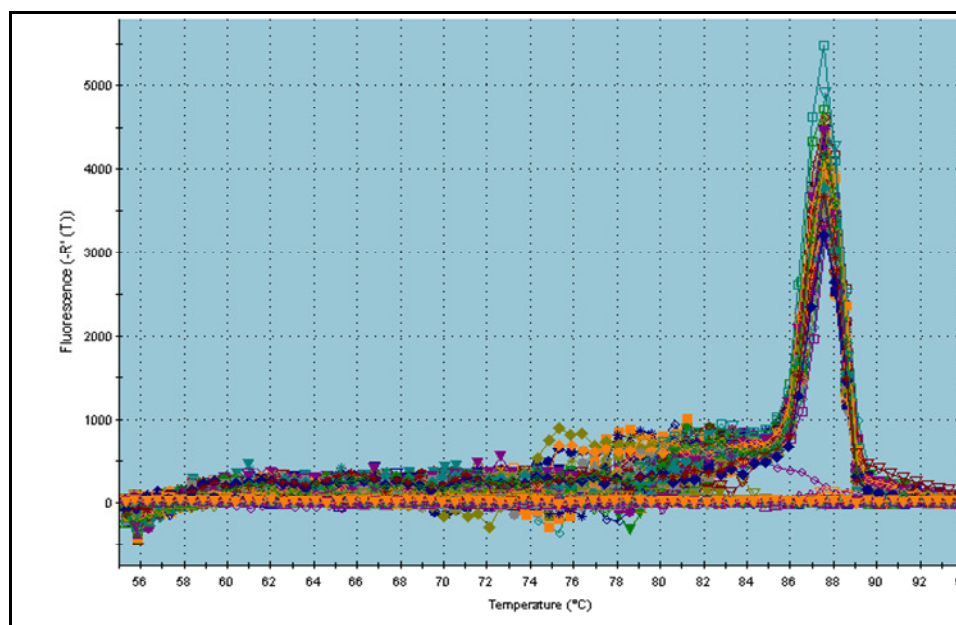

Figure 48 Representative melting curve analysis for control of amplification products exemplified by primer pair *NR2B*

Data obtained from *ProT*$^{-/-}$- and *ProT*$^{+/+}$-genotypes were normalized by the reference gene *β-actin* and set in relation to each other.

9.3   Manufacturer

Agilent Technologies	D-76337 Waldbronn
Applichem	D-64291 Darmstadt
Applied Biosystems	CA 92008, USA
Berthold technologies	D-75323 Bad Wildbad
Bioplastics BV	6374 XW Landgraaf, NL
Bio Rad	CA 94547, USA
Biozol	D-85386 Eching
Cayman Chemical Company	MI 48108, USA
Chemicon® (Millipore)	MA 01821, USA
Cisbio Bioassays	BP 84175, France
Corning® Incorporated	NY 14831, USA
CyBio	D-07745 Jena
Decon Science Tec GmbH	D-37318 Hohengandern
Enzo Life Sciences	PA 19462-1202, USA

Eppendorf	D-22339 Hamburg
Fermentas	D-68789 St. Leon-Rot
Fisher Scientific	Leicestershire LE11 5R6, UK
Fluka	D-21147 Hamburg
Genex Lab	Torquay TQ2 8JG, UK
Gibco	Paisley PA4 9RF, UK
Gold Biotechnology	MO 63132, USA
GraphPad Software, Inc	CA 92037, USA
Greiner bio one	4550 Kremsmünster, Austria
Grüssing GmbH Analytika	D-26849 Filsum
Heraeus	D-63450 Hanau
HLC BioTech	D-37120 Bovenden
Invitrogen™	D-64293 Darmstadt
KMF Laborchemie Handels GmbH	D-53785 Lohmar
Labomedic GmbH	D-53115 Bonn
Leica	D-35578 Wetzlar
Merck	D-64293 Darmstadt
Mettler Toledo	D-35353 Giessen
Microsoft® Corporation	D-85716 Unterschleißheim
Moravek Biochemicals	CA 92821, USA
New England BioLabs® (NEB)	MA 01938-2723, USA
Olympus	D-20097 Hamburg
PerkinElmer Life Sciences	MA 02451, USA
Promega	WI 53711, USA
QIAGEN GmbH	D-40724 Hilden
Riedel-de Haen	D-30926 Seelze
Ritter GmbH	D- 86830 Schwabmünchen
Roth	D-76231 Karlsruhe
SAFC Supply Solutions	MO 63103, USA
Sarstedt	D-51582 Nümbrecht
Sartorius	D-37075 Göttingen
Sigma	D-21147 Hamburg
Thermo Fisher Scientific Germany Ltd. & Co. KG.	D-53113 Bonn
Tocris	Bristol BS11 0QL, UK